THE FUNCTIONS OF THE CULLIN-2-ZYG-11 COMPLEX IN PROMOTING MEIOSIS AND ANTERIOR-POSTERIOR POLARITY IN C. ELEGANS

by

SRIVIDYA VASUDEVAN

(Under the Direction of Edward T. Kipreos)

ABSTRACT

Chromosome segregation is one of the most important events in the life cycle of a cell. Unequal segregation of chromosomes is the cause of a number of disorders in humans and other organisms.

In this study we demonstrate that in *Caenorhabditis elegans,* the ubiquitin ligase CUL-2 is required for chromosome segregation during meiosis. In *cul-2* mutant zygotes, the maternal chromosomes fail to complete the second meiotic division. Inspection of chromosome and spindle dynamics has revealed that in *cul-2* zygotes the meiotic apparatus spends an extended amount of time in the metaphase configuration and fails to proceed towards anaphase. During the metaphase II arrest, premature establishment of anterior-posterior polarity and cytoskeletal defects are observed in the zygote.

A second gene, *zyg-11,* has similar meiosis defects as *cul-2*. In this report we demonstrate that ZYG-11 serves as a substrate recognition subunit for the CUL-2 ubiquitin ligase. Here we find that ZYG-11 interacts with the CUL-2 complex adaptor Elongin C through a nematode specific VHL box motif. ZYG-11 homologs in *C. elegans* and humans also function as substrate recognition subunits of CUL-2.

To identify the substrates of the CUL-2 $^{ZYG-11}$ complex we have undertaken a *zyg-11* suppressor screen. We anticipate that this screen will identify novel cell cycle regulators that will explain the complex phenotypes observed in *cul-2* and *zyg-11* mutants.

INDEX WORDS: *Caenorhabditis elegans*, CUL-2, ZYG-11, Meiosis, Anterior-Posterior Polarity, Ubiquitin Ligase.

THE FUNCTIONS OF THE CULLIN-2-ZYG-11 COMPLEX IN PROMOTING MEIOSIS AND ANTERIOR-POSTERIOR POLARITY IN C. ELEGANS

by

SRIVIDYA VASUDEVAN

B.Sc., Sophia College, University of Mumbai, India, 1998

M.Sc., Mithibai College, University of Mumbai, India, 2000

A Dissertation Submitted to the Graduate Faculty of The University of Georgia in Partial Fulfillment of the Requirements for the Degree

DOCTOR OF PHILOSOPHY

ATHENS, GEORGIA

2007

THE FUNCTIONS OF THE CULLIN-2-ZYG-11 COMPLEX IN PROMOTING MEIOSIS AND ANTERIOR-POSTERIOR POLARITY IN C. ELEGANS

by

SRIVIDYA VASUDEVAN

Major Professor: Edward T. Kipreos

Committee: Haini Cai
Scott Dougan
Marcus Fechheimer
Jacek Gaertig

Electronic Version Approved:

Maureen Grasso
Dean of the Graduate School
The University of Georgia
December 2007

ACKNOWLEDGEMENTS

It is my pleasure in presenting this dissertation “THE FUNCTIONS OF THE CULLIN-2-ZYG-11 COMPLEX IN PROMOTING MEIOSIS AND ANTERIOR-POSTERIOR POLARITY IN C. ELEGANS”.

I express my deepest gratitude to Dr. Edward T. Kipreos whose precious advice, constant support and guidance has helped me accomplish my dissertation. I thank my committee members Drs. Haini Cai, Scott Dougan, Marcus Fechheimer, and Jacek Gaertig for their keen interest and involvement in my Ph. D program. I am grateful to Drs. Jacek Gaertig, Charles Keith, James Lauderdale and John Willis for permitting us to use their laboratory facilities.

Special thanks to Dr. Marcus Fechheimer, Marian Thomas and everyone in the Cellular Biology department at the University of Georgia for their patience, advice and help.

I thank former graduate students Ji Liu and Hui Feng for initiating the CUL-2 projects, Ji Liu and Natalia Starostina for excellent collaborations, Christopher Dowd for technical help and Drs. Kenneth Kemphues and Geraldine Seydoux for valuable reagents. Sincere thanks to current members Dimple Bosu, Jihyun Kim, Kathryn Williams, Mohammad Rahman, Natalia Starostina, and Youngjo Kim and former members Ji Liu, Hui Feng, Vikas Dhingra, Weiwei Zhong, Fernando Santiago and Christopher Dowd for helpful suggestions.

I am very grateful to my family and friends for providing constant encouragement throughout.

TABLE OF CONTENTS

Page

CHAPTER 1

INTRODUCTION

Structure of the dissertation

CUL-2 is a member of the E3 ubiquitin-ligase family. In humans, CUL-2 is present in a protein complex with Elongin B, Elongin C, a substrate recognition subunit such as the tumor suppressor protein VHL and RBX-1. This protein complex is known to target the hypoxia inducible factor, HIF-1α for degradation via the ubiquitin-proteosome pathway under normal oxygen conditions (Maxwell et al., 1999; Pause et al., 1999).

Deletion of the *C. elegans cul-2* gene causes an abnormal metaphase arrest in zygotes undergoing the second meiotic cycle, and a host of other defects (Feng et al., 1999; Starostina et al., 2007; Vasudevan et al., 2007). Null mutations in a second gene, *zyg-11,* causes a similar metaphase II arrest (Carter et al., 1990; Liu et al., 2004; Sonneville and Gonczy, 2004). CUL-2 and ZYG-11 are dispensable for the first meiosis but are required for completing meiosis II. The mechanisms by which CUL-2 and ZYG-11 regulate meiosis are not known.

The goal of this dissertation is to

a. Characterize the meiotic defects in *cul-2* and *zyg-11*.
b. Test for interaction between *cul-2* and *zyg-11* by biochemical and genetic means.
c. Identify and characterize suppressors of *zyg-11*.

The second chapter of this dissertation is a literature review that explains the background and how this research work has contributed to our further understanding about protein degradation, ubiquitin ligases, chromosome segregation, meiosis, and anterior-posterior polarity.

The third chapter is the manuscript "CUL-2 and ZYG-11 promote meiotic anaphase II and the proper placement of the anterior-posterior axis in *C. elegans*." Here we characterize the meiotic and anterior-posterior polarity defects in *cul-2* and *zyg-11* mutants. The major results of this manuscript are as follows:

1. *cul-2* and *zyg-11* are required to promote the metaphase to anaphase transition during meiosis II.
2. In *cul-2* mutants, the cohesin REC-8 is removed during metaphase suggesting that the failure to complete anaphase is due to defects in chromosome movement rather than from a failure to sever chromosome attachments.
3. CUL-2 and ZYG-11 are required for the degradation of cyclin B1, and the inactivation of cyclin B1 partially rescues the meiotic delay in *cul-2* mutants.
4. The metaphase II delay in *cul-2* and *zyg-11* mutants induces polarity reversals of PAR proteins, P granules, pronuclei migration, and asymmetric cell division.
5. CUL-2 is required to limit the initiation of PAR-2 in regions distant from microtubule organizing centers (Liu et al., 2004).

The fourth chapter of this dissertation is the manuscript "The Caenorhabditis elegans cell-cycle regulator ZYG-11 defines a conserved family of CUL-2 complex components." The major results of this work are as follows:

1. ZYG-11 interacts with CUL-2 *in vivo.*

2. ZYG-11 binds to the adaptor protein Elongn C using a nematode variant of the VHL-box motif.
3. The ZYG-11 homologs in *C. elegans* and humans are conserved components of the CUL-2 ubiquitin ligases (Vasudevan et al., 2007).

The fifth chapter is a temperature sensitive suppressor screen aimed to identify substrates and regulators of the CUL-2-ZYG-11 complex. The sixth chapter is a discussion of this work.

REFERENCES

Carter, P.W., Roos, J.M., and Kemphues, K.J. (1990). Molecular analysis of zyg-11, a maternal-effect gene required for early embryogenesis of Caenorhabditis elegans. Mol Gen Genet *221*, 72-80.

Feng, H., Zhong, W., Punkosdy, G., Gu, S., Zhou, L., Seabolt, E.K., and Kipreos, E.T. (1999). CUL-2 is required for the G1-to-S-phase transition and mitotic chromosome condensation in Caenorhabditis elegans. Nature cell biology *1*, 486-492.

Liu, J., Vasudevan, S., and Kipreos, E.T. (2004). CUL-2 and ZYG-11 promote meiotic anaphase II and the proper placement of the anterior-posterior axis in C. elegans. Development (Cambridge, England) *131*, 3513-3525.

Maxwell, P.H., Wiesener, M.S., Chang, G.W., Clifford, S.C., Vaux, E.C., Cockman, M.E., Wykoff, C.C., Pugh, C.W., Maher, E.R., and Ratcliffe, P.J. (1999). The tumour suppressor protein VHL targets hypoxia-inducible factors for oxygen-dependent proteolysis. Nature *399*, 271-275.

Pause, A., Peterson, B., Schaffar, G., Stearman, R., and Klausner, R.D. (1999). Studying interactions of four proteins in the yeast two-hybrid system: structural resemblance of the pVHL/elongin BC/hCUL-2 complex with the ubiquitin ligase complex SKP1/cullin/F-box protein. Proceedings of the National Academy of Sciences of the United States of America *96*, 9533-9538.

Sonneville, R., and Gonczy, P. (2004). Zyg-11 and cul-2 regulate progression through meiosis II and polarity establishment in C. elegans. Development (Cambridge, England) *131*, 3527-3543.

Starostina, N.G., Lim, J.M., Schvarzstein, M., Wells, L., Spence, A.M., and Kipreos, E.T. (2007). A CUL-2 ubiquitin ligase containing three FEM proteins degrades TRA-1 to regulate C. elegans sex determination. Developmental cell *13*, 127-139.

Vasudevan, S., Starostina, N.G., and Kipreos, E.T. (2007). The Caenorhabditis elegans cell-cycle regulator ZYG-11 defines a conserved family of CUL-2 complex components. EMBO reports *8*, 279-286.

CHAPTER 2

LITERATURE REVIEW

This section provides background and highlights the major discoveries of this research

Biological Processes associated with protein degradation

Protein degradation by the ubiquitin proteosome system (UPS) is one of the major pathways by which proteins are degraded in the cell. Various biological processes such as cell division, embryogenesis, antigen-presentation, quality control, signal transduction, programmed cell death, and activities of the nervous system require ubiquitin-dependent proteolysis for proper function (Chen, 2005; DeRenzo and Seydoux, 2004; Hampton, 2002; Jesenberger and Jentsch, 2002; Korhonen and Lindholm, 2004; Lord et al., 2005; Peters, 2002; Rock and Goldberg, 1999).

MITOSIS

During mitosis, Anaphase Promoting Complex is the major ubiquitin ligase that brings about the destruction of key cell cycle regulators. The Cyclin B/CDK complex initiates mitosis in all eukaryotes and the degradation of cyclin B is required for the exit from telophase to the subsequent interphase. The APC was discovered as a mitosis and cyclin B specific ubiquitin ligase in clam and *Xenopus* extracts. Expression of nondegradable cyclin mutants causes fungal, plant and animal cells to arrest in telophase; however inactivation of APC blocks mitosis before sister chromatids have separated in anaphase. Separase is essential for sister chromatid

separation and its activation depends on securin proteolysis. APC's essential functions in promoting mitosis is via the degradation of securin, which releases active separase during anaphase, followed by the degradation of cyclins during telophase (Peters, 2002).

OOCYTE TO EMBRYO TRANSITION

During the oocyte-embryo transition a change from a germ cell character to a zygote that can generate both somatic and germ cells is required. In *C. elegans,* three RNA binding proteins PIE-1, POS-1 and MEX-1 are required for germline specification. They are segregated preferentially to the germline daughter and are actively degraded in the somatic blastomeres by the ubiquitin ligase CUL-2 (DeRenzo et al., 2003).

Fertilization triggers the completion of meiosis and the transition into mitosis. The meiotic and mitotic spindles are functionally and morphologically different, and form in the same cytoplasm within minutes of each other. In *C. elegans,* the transition from the small meiotic spindle to the large mitotic spindle requires the down-regulation of the microtubule severing complex katanin (MEI-1 and MEI- 2). MEI-1 and MEI-2 proteins accumulate on the meiotic spindle keeping it small and are immediately degraded after meiosis to allow the formation of the large mitotic spindle. Degradation of MEI-1 is brought about by the ubiquitin ligase CUL-3 (Pintard et al., 2003). Mutations that block the degradation of MEI-1 and MEI-2 cause these proteins to accumulate on the mitotic spindle and interfere with spindle elongation and rotation (DeRenzo and Seydoux, 2004).

The ubiquitin proteosome system is indispensable and is required for many biological processes.

Ubiquitin

Ubiquitin is a small 76 residue polypeptide that shows remarkable conservation in evolution. The primary structure of ubiquitin is identical in organisms as diverse as insects, trout, cattle, and man. The role of ubiquitin in intracellular protein degradation was demonstrated by Rose, Hershko and Ceichanover (Hershko, 1983).

The protein degradation machinery

The proteins that are to be degraded, called substrates, are conjugated to a polyubiquitin chain and degraded by the 26S proteosome (Pickart and Cohen, 2004). The 26S proteosome consists of a catalytic 20S core that is capped at each end by a regulatory 19S particle. The substrate linked poly-ubiquitin chain is recognized by a component in the 19S particle. The substrate along with the poly-ubiquitin chain is unfolded in the 19S particle and hydrolysed to peptides as the protein passes through the core of the 20S particle. The poly-ubiquitin chain is then disassembled by deubiquitinating enzymes and recycled.

Ubiquitination Reaction

Ubiquitination results in the formation of a bond between the C terminus of ubiquitin (Glycine 76) and the ε-amino group of a substrate lysine residue (Figure. 2.1). Ubiquitination reactions require the sequential activities of three enzymes, namely the ubiquitin activating enzyme (E1), the ubiquitin conjugating enzyme (E2), and the ubiquitin ligase (E3).

E1

In most organisms, including humans and yeast, there is a single E1 enzyme. The ubiquitin activation reaction begins with the ordered binding of MgATP and then ubiquitin to the E1 leading to the formation of ubiquitin adenylate intermediate that serves as the donor for conjugating ubiquitin to a cysteine in the E1 active site. Each E1 carries two molecules of activated ubiquitin one as a thiol ester and the other as an adenylate.

E2

After activation by the E1, ubiquitin is trans-esterified to a conserved cysteine of an E2 enzyme. There are 13 E2s in yeast, 21 in *C. elegans* and probably a similar number in vertebrates (Kipreos, 2005). The E2 proteins catalyze substrate ubiquitination in conjunction with a ubiquitin-protein ligase (E3) (Pickart, 2001).

E3

The E3 ubiquitin ligase are known to have several functions:

1. For most ubiquitination reactions, the E3 appears to function as an adaptor that positions the substrate in close proximity to the reactive E2~Ubiquitin thioester bond.
2. In the "HECT" E3 ubiquitin ligases, the ubiquitin is first transferred to a conserved cysteine of the E3 before the final transfer to a substrate group.
3. In addition to substrate recognition, other roles for E3s are in the allosteric activation of the E2.

There are various types of E3 ubiquitin-ligase:

1. The HECT domain proteins are found in eukaryotes from yeast to humans and are characterized by the presence of a 350 amino acid HECT domain. In this class of ubiquitin ligases, the N-terminus confers the ability to bind the substrate and the C-terminal HECT domain serves to directly transfer ubiquitin from a thioester linkage to the substrate. The HECT domain proteins were originally identified in E6-AP, a cellular ubiquitin ligase recruited by the human papilloma virus E6 oncoprotein to induce degradation of the p53 tumor suppressor.
2. The RING E3s display a series of histidine and cysteine residues with a characteristic spacing that allows for the coordination of two zinc ions in a cross-brace structure called the RING finger.
    A. The single-subunit RING E3s consists of just the RING finger protein. The E2 enzyme can directly bind to the RING finger protein and the E3 might directly bind to the substrate.
    B. The multisubunit RING E3s consists of several proteins in addition to the RING protein. The two main types of multi-subunit RING E3 are the Anaphase Promoting Complex (APC) and Cullin-RING superfamily of ubiquitin ligase that associate with the Roc1/Rbx1/Hrt1 RING protein. The APC in humans and yeast contain at least 11 components. Apc11 is the RING finger protein and in conjuction with Ubc4 displays core ligase activity (Hochstrasser, 2006; Jackson et al., 2000; Pickart, 2001).

<u>The objective of this research is to understand the functions of a sub-class of Cullin-RING ubiquitin ligase containing the cullin CUL-2</u>

Cullin-RING superfamily of ubiquitin ligase

Ethylmethanesulfonate mutagenesis screen for genes exhibiting hyperplasia in *C. elegans* resulted in the isolation of two independent alleles of *cul-1*. Kipreos et al. 1996 cloned this gene and discovered a novel family of proteins called cullins. Searches of the Expressed Sequence Tag database revealed the presence of three cullin paralogs in yeast, five in *C. elegans* and six in humans (Kipreos et al., 1996). The yeast ortholog of *cul-1, cdc53* was identified by two research groups as a protein that associates with the S-phase cyclin, Cln2 and in a temperature sensitive screen for mutants that resemble Cdc34 (E2) mutants. The fact that Cdc53 is required for Cln2 ubiquitination and co-immunoprecipitated with the ubiquitin conjugating enzyme Cdc34, led these groups to believe that Cdc53 is an E3 ubiquitin-ligase (Mathias et al., 1996; Willems et al., 1996).

The crystal structure of the human Cul1 complex also known as the Skp1-Cullin-F-Box (SCF) complex was elucidated (Zheng et al., 2002) (Figure. 2.2). Cul1 is a stalk like protein that serves as a scaffold to bring in close proximity all the components necessary for substrate ubiquitination. The N terminus of Cul1 interacts with Skp1 while the C terminus interacts with Rbx1. Skp1 and Rbx1 associate with the substrate binding component, an F-box protein and the E2 ubiquitin conjugating enzyme, respectively (Zheng et al., 2002). All cullin members, CUL1 through CUL5 are post-translationally modified by a ubiquitin like protein called NEDD8 at the C-terminus (Hori et al., 1999). Cullins are regulated by neddylation and deneddylation. In the deneddylated state the cullins are bound to a horseshoe-shaped protein called CAND1. The central elongated region of CUL-1 interacts with CAND1 and contacts are also made with the N and C terminus of the cullin. In the CAND1-bound this state CUL1 is not able to bind the SKP1 adaptor (Goldenberg et al., 2004).

Based upon the nature of the F-box protein employed, the SCF complexes are variously named, e.g., SCF^{Grr1}, whereby Grr1 is the F-box protein targeting the substrate Cln-2 for ubiquitination. Similarly SCF^{Cdc4} targets Sic1 the S phase inhibitor; $SCF^{\beta TrCp}$ targets IkBα, and so on. A partial list of substrates and their substrate recognition subunits in various organisms is given in the following review article (Deshaies, 1999).

The other members of the cullin family are predicted to have a similar structure to CUL1; indeed CUL4A, a paralogue of CUL1, adopts a CUL1-like structure (Angers et al., 2006) (Figure. 2.2). All cullin family members interact with the RING finger proteins Rbx1/ROC1 or Rbx-2/ROC2 at their C-terminus (Ohta et al., 1999). Substrates are recruited to the N-terminal domains of cullins through substrate recongnition subunits that bind the adaptors. CUL2 interacts with adaptor Elongin C which is a SKP1 like protein. CUL3 interacts with BTB domain containing proteins that has the properties of an adaptor as well as the substrate recognition subunit and CUL4 with the β propeller domain of DDB1. The cullin binding domain of Skp1, Elongin C, and BTB proteins share structural homology, however this domain is absent in DDB1 (Angers et al., 2006; Petroski and Deshaies, 2005).

The mammalian CUL-2 ubiquitin ligase complex

The CUL-2 based ubiquitin ligase complex consists of the adaptor Elongin C, a ubiquitin-like protein Elongin B and Rbx1 (Figure. 2.2). Elongin C is a Skp-1 related protein that binds to the N-terminus of CUL-2 in combination with Elongin B. Elongin C binds to substrate recognition subunit (SRS) through a sequence motif on the SRS that has been variously called the BC-box, VHL-box or SOCS-box (Kamura et al., 2004; Pause et al., 1999). The CUL-2-Elongin BC^{VHL} (CBC^{VHL}) complex has been the most intensively studied CBC complex. VHL was the first

reported SRS for CUL2 that targets the substrate hypoxia inducible transcription factor Hif1α for degradation by the proteosome under normal oxygen levels (Maxwell et al., 1999). The interaction of Elongin C with VHL depends on the presence of a ten amino acid degenerate sequence motif called the BC box that lies within the α domain of VHL (Ohh et al., 1999; Stebbins et al., 1999). The α domain of VHL composed of three α-helices (H1, H2 and H3) and the BC box lies in the H1 helix of VHL. The BC box makes extensive contact with Elongin C and mutations in this region abolish interaction of VHL with Elongin C. The α domain of VHL which is referred to as the VHL box, is structurally and functionally homologous to the SOCS box, and several SOCS box containing proteins can bind Elongin BC (Kamura et al., 2004; Stebbins et al., 1999). However, it has recently been shown that SOCS-box proteins bind Elongin C in CUL-5 complexes while the distinct motif called the VHL-box mediates binding to Elongin C in CUL2 complexes. Mammalian SRSs for the CBC complex that contain domains homologous to the VHL or SOCS box are mMED8, LRR-1 and FEM1B (Kamura et al., 2004).

In this study we have identified ZYG-11 family members as SRSs for CUL-2 and demonstrate that mutations in the VHL box disrupts the interaction of ZYG-11 with Elongin C (Vasudevan et al., 2007).

Cullin functions in *C. elegans*

CUL-1

In *C. elegans,* lack of the *cul-1* gene causes hyperplasia in all larval tissues. Excess cells are observed in the ectoderm, mesoderm, endoderm, and the germline indicating a requirement for CUL-1 in cell cycle exit (Kipreos et al., 1996). CUL-1 also has additional roles in the regulation of life span and the nervous system of *C. elegans* (Ding et al., 2007; Fielenbach et al., 2007).

CUL-3

A CUL-3 ubiquitin-ligase employs the BTB domain containing protein MEL-26 as the substrate binding component and degrades MEI-1, a katanin like protein associated with the *C. elegans* meiotic spindle. CUL-3 degrades MEI-1 at the meiosis to mitosis transition. MEI-1 decorates the polar ends of the microtubule and the meiotic chromatin. The microtubule severing activity of MEI-1 is required for meiotic spindle organization in *C. elegans.* In *cul-3 (RNAi)* animals or in animals expressing a non-degradable form of MEI-1, the MEI-1 protein is incorporated into the mitotic spindle, leading to defects in mitotic spindle positioning, elongation, and cytokinesis (Pintard et al., 2003; Srayko et al., 2000).

CUL-4

The CUL-4/DDB-1 E3 complex has been implicated in maintaining genome stability by degrading the DNA-replication licensing factor CDT-1. Inactivation of CUL-4 causes massive DNA- re-replication in *C. elegans* producing seam cells with upto 100C DNA content (Kim and Kipreos, 2007; Zhong et al., 2003). CUL-4 also maintains genome stability by exporting the replication licensing factor CDC-6 after origin firing. In CUL-4 mutants, CDC-6 export from the nucleus is not observed and this phenomenon is thought be an additional factor contributing to DNA rereplication (Kim et al., 2007).

CUL-5 and CUL-6

Loss of *cul-5* and *cul-6* do not lead to defects in growth and development in *C. elegans*, however they are required to prevent spontaneous mutations in the germline (Kamath et al., 2003; Pothof et al., 2003).

CUL-2

The goal of this report is to understand the functions of CUL-2 in *C. elegans*. *cul-2* homozygous progeny have normal embryonic and post embryonic somatic divisions. However, *cul-2* mutant worms have fewer and larger germ cells than wild type. The progeny of *cul-2* homozygous hermpaphrodites arrest development at approximately the 24 cell stage with lengthened mitosis, defects in mitotic chromosome condensation and cytoskeletal organization (Feng et al., 1999). CUL-2 is also required to promote meiotic anaphase II, proper placement of the anterior-posterior axis, Cyclin B degradation, degradation of CCCH-finger polarity proteins and sex determination (DeRenzo et al., 2003; Liu et al., 2004; Starostina et al., 2007). *cul-2* mutant males are feminized in that they produce oocyte like cells and an incomplete male tail due to high levels of TRA-1 (Starostina et al., 2007).

ZIF-1, has been identified as a substrate recognition subunit and is required for the degradation of CCCH polarity proteins, while FEM-1 degrades the inhibitor of male development TRA-1 (DeRenzo et al., 2003; Starostina et al., 2007). The SRSs for the CBC complex that are responsible for most of the known *cul-2* phenotypes had not been identified.

In this study we have identified ZYG-11 as the substrate recognition subunit required for the execution of meiosis II, proper establishment of anterior-posterior polarity, degradation of cyclin B1 in the zygote and maintainance of a proper cytoplasm.

Meiosis

Meiosis is a specialized form of cell division whereby sexually reproducing organisms reduce their chromosome number while generating gametes. Meiosis consists of one round of DNA

replication followed by two rounds of chromosome segregation with no intervening DNA replication (Figure 2.3).

After premeiotic S phase, prophase begins with leptotene, which marks the condensation of chromosomes and the formation of axial elements between sister chromatids, followed by zygotene whereby the formation of the synaptonemal complex (SC) is initiated between homologs; pachytene signifies the completion of synaptonemal complex and the formation of mature bivalent. During the diplotene/diakinesis stage, the SC is disassembled and the chiasmata that began to form during zygotene becomes evident. The chiasmata is formed as a result of reciprocal exchange of strands between the sister chromatids of homologous chromosomes. The reciprocal exchanges are created by the double stranded break repair model of meiotic recombination. After diakinesis, the chromosomes complete two rounds of reductional division whereby the chromosome number is reduced from 4n to 1n (Petronczki et al., 2003).

The oocytes in animals are arrested in prophase I. Upon receiving the maturation signal they are released from the prophase arrest and proceed to meiotic maturation. A second arrest is observed at a later stage that is released upon fertilization. However, the second stage of arrest differs from one species to the other. In humans, oocytes enter meiosis during fetal development and arrest in prophase I. Resumption of meiosis and completion of the first division occurs years later in the ovary just before ovulation. After completion of MI, the oocytes arrest again at metaphase of MII and the second division is completed only after the egg is fertilized. The second arrest occurs during metaphase I in invertebrates, during metaphase II in most vertebrates including frog and mouse, and at G1 phase after meiosis II in starfish and sea urchins. In the nematode *C. elegans,* the growing oocytes are arrested in the pachytene stage of prophase I. Upon entering diakinesis, they are fertilized resulting in the release of the prophase I arrest and

completion of two consecutive rounds of chromosome segregation (Kishimoto, 2003; Page and Orr-Weaver, 1997). While the basic process of reducing chromosome number during meiosis remains conserved, the stages of arrest during oocyte growth and maturation and the mechanisms of chromosome segregation are different among species.

Molecular mechanism of chromosome segregation

As cells exit from mitotic cell division, the sister chromatids lose cohesion and separate to opposite poles of the dividing cell resulting in equal chromosome segregation. In contrast, the reductional segregation of the first stage of meiotic cell division (meiosis I) requires that sister chromatids remain associated through their centromeres and move together to the same pole. Centromeric cohesion is lost as cells exit from meiosis II resulting in the separation of sister chromatids (Figure 2.3).

Cohesins are chromosomal proteins that prevent premature separation of sister chromatids. In *S. cerevisiae* separation of sister chromatids at the metaphase to anaphase transition is promoted by the Anaphase Promoting Complex (Irniger et al., 1995). In order to identify proteins required for sister chromatid cohesion, Michaelis et al. 1997 screened for mutants that separate sister chromatids in the absence of APC function. They describe three proteins, Scc1, Smc1 and Smc3 whose absence causes premature separation of sister chromatids (Michaelis et al., 1997). The cohesin complex consists of at least four subunits Scc1, Scc3, Smc1 and Smc3 that assemble to form a ring like structure. It has been suggested that the cohesins may hold the sister chromatids together by entrapping them at the center of the ring (Gruber et al., 2003). A similar cohesin complex containing XSMC1, XSMC3 and p120 (Xenopus homolog of budding yeast Scc1) has been identified in *X. laevis* (Losada et al., 1998). The *S. cerevisiae* Scc1

is an unstable protein that is absent in G1 cells, accumulates during S, G2 and metaphase and declines during anaphase. It associates with chromosomes during S phase and dissociates at the metaphase to anaphase transition (Michaelis et al., 1997). Uhlmann et al. 1999 propose that sister chromatid separation in yeast is triggered by the sudden cleavage of Scc1, dependent on the activity of the protease Esp1 separase (Uhlmann et al., 1999). Esp1 forms a stable complex with the anaphase inhibitor Pds1 also known as securin. The Anaphase Promoting Complex promotes sister chromatid separation by destroying Pds1 (securin) and thus liberating the separase Esp1 (Ciosk et al., 1998).

The Rec8 protein of the fission yeast *Schizosaccharomyces pombe* bears significant homology to cohesins and is expressed only during meiosis. Rec8 appears on centromeres and adjacent chromosome arms during premeiotic S phase. The centromeric Rec8 persists throughout meiosis I and disappears at anaphase of meiosis II. In the absence of the Rec8 protein, the chromosomes undergo equational chromosomal segregation instead of reductional division (Watanabe and Nurse, 1999). In *esp 1-2* (separase) mutants or yeast cells expressing non cleavable form of Rec8, dissociation of Rec8 from chromosome arms, chiasmata resolution and loss of sister chromatid cohesion are abolished (Ciosk et al., 1998). It has been hypothesized that cohesion between sister chromatids distal to chiasmata is responsible for holding homologous chromosomes together while the cohesion at the centromere that is protected during meiosis I is responsible for holding sister chromatids until anaphase II. The *C. elegans* meiotic chromosomes are holocentric. In *C. elegans*, Rec8 localizes to chromosome arms during meiosis I, and between sister chromatids during meiosis II (Pasierbek et al., 2001). This leads to the next obvious question as to what protects the centromeric cohesin from separin during meiosis I. Kitajima et al. have identified a meiosis-specific protein Sgo1 in fission yeast that protects

centromeric Rec8 from degradation during meiosis I (Kitajima et al., 2004). In *C. elegans*, loss of separase or the components of the Anaphase Promoting Complex causes a metaphase arrest during meiosis I. However, loss of Rec8 by RNAi does not bypass the metaphase I arrest indicating that there might be additional substrates of the APC required for meiosis I exit (Davis et al., 2002; Siomos et al., 2001).

In *Drosophila*, the cell cycle mutants *grauzone* and *cortex* are arrested in metaphase of meiosis II (Page and Orr-Weaver, 1996). It was subsequently found that cortex is a member of the Cdc20/Fizzy family (the activator of APC), and *grauzone* is the transcriptional activator for cortex (Chu et al., 2001; Harms et al., 2000). In this work, we show that *cul-2* zygotes complete meiosis I with normal chromosome dynamics approximately 15 minutes post-fertilization similar to wild type. Meiosis II is lengthened and takes an average of 50 to 60 minutes in *cul-2* zygotes as compared to 15 minutes in wild type. The meiosis II delay in *cul-2* zygotes is due to a failure of the chromosomes to segregate at the metaphase to anaphase transition. In *cul-2* zygotes, the chromosomes separate at the metaphase to anaphase transition as observed by the disappearance of the cohesin Rec8 but are not able to move the chromosomes apart that is characteristic of anaphase (Liu et al., 2004).

This is the first demonstration of a ubiquitin ligase other than the Anaphase Promoting Complex that is involved in chromosome segregation during meiosis. It also demonstrates that the two meiotic stages are differentially regulated.

The Spindle

The accurate segregation of chromosomes during both mitosis and meiosis is essential for the propagation of cells and species. Segregation errors during mitosis leads to the development of

cancer while errors in meiosis cause birth defects. A complex protein superstructure called the spindle mediates chromosome segregation. The primary function of the spindle is the equal segregation of sister chromatids during cell division. In animal cells, the bipolar mitotic spindle is characterized by the presence of two centrosomes. The two chromosomes are captured by microtubules between the two centrosome-nucleated mitotic asters. A subset of specialized cell types undergo cell division in the absence of conventional centrosomes using the chromatin-driven spindle assembly pathway. These include plant cells during mitosis and oocytes in many animal species (Compton, 2000).

In most species, microtubules interact with localized regions of the chromosome called kinetochores, while in other species the kinetochore extends along the entire length of the mitotic chromosome rather than a single centromere region located at the primary constriction of monocentric chromosomes. In *C. elegans,* the chromosomes are holocentric and the microtubules interact with the chromosome along the entire axis of the chromosome. The *C. elegans* female meiotic spindle is acentriolar and assumes an elongated pointed morphology upon fertilization. As the chromosomes congress to form a pentagonal array the spindle assumes a barrel shape. Prior to chromosome separation the barrel shaped spindle shrinks in size and at anaphase the microtubules are observed between the separating pieces of DNA appearing to push them apart (Albertson and Thomson, 1993). The spindle dynamics also differ among the various organisms. In mice, the chromosomes contain a centromere and at metaphase the chromosomes are positioned equidistantly between the poles of a barrel-shaped MI spindle. The anaphase configuration can be observed as two groups of chromosomes moving to opposite poles and formation of a dark spindle midzone. This suggests that in mouse oocytes the chromosomes are pulled apart at anaphase (Woods et al., 1999). In *cul-2* and *zyg-11* zygotes, the characteristic

anaphase II figures are never observed (i.e. microtubules fail to polymerize between the separating pieces of DNA) and the meiotic spindle remains in the barrel shaped metaphase configuration for an extended period of time (Liu et al., 2004). This indicates that *cul-2* and *zyg-11* are required to reorganize the meiotic spindle at the metaphase II to anaphase II transition.

Establishment of Polarity in *C. elegans*

Development of the anterior-posterior axis in the *C. elegans* zygote is one of the best-studied examples of polarity (Figure 2.4). *C. elegans* oocytes do not have any predetermined polarity. As the mature oocyte passes through the spermatheca it is fertilized by the sperm and completes two rounds of meiosis. The sperm DNA that remains condensed until the completion of maternal meiosis now decondenses to form the sperm pronucleus at the posterior. During the same time frame, the oocyte DNA that has completed the meiotic divisions decondenses at the anterior. After completion of meiosis, the centrosomes brought in by the sperm organize large microtubule asters and the oocyte pronucleus migrates to meet the sperm pronucleus at the posterior. The two pronuclei meet in the posterior and then migrate to the center of the embryo. The nuclear membrane of the fused pronuclei breaks down and the embryo enters the first mitotic cycle. The first division gives rise to two daughter cells of different size: a large anterior cell, AB and a small posterior cell P1.

In the oocyte, and early zygotes undergoing meiosis, a group of proteins that are critical for overall polarity are distributed uniformly. At the two-cell stage, PAR-1, a serine-threonine kinase and PAR-2, a RING finger protein, localizes to the posterior cortex of P1. PAR-3 and PAR-6 that contain PDZ domains and PKC-3, an atypical protein kinase C localize reciprocally at the anterior cortex in the AB cell. The first manifestations of polarity are observed roughly 30

minutes after fertilization whereby PAR-2 localizes to the cortex near the sperm pronucleus (Nance, 2005). Wallenfang and Seydoux have demonstrated that a microtubule – organizing center is necessary and sufficient to establish several aspects of A/P polarity (Wallenfang and Seydoux, 2000). In wild-type embryos nucleation of microtubules by sperm derived microtubules expels the PAR-3/6/PKC-3 on the posterior cortex and allows PAR-2 to accumulate there during the "establishment" phase (i.e. after completion of meiosis during pronuclei formation). During the "maintenance" phase that occurs after pronuclei meeting, PAR-2 prevents PAR-3/6/PKC-3 from re-entering the posterior domain (Cuenca et al., 2003). Anaphase Promoting Complex mutants are arrested in metaphase of meiosis I and the sperm asters never form. In such mutants, posterior is defined by the persistent meiotic spindle and a reversal of localization of all polarity determinants are seen (Wallenfang and Seydoux, 2000).

We observe a similar situation with *cul-2* and *zyg-11* zygotes. PAR-1 and PAR-2 are observed near the perduring meiotic spindle whereas PAR-3 and PAR-6 are observed at the posterior cortex (Liu et al., 2004; Sonneville and Gonczy, 2004). When we remove the meiotic spindle in *cul-2* zygotes by tubulin RNAi, we observe a small percentage of zygotes where PAR-2 has localized on the cortex away from any microtubule structures.

These results suggest that during meiosis CUL-2 restrains PAR-2 from localizing to the cortex (Liu et al., 2004; Nance, 2005). This study also aims to understand the regulation of polarity between the fertilization and "establishment" phases in *C. elegans* zygotes.

Role of Cyclin B1 in meiotic progression

High levels of CDK1/Cyclin B1 activity prevents sister chromatid separation and segregation in *Xenopus* extracts (Stemmann et al., 2001). To determine if the separation of homologous

chromosomes was inhibited by non-degradable cyclin B1, a destruction box (D box)-truncated form of cyclin B1- GFP mRNA was injected into mouse oocytes. The D-box is required for the degradation of cyclin B1 and timelapse fluorescence measurements demonstrated that the D-box truncated form of cyclin B1-GFP was stable in MI oocytes. In oocytes that were injected with stable cyclin B1 both polar body formation as well as homologue disjunction were inhibited (Herbert et al., 2003). Thus cyclin B1 needs to be degraded to promote homologue disjunction in mice. The behavior of cyclin B1 in *C. elegans* was not understood. In this study we show that maternal cyclin B1 is expressed in oocytes, zygotes and localizes to the meiotic spindle. Cyclin B1 is rapidly degraded during meiosis and by the time of pronuclear formation it completely disappears. We also observe that cyclin B1 RNAi partially suppresses the meiosis II delay in *cul-2* mutants (Liu et al., 2004).

REFERENCES

Albertson, D.G., and Thomson, J.N. (1993). Segregation of holocentric chromosomes at meiosis in the nematode, Caenorhabditis elegans. Chromosome Res *1*, 15-26.

Angers, S., Li, T., Yi, X., MacCoss, M.J., Moon, R.T., and Zheng, N. (2006). Molecular architecture and assembly of the DDB1-CUL4A ubiquitin ligase machinery. Nature *443*, 590-593.

Chen, Z.J. (2005). Ubiquitin signalling in the NF-kappaB pathway. Nature cell biology *7*, 758-765.

Chu, T., Henrion, G., Haegeli, V., and Strickland, S. (2001). Cortex, a Drosophila gene required to complete oocyte meiosis, is a member of the Cdc20/fizzy protein family. Genesis *29*, 141-152.

Ciosk, R., Zachariae, W., Michaelis, C., Shevchenko, A., Mann, M., and Nasmyth, K. (1998). An ESP1/PDS1 complex regulates loss of sister chromatid cohesion at the metaphase to anaphase transition in yeast. Cell *93*, 1067-1076.

Compton, D.A. (2000). Spindle assembly in animal cells. Annual review of biochemistry *69*, 95-114.

Cuenca, A.A., Schetter, A., Aceto, D., Kemphues, K., and Seydoux, G. (2003). Polarization of the C. elegans zygote proceeds via distinct establishment and maintenance phases. Development (Cambridge, England) *130*, 1255-1265.

Davis, E.S., Wille, L., Chestnut, B.A., Sadler, P.L., Shakes, D.C., and Golden, A. (2002). Multiple subunits of the Caenorhabditis elegans anaphase-promoting complex are required for chromosome segregation during meiosis I. Genetics *160*, 805-813.

DeRenzo, C., Reese, K.J., and Seydoux, G. (2003). Exclusion of germ plasm proteins from somatic lineages by cullin-dependent degradation. Nature *424*, 685-689.

DeRenzo, C., and Seydoux, G. (2004). A clean start: degradation of maternal proteins at the oocyte-to-embryo transition. Trends in cell biology *14*, 420-426.

Deshaies, R.J. (1999). SCF and Cullin/Ring H2-based ubiquitin ligases. Annu Rev Cell Dev Biol *15*, 435-467.

Ding, M., Chao, D., Wang, G., and Shen, K. (2007). Spatial regulation of an E3 ubiquitin ligase directs selective synapse elimination. Science (New York, NY *317*, 947-951.

Feng, H., Zhong, W., Punkosdy, G., Gu, S., Zhou, L., Seabolt, E.K., and Kipreos, E.T. (1999). CUL-2 is required for the G1-to-S-phase transition and mitotic chromosome condensation in Caenorhabditis elegans. Nature cell biology *1*, 486-492.

Fielenbach, N., Guardavaccaro, D., Neubert, K., Chan, T., Li, D., Feng, Q., Hutter, H., Pagano, M., and Antebi, A. (2007). DRE-1: an evolutionarily conserved F box protein that regulates C. elegans developmental age. Developmental cell *12*, 443-455.

Goldenberg, S.J., Cascio, T.C., Shumway, S.D., Garbutt, K.C., Liu, J., Xiong, Y., and Zheng, N. (2004). Structure of the Cand1-Cul1-Roc1 complex reveals regulatory mechanisms for the assembly of the multisubunit cullin-dependent ubiquitin ligases. Cell *119*, 517-528.

Gruber, S., Haering, C.H., and Nasmyth, K. (2003). Chromosomal cohesin forms a ring. Cell *112*, 765-777.

Hampton, R.Y. (2002). ER-associated degradation in protein quality control and cellular regulation. Current opinion in cell biology *14*, 476-482.

Harms, E., Chu, T., Henrion, G., and Strickland, S. (2000). The only function of Grauzone required for Drosophila oocyte meiosis is transcriptional activation of the cortex gene. Genetics *155*, 1831-1839.

Herbert, M., Levasseur, M., Homer, H., Yallop, K., Murdoch, A., and McDougall, A. (2003). Homologue disjunction in mouse oocytes requires proteolysis of securin and cyclin B1. Nature cell biology *5*, 1023-1025.

Hershko, A. (1983). Ubiquitin: roles in protein modification and breakdown. Cell *34*, 11-12.

Hochstrasser, M. (2006). Lingering mysteries of ubiquitin-chain assembly. Cell *124*, 27-34.

Hori, T., Osaka, F., Chiba, T., Miyamoto, C., Okabayashi, K., Shimbara, N., Kato, S., and Tanaka, K. (1999). Covalent modification of all members of human cullin family proteins by NEDD8. Oncogene *18*, 6829-6834.

Irniger, S., Piatti, S., Michaelis, C., and Nasmyth, K. (1995). Genes involved in sister chromatid separation are needed for B-type cyclin proteolysis in budding yeast. Cell *81*, 269-278.

Jackson, P.K., Eldridge, A.G., Freed, E., Furstenthal, L., Hsu, J.Y., Kaiser, B.K., and Reimann, J.D. (2000). The lore of the RINGs: substrate recognition and catalysis by ubiquitin ligases. Trends in cell biology *10*, 429-439.

Jesenberger, V., and Jentsch, S. (2002). Deadly encounter: ubiquitin meets apoptosis. Nature reviews *3*, 112-121.

Kamath, R.S., Fraser, A.G., Dong, Y., Poulin, G., Durbin, R., Gotta, M., Kanapin, A., Le Bot, N., Moreno, S., Sohrmann, M., *et al.* (2003). Systematic functional analysis of the Caenorhabditis elegans genome using RNAi. Nature *421*, 231-237.

Kamura, T., Maenaka, K., Kotoshiba, S., Matsumoto, M., Kohda, D., Conaway, R.C., Conaway, J.W., and Nakayama, K.I. (2004). VHL-box and SOCS-box domains determine binding specificity for Cul2-Rbx1 and Cul5-Rbx2 modules of ubiquitin ligases. Genes & development *18*, 3055-3065.

Kim, J., Feng, H., and Kipreos, E.T. (2007). C. elegans CUL-4 prevents rereplication by promoting the nuclear export of CDC-6 via a CKI-1-dependent pathway. Curr Biol *17*, 966-972.

Kim, Y., and Kipreos, E.T. (2007). The Caenorhabditis elegans Replication Licensing Factor CDT-1 Is Targeted for Degradation by the CUL-4/DDB-1 Complex. Mol Cell Biol *27*, 1394-1406.

Kipreos, E.T. (2005). Ubiquitin-mediated pathways in C. elegans. The C elegans Research Community WormBook, 1551-8507.

Kipreos, E.T., Lander, L.E., Wing, J.P., He, W.W., and Hedgecock, E.M. (1996). cul-1 is required for cell cycle exit in C. elegans and identifies a novel gene family. Cell *85*, 829-839.

Kishimoto, T. (2003). Cell-cycle control during meiotic maturation. Current opinion in cell biology *15*, 654-663.

Kitajima, T.S., Kawashima, S.A., and Watanabe, Y. (2004). The conserved kinetochore protein shugoshin protects centromeric cohesion during meiosis. Nature *427*, 510-517.

Korhonen, L., and Lindholm, D. (2004). The ubiquitin proteasome system in synaptic and axonal degeneration: a new twist to an old cycle. The Journal of cell biology *165*, 27-30.

Liu, J., Vasudevan, S., and Kipreos, E.T. (2004). CUL-2 and ZYG-11 promote meiotic anaphase II and the proper placement of the anterior-posterior axis in C. elegans. Development (Cambridge, England) *131*, 3513-3525.

Lord, J.M., Roberts, L.M., and Stirling, C.J. (2005). Quality control: another player joins the ERAD cast. Curr Biol *15*, R963-964.

Losada, A., Hirano, M., and Hirano, T. (1998). Identification of Xenopus SMC protein complexes required for sister chromatid cohesion. Genes & development *12*, 1986-1997.

Mathias, N., Johnson, S.L., Winey, M., Adams, A.E., Goetsch, L., Pringle, J.R., Byers, B., and Goebl, M.G. (1996). Cdc53p acts in concert with Cdc4p and Cdc34p to control the G1-to-S-phase transition and identifies a conserved family of proteins. Mol Cell Biol *16*, 6634-6643.

Maxwell, P.H., Wiesener, M.S., Chang, G.W., Clifford, S.C., Vaux, E.C., Cockman, M.E., Wykoff, C.C., Pugh, C.W., Maher, E.R., and Ratcliffe, P.J. (1999). The tumour suppressor protein VHL targets hypoxia-inducible factors for oxygen-dependent proteolysis. Nature *399*, 271-275.

Michaelis, C., Ciosk, R., and Nasmyth, K. (1997). Cohesins: chromosomal proteins that prevent premature separation of sister chromatids. Cell *91*, 35-45.

Nance, J. (2005). PAR proteins and the establishment of cell polarity during C. elegans development. Bioessays *27*, 126-135.

Ohh, M., Takagi, Y., Aso, T., Stebbins, C.E., Pavletich, N.P., Zbar, B., Conaway, R.C., Conaway, J.W., and Kaelin, W.G., Jr. (1999). Synthetic peptides define critical contacts between elongin C, elongin B, and the von Hippel-Lindau protein. The Journal of clinical investigation *104*, 1583-1591.

Ohta, T., Michel, J.J., Schottelius, A.J., and Xiong, Y. (1999). ROC1, a homolog of APC11, represents a family of cullin partners with an associated ubiquitin ligase activity. Molecular cell *3*, 535-541.

Page, A.W., and Orr-Weaver, T.L. (1996). The Drosophila genes grauzone and cortex are necessary for proper female meiosis. Journal of cell science *109 (Pt 7)*, 1707-1715.

Page, A.W., and Orr-Weaver, T.L. (1997). Stopping and starting the meiotic cell cycle. Current opinion in genetics & development *7*, 23-31.

Pasierbek, P., Jantsch, M., Melcher, M., Schleiffer, A., Schweizer, D., and Loidl, J. (2001). A Caenorhabditis elegans cohesion protein with functions in meiotic chromosome pairing and disjunction. Genes & development *15*, 1349-1360.

Pause, A., Peterson, B., Schaffar, G., Stearman, R., and Klausner, R.D. (1999). Studying interactions of four proteins in the yeast two-hybrid system: structural resemblance of the pVHL/elongin BC/hCUL-2 complex with the ubiquitin ligase complex SKP1/cullin/F-box protein. Proceedings of the National Academy of Sciences of the United States of America *96*, 9533-9538.

Peters, J.M. (2002). The anaphase-promoting complex: proteolysis in mitosis and beyond. Molecular cell *9*, 931-943.

Petronczki, M., Siomos, M.F., and Nasmyth, K. (2003). Un menage a quatre: the molecular biology of chromosome segregation in meiosis. Cell *112*, 423-440.

Petroski, M.D., and Deshaies, R.J. (2005). Function and regulation of cullin-RING ubiquitin ligases. Nature reviews *6*, 9-20.

Pickart, C.M. (2001). Mechanisms underlying ubiquitination. Annual review of biochemistry *70*, 503-533.

Pickart, C.M., and Cohen, R.E. (2004). Proteasomes and their kin: proteases in the machine age. Nature reviews *5*, 177-187.

Pintard, L., Willis, J.H., Willems, A., Johnson, J.L., Srayko, M., Kurz, T., Glaser, S., Mains, P.E., Tyers, M., Bowerman, B., *et al.* (2003). The BTB protein MEL-26 is a substrate-specific adaptor of the CUL-3 ubiquitin-ligase. Nature *425*, 311-316.

Pothof, J., van Haaften, G., Thijssen, K., Kamath, R.S., Fraser, A.G., Ahringer, J., Plasterk, R.H., and Tijsterman, M. (2003). Identification of genes that protect the C. elegans genome against mutations by genome-wide RNAi. Genes & development *17*, 443-448.

Rock, K.L., and Goldberg, A.L. (1999). Degradation of cell proteins and the generation of MHC class I-presented peptides. Annual review of immunology *17*, 739-779.

Siomos, M.F., Badrinath, A., Pasierbek, P., Livingstone, D., White, J., Glotzer, M., and Nasmyth, K. (2001). Separase is required for chromosome segregation during meiosis I in Caenorhabditis elegans. Curr Biol *11*, 1825-1835.

Sonneville, R., and Gonczy, P. (2004). Zyg-11 and cul-2 regulate progression through meiosis II and polarity establishment in C. elegans. Development (Cambridge, England) *131*, 3527-3543.

Srayko, M., Buster, D.W., Bazirgan, O.A., McNally, F.J., and Mains, P.E. (2000). MEI-1/MEI-2 katanin-like microtubule severing activity is required for Caenorhabditis elegans meiosis. Genes & development *14*, 1072-1084.

Starostina, N.G., Lim, J.M., Schvarzstein, M., Wells, L., Spence, A.M., and Kipreos, E.T. (2007). A CUL-2 ubiquitin ligase containing three FEM proteins degrades TRA-1 to regulate C. elegans sex determination. Developmental cell *13*, 127-139.

Stebbins, C.E., Kaelin, W.G., Jr., and Pavletich, N.P. (1999). Structure of the VHL-ElonginC-ElonginB complex: implications for VHL tumor suppressor function. Science (New York, NY *284*, 455-461.

Stemmann, O., Zou, H., Gerber, S.A., Gygi, S.P., and Kirschner, M.W. (2001). Dual inhibition of sister chromatid separation at metaphase. Cell *107*, 715-726.

Uhlmann, F., Lottspeich, F., and Nasmyth, K. (1999). Sister-chromatid separation at anaphase onset is promoted by cleavage of the cohesin subunit Scc1. Nature *400*, 37-42.

Vasudevan, S., Starostina, N.G., and Kipreos, E.T. (2007). The Caenorhabditis elegans cell-cycle regulator ZYG-11 defines a conserved family of CUL-2 complex components. EMBO reports *8*, 279-286.

Wallenfang, M.R., and Seydoux, G. (2000). Polarization of the anterior-posterior axis of C. elegans is a microtubule-directed process. Nature *408*, 89-92.

Watanabe, Y., and Nurse, P. (1999). Cohesin Rec8 is required for reductional chromosome segregation at meiosis. Nature *400*, 461-464.

Willems, A.R., Lanker, S., Patton, E.E., Craig, K.L., Nason, T.F., Mathias, N., Kobayashi, R., Wittenberg, C., and Tyers, M. (1996). Cdc53 targets phosphorylated G1 cyclins for degradation by the ubiquitin proteolytic pathway. Cell *86*, 453-463.

Woods, L.M., Hodges, C.A., Baart, E., Baker, S.M., Liskay, M., and Hunt, P.A. (1999). Chromosomal influence on meiotic spindle assembly: abnormal meiosis I in female Mlh1 mutant mice. The Journal of cell biology *145*, 1395-1406.

Zheng, N., Schulman, B.A., Song, L., Miller, J.J., Jeffrey, P.D., Wang, P., Chu, C., Koepp, D.M., Elledge, S.J., Pagano, M., *et al.* (2002). Structure of the Cul1-Rbx1-Skp1-F boxSkp2 SCF ubiquitin ligase complex. Nature *416*, 703-709.

Zhong, W., Feng, H., Santiago, F.E., and Kipreos, E.T. (2003). CUL-4 ubiquitin ligase maintains genome stability by restraining DNA-replication licensing. Nature *423*, 885-889.

FIGURE LEGENDS

Figure 2.1. Schematic representation of the ubiquitin proteosome system.

Ubiquitin is activated in two steps: It is first adenylated then attacked by a cysteine side chain to form a thioester bond with E1. The activated ubiquitin then forms a thioesterbond with E2. The ubiquitin is passed from the E2 to a substrate lysine residue in the presence of an E3 ligase. Once a polyubiquitin chain is synthesized on the protein susbstrate, it is hydrolysed to peptides by the 26S proteosome and the ubiquitin molecues are recycled.

Figure 2.2. Structures of the Cullin-RING ligases.

All cullin members bind to the RING finger protein at the C-terminus. At the N terminus CUL1 binds the adaptors Skp1, CUL2 and CUL5 binds the Elongin C/ElonginB complex, CUL3 binds the BTB domain protein while CUL4 binds DDB1. The substrate reconginition subunits (SRS) for CUL1 binds SKP1, the SRSs for CUL2 and CUL5 bind Elongin C through the VHL and SOCS box respectively. For the ubiquitin ligase CUL3, the BTB domain protein serves as the adaptor as well as the substrate recognition subunit. For the CUL4 protein it is not clear whether DDB-1 serves as the adaptor or the substrate recongnition subunit. The substrate recognition subunit confers substrate specificity.

Figure 2.3. Flow - chart of meiosis in *C. elegans*.

During premeiotic DNA replication, cohesion between sister chromatids is established by the cohesin complex containing Rec8. During prophase I which is composed of several stages, the homologous chromosomes are aligned and homologs undergo recombination. During meiois I the cohesin on the chromosome arm is degraded and the chromosome number is reduced from 4n to n. During meiois II the centromeric Rec8 is degraded and sister chromatids are separated resulting in the reduction of chromosome number from 2n to n.

Figure 2.4. Establishment and maintenance of polarity in *C. elegans* embryos.

In wild type zygotes PAR-3/6/PKC (Red) is observed all around the cortex. As the sperm asters form at the posterior and interact with the actin cytoskeleton, PAR-3/6/PKC is expelled at the posterior and PAR-2 (Green) accumulates at that position. In wild-type transient PAR-2 may be observed near the meiotic spindle, however this disappears as the sperm asters are set up. In *cul-2* mutant zygotes PAR-2 is established and maintained at the anterior near the meiotic spindle leading to a reversal in downstream events.

Fig. 2.1.

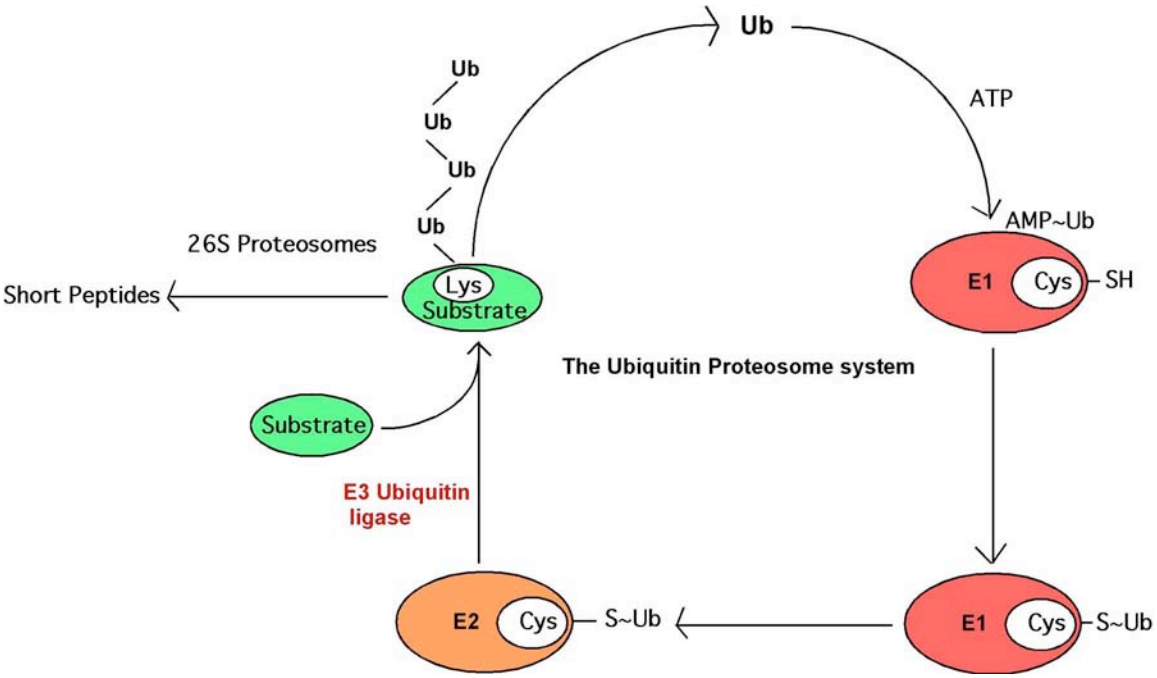
Ub
ATP
AMP~Ub
E1
Cys
SH
Ub
Ub
Ub
Ub
26S Proteosomes
Short Peptides
Lys
Substrate
The Ubiquitin Proteosome system
Substrate
E3 Ubiquitin
ligase
E2
Cys
S~Ub
E1
Cys
S~Ub

Fig. 2.2.

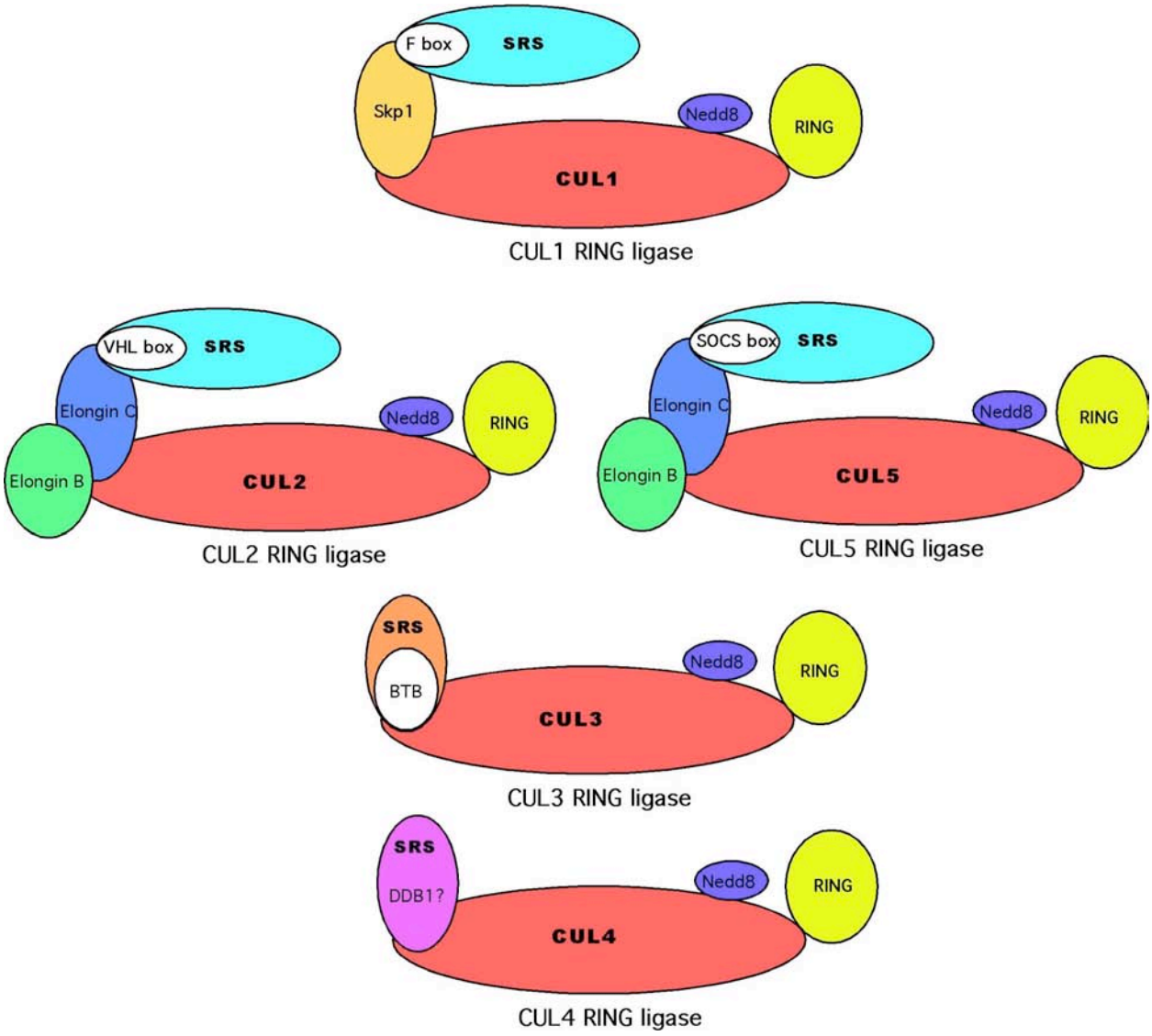
F box
SRS
Skp1
Nedd8
RING
CUL1
CUL1 RING ligase
VHL box
SRS
Elongin C
Nedd8
RING
Elongin B
CUL2
CUL2 RING ligase
SOCS box
SRS
Elongin C
Nedd8
RING
Elongin B
CUL5
CUL5 RING ligase
SRS
BTB
Nedd8
RING
CUL3
CUL3 RING ligase
SRS
DDB1?
Nedd8
RING
CUL4
CUL4 RING ligase

Fig. 2.3.

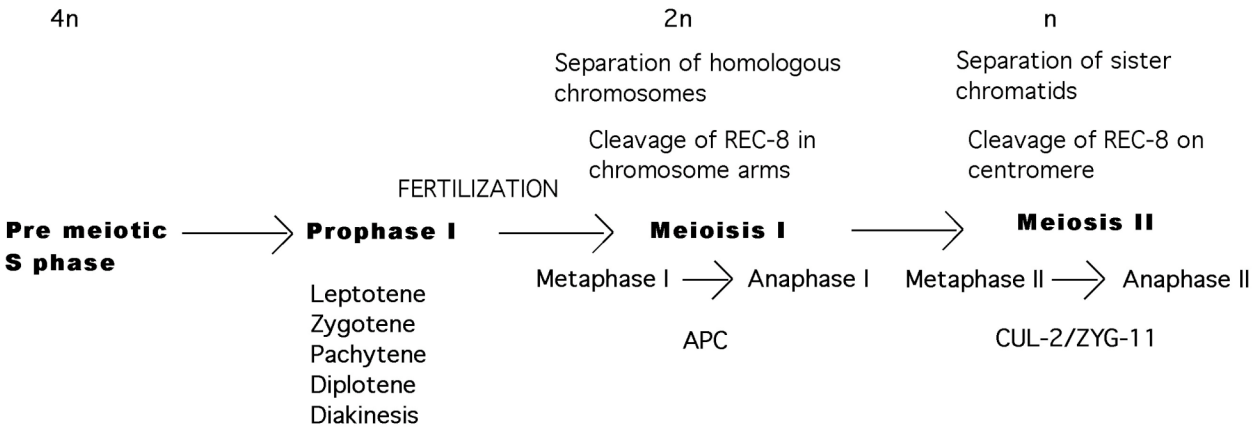
4n
2n
n
Separation of homologous chromosomes
Separation of sister chromatids
Cleavage of REC-8 in chromosome arms
Cleavage of REC-8 on centromere
FERTILIZATION
Pre meiotic S phase
Prophase I
Meioisis I
Meiosis II
Metaphase I
Anaphase I
Metaphase II
Anaphase II
Leptotene
Zygotene
Pachytene
Diplotene
Diakinesis
APC
CUL-2/ZYG-11

Fig. 2.4.

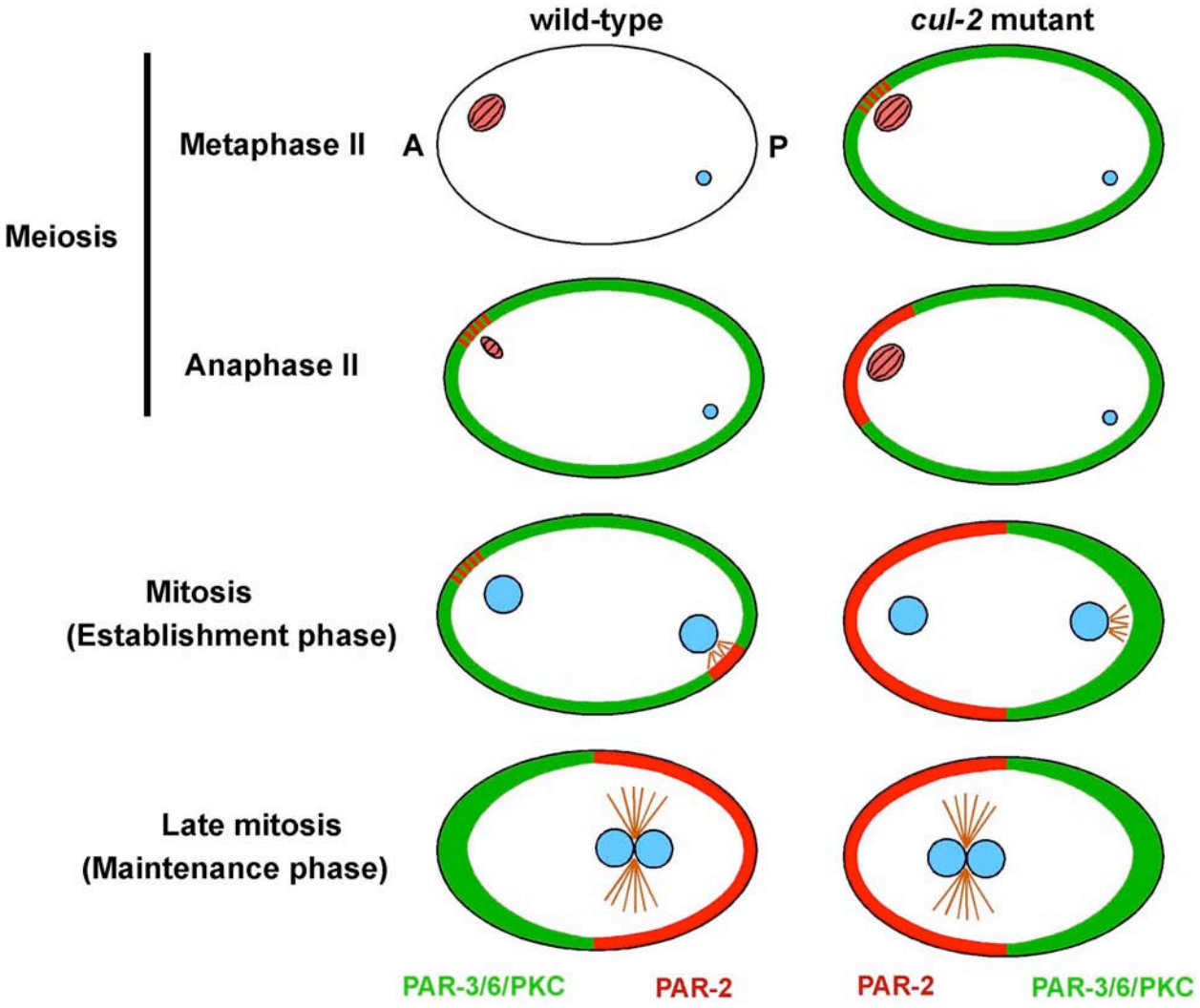
wild-type
cul-2 mutant
Meiosis
Metaphase II
A
P
Anaphase II
Mitosis
(Establishment phase)
Late mitosis
(Maintenance phase)
PAR-3/6/PKC
PAR-2
PAR-2
PAR-3/6/PKC

CHAPTER 3

CUL-2 AND ZYG-11 PROMOTE MEIOTIC ANAPHASE II AND THE PROPER PLACEMENT OF THE ANTERIOR-POSTERIOR AXIS IN *C. elegans*[1]

[1] **Srividya Vasudevan*, Ji Liu* and Edward T. Kipreos.**
Development. 2004 Aug; 131(15): 3513-25
*Authors contributed equally to this work
Reprinted here with the permission of the publisher.

ABSTRACT

The faithful segregation of chromosomes during meiosis is vital for sexual reproduction. Currently, little is known about the molecular mechanisms regulating the initiation and completion of meiotic anaphase. Here we show that inactivation of CUL-2, a member of the cullin family of ubiquitin ligases, delays or abolishes meiotic anaphase II with no effect on anaphase I, indicating differential regulation during the two meiotic stages. In *cul-2* mutants, the cohesin REC-8 is removed from chromosomes normally during meiosis II and sister chromatids separate, suggesting that the failure to complete anaphase results from a defect in chromosome movement rather than from a failure to sever chromosome attachments. CUL-2 is required for the degradation of cyclin B1 in meiosis and inactivation of cyclin B1 partially rescued the meiotic delay in *cul-2* mutants. In *cul-2* mutants, the failure to degrade cyclin B1 precedes the metaphase II arrest. CUL-2 is also required for at least two aspects of embryonic polarity. The extended meiosis II in *cul-2* mutants induces polarity reversals that include reversed orientation of polarity proteins, P granules, pronuclei migration, and asymmetric cell division. Independently of its role in meiotic progression, CUL-2 is required to limit the initiation/spread of the polarity protein PAR-2 in regions distant from microtubule organizing centers. Finally, we show that inactivation of the leucine-rich repeat protein ZYG-11 produces meiotic and polarity reversal defects similar to those observed in *cul-2* mutants, suggesting that the two proteins function in the same pathways.

INTRODUCTION

The faithful segregation of chromosomes during meiosis is vital for sexual reproduction, as missegregation leads to aneuploidy. Meiotic chromosome segregation involves two processes: loss of cohesion between chromosome homologs and the movement of chromosomes to opposite spindle poles. The molecular mechanisms that regulate meiotic chromosome cohesion are relatively well understood. Central to chromosome cohesion is the REC-8 cohesin complex, which holds chromosomes together from premeiotic S phase until anaphase (Petronczki et al., 2003). In budding and fission yeast, Rec8 is cleaved during meiosis I by separase in non-centromeric regions to allow the separation of chromosome homologs (Buonomo et al., 2000; Kitajima et al., 2003). In meiosis II, the remaining centromeric Rec8 is removed to allow sister chromatid separation; and this has been shown to require separase activity in fission yeast (Kitajima et al., 2003). In *C. elegans*, REC-8 is partially removed from chromosomes at anaphase I and is completely removed at anaphase II (Pasierbek et al., 2001). Inactivation of a *C. elegans* separase homolog leads to failures of chromosome separation, suggesting that the cohesin degradation mechanism is conserved (Siomos et al., 2001). In contrast to the detailed information about chromosome cohesion and its dissolution, little is known about the mechanisms that regulate chromosome movement during meiotic anaphase.

In many metazoa, the anterior-posterior (A-P) body axis is defined at a very early stage when patterning molecules are asymmetrically distributed in the embryo (Pellettieri and Seydoux, 2002). In the nematode *C. elegans*, A-P polarity is initiated in the zygote immediately after meiosis by the sperm pronucleus/centrosomes complex (SPCC) (Goldstein and Hird, 1996). In response to the SPCC, the PDZ-domain polarity protein PAR-6 becomes excluded from the posterior cortex. PAR-6 functions in a complex with the PDZ-domain protein PAR-3 and the

atypical protein kinase C PKC-3 (Tabuse et al., 1998; Hung and Kemphues, 1999; Joberty et al., 2000). The exclusion of PAR-6 from the posterior allows the RING finger protein PAR-2 to accumulate on the posterior cortex (Watts et al., 1996; Boyd et al., 1996; Hung and Kemphues, 1999; Cuenca et al., 2003). This redistribution of PAR-2 and PAR-6 is required for subsequent A-P asymmetries, including the polarized localization of maternal proteins to specify different cell fates and the asymmetric orientation of the mitotic spindle to generate unequal cell divisions (Schneider and Bowerman, 2003; Pellettieri and Seydoux, 2002).

Ubiquitin-mediated protein degradation is an essential aspect of many dynamic cellular processes, including cell cycle progression, signal transduction, and transcription (Pickart, 2001). The covalent attachment of poly-ubiquitin chains to proteins can signal degradation by the 26S proteasome (Pickart, 2001). The addition of ubiquitin to proteins is highly regulated and requires the action of a ubiquitin activating enzyme (E1), a ubiquitin conjugating enzyme (E2), and a ubiquitin ligase (E3). The substrate specificity of ubiquitination derives from the recognition of the substrate by the ubiquitin ligase. A major class of E3s are the cullin/RING finger ubiquitin ligases (Tyers and Jorgensen, 2000). The cullin gene family comprises five major groupings in metazoa, CUL-1 through CUL-5 (Tyers and Jorgensen, 2000). In mammals, CUL2 functions in an E3 complex that contains the core components elongin C, elongin B, and the RING-H2 finger protein RBX1/ROC1 (Kim and Kaelin, 2003).

Here we show that CUL-2, as well as orthologs of elongin C and RBX1, are required for the initiation of meiotic anaphase II but not for anaphase I. The meiotic delay in *cul-2* mutants causes a reversal of A-P polarity. By titrating the length of the delay, we demonstrate that there is a tight linkage between meiotic timing and the placement of the A-P axis. We also show that

CUL-2 has an additional role to prevent the ectopic localization or spreading of PAR-2 on the cortex.

MATERIALS AND METHODS

Strains and alleles

C. elegans strains were cultured as previously described (Brenner, 1974). Strains and alleles used were: Bristol N2; AZ212 [*unc-119(ed3)*; ruIs32 (pAZ132: *pie-1* promoter/histone H2B::GFP)]; AZ244 [*unc-119(ed3)*; ruIs57 (pAZ147: *pie-1* promoter/β-tubulin::GFP; *unc-119(+)*)]; KK866 [itIs153 (*pie-1* promoter/PAR-2::GFP, pRF4, N2 genomic DNA)]; JH1461 [axEx1121 (*pie-1* promoter/PAR-6::GFP, pRF4, N2 DNA)]; JH1473 [itIs153; ruIs57]; ET108 [*cul-2(ek1)*/*unc-64(e246)*; ruIs32]; ET129 [*unc-119(ed3)*; itIs153; ruIs32]; DG627 [*emb-30(tn377*ts)]; ET143 [*zyg-11(mn40) unc-4(e120)*/*mnC1; cul-2(ek1)*/*unc-64(e246)*]; ET144 [*zyg-11(mn40) unc-4(e120)*/*mnC1; cul-2(ek1)*/*unc-64(e246)*; ruIs32]; SP152 [*him-1(e879); zyg-11(mn40) unc-4(e120)*/*mnC1*]; ET155 [*zyg-11(mn40) unc-4(e120)*/*mnC1*; ruIs32]; and ET113 [*unc-119(ed3)*; ekIs2 (*pie-1* promoter/CYB-1::GFP; *unc-119(+)*). N2 and ET108 were maintained at 20° C, DG627 was maintained at 15° C, and all other strains were maintained at 24° C.

RNAi

RNAi was performed either by injection of dsRNA into hermaphrodites or by feeding with bacteria expressing dsRNA, as described (Feng et al., 1999; Timmons et al., 2001). To produce a partial loss of CUL-2 function, embryos were observed between 4 and 12 hours post-injection of *cul-2* dsRNA into adult hermaphrodites. The *cul-2; rec-8* double RNAi experiment followed the protocol of Davis et al., 2002, except that after injection of *rec-8* dsRNA into adult

hermaphrodites, L4-stage progeny were placed on *cul-2* RNAi bacteria feeding plates for 24 hours prior to observation. Inactivation of *cul-2* in double RNAi experiments was assessed by observation of multinuclei and cytoplasmic extensions that occur in *cul-2* mutant embryos (Feng et al., 1999). The effectiveness of *cyb-1* RNAi was confirmed by the elimination of CYB-1::GFP signal.

Microscopy

Time-lapse movies were made of embryos *in utero*. Young adult hermaphrodites were anesthetized either with 0.1% tricaine, 0.01% tetramisole (Sigma) in M9 solution or 10 mM levamisole (Sigma) in M9 solution. To observe the initiation of PAR-2 cortical localization, zygotes were cut from the uterus into EBGM medium (Shelton and Bowerman, 1996) on 12x12 mm cover slips. The cover slip was mounted on 4% agarose pads with a thin layer of petroleum jelly applied between the cover slip and the pad to eliminate pressure on the zygotes. Automatic time-lapse imaging was performed with a Zeiss Axioplan microscope equipped with a Hamamatsu ORCA-ER CCD camera, LUDL hardware controller, automated filter wheels and shutters, and an Apple G4 computer running Openlab software (Improvision). Movies were made with pulsed 100 msec exposures for DIC and epifluorescence every 40-80 sec; epifluorescent illumination was from a 100 W HBO mercury lamp that was filtered to 25% of normal levels. PAR-2::GFP cortical patches were only scored when they were of higher epifluorescent intensity than the interior cytoplasm, except in Table 2 where they were noted as being transient and weak. For the timing of meiosis, the following number of embryos were observed for wild type, *cul-2(RNAi)*, *cul-2(ek1)*, *elc-1(RNAi)*, *rbx-1(RNAi)*, *elb-1(RNAi)*, *zyg-11(RNAi)*, and *zyg-11(mn40)*, and *zyg-11(mn40); cul-2(ek1)*: n = 5, 5, 5, 3, 4, 6, 9, 3, and 5 respectively, for meiosis I; and n = 5, 5, 5, 5, 4, 9, 9, 4, and 5 respectively, for meiosis II.

Quantitation of CYB-1::GFP levels was performed by measuring the fluorescent signal with OpenLab software and subtracting background fluorescence.

The following primary antibodies were used for immunofluorescence: anti-REC-8 (Pasierbek et al., 2001); anti-PAR-2 (Boyd et al., 1996); anti-PAR-6 (Hung and Kemphues, 1999); anti-P granules, OI1CD4 (Strome and Wood, 1982), and our monoclonal 4G8; anti-α-tubulin (N356, Amersham); and anti-GFP, 3E6, Molecular Probes, and ab6556, AbCam. Secondary antibodies used were: anti-mouse rhodamine (Cappel); and anti-rabbit Alexa Fluor 488 (Molecular Probes). Slides were incubated with 1 μg/ml DAPI to stain DNA prior to mounting in 90% glycerol/PBS with 1 mg/ml p-phenylenediamine (Sigma). The anti-α-tubulin and DAPI-stained meiotic spindle images were obtained as 0.3 μm z-sections and processed with Openlab multi-neighbor deconvolution software. For *emb-30(tn377)* immunofluorescence experiments, only zygotes that were arrested in meiosis I with the meiotic spindle associated with the anterior cortex and no sperm asters were scored for PAR-2 and PAR-6 localization; this represents relatively younger arrest embryos prior to the wandering of the meiotic spindle or the formation of sperm asters. Images were processed with Adobe Photoshop software (6.0). The chi-squares test was used to determine statistical significance. Means are given with s.e.m.

RESULTS

CUL-2 is required for meiotic anaphase II

Following fertilization in wild-type zygotes, the six maternal chromosome bivalents align in a pentagonal array at metaphase I (Albertson and Thomson, 1993) (Fig. 3.1A). In anaphase I, homologs segregate and a 2N polar body is extruded from the zygote. In metaphase II, the remaining six sister chromatids again adopt a pentagonal array (Fig. 3.1A). After the second

polar body is extruded from the zygote, the maternal chromatids decondense, marking the completion of meiosis.

We examined meiotic chromosome dynamics using time-lapse movies of chromosomes visualized by transgenic expression of histone H2B::GFP. Zygotes homozygous for the *cul-2(ek1)* null allele (Feng et al., 1999) or zygotes depleted of CUL-2 by RNA-mediated interference *(RNAi)* (Fire et al., 1998) had indistinguishable phenotypes. They both completed meiosis I with normal chromosome dynamics approximately 15 minutes post-fertilization, similar to wild type (Fig. 3.1A,B). Significantly, while meiosis II lasted approximately 15 minutes in wild type, it took an average of 50 to 60 minutes in *cul-2(RNAi)* and *cul-2(ek1)* zygotes (Fig. 3.1A,B). Afterwards, the chromosomes generally congressed and individual chromosomes could not be discerned; this was followed by decondensation. Of 18 zygotes observed, ten never executed anaphase II (Fig. 1A), while in the other eight the DNA split immediately before or after chromosome decondensation with DNA bridges observed in the majority of cases (7/8). RNAi depletion of the orthologs of mammalian CUL-2 complex components elongin C, *elc-1*, and RBX1/ROC1, *rbx-1*, produced metaphase II arrest phenotypes similar to that of *cul-2* mutants (Fig. 3.1 A,B). This suggests that CUL-2 normally promotes entry into anaphase in the context of a conserved ubiquitin ligase complex.

cul-2 and *zyg-11* mutants have a similar meiosis II arrest

The failure of *cul-2* mutant embryos to initiate anaphase II was reminiscent of the *zyg-11* mutant phenotype. In a study by Kemphues et al, 1986, embryos homozygous for the hypomorphic allele *zyg-11(bn2)* were found to progress through meiosis I with normal timing, while meiosis II was extended to 26 minutes. We analyzed embryos homozygous for the null allele *zyg-*

11(mn40) as well as *zyg-11(RNAi)* embryos and found a longer meiosis II delay of 50.2 ± 4.0 minutes (n=5) and 43.6 ± 3.1 minutes (n=9), respectively, comparable to the delay observed in *cul-2* mutants (Fig. 3.1 A,B). To test whether simultaneous inactivation of both genes increased the severity of the meiotic arrest, as might occur if the two genes affected meiotic progression through independent pathways, we created a double heterozygous mutant strain (ET144) using null alleles for each gene. Double homozygous *zyg-11(mn40); cul-2(ek1*) embryos from this strain remained in meiosis II for 53 ± 4.5 minutes (n=5), equivalent to the timings seen upon individual inactivation of each gene (Fig. 3.1B). This result is consistent with the two genes functioning in the same pathway to regulate anaphase II.

In addition to defective meiosis II, *zyg-11* and *cul-2* mutant embryos share other phenotypes, including the presence of multinuclei and cytoplasmic extensions during mitotic divisions (Feng et al., 1999; Kemphues et al., 1986). One difference between the two mutants is the presence of G1-phase arrested germ cells in *cul-2* mutants (Feng et al., 1999), which are not observed in *zyg-11* mutants. The decreased number of germ cells in *cul-2* mutants leads to lower numbers of eggs. We sought to test whether combining the *cul-2* mutant with the *zyg-11* mutant would enhance the *cul-2* egg production defect. *zyg-11(mn40); cul-2(ek1)* double homozygotes produced a low number of eggs (35.2 ± 4.7; n=18) that was comparable to the egg numbers in *cul-2(ek1)* homozygotes (Feng et al., 1999) or hermaphrodites that are homozygous for *cul-2(ek1)* and heterozygous for *zyg-11(mn40)* (29.3 ± 5.5; n=19). Conversely, animals homozygous for *zyg-11(mn40)* but heterozygous for *cul-2(ek1)* had egg numbers (333 ± 3.2; n =10) similar to wild type, indicating that the loss of *zyg-11* cannot induce a germline arrest phenotype in *cul-2(ek1)* heterozygotes. These results suggest that ZYG-11 is unlikely to function with CUL-2 in promoting germline proliferation.

CUL-2 is not required for the removal of REC-8 from sister chromatids

A failure to segregate chromosomes during meiosis could result from defects in either chromosome separation or chromosome movement. In yeast, cohesin degradation is sufficient for the initiation of anaphase chromosome segregation (Uhlmann et al., 2000). In *C. elegans*, RNAi depletion of the cohesion REC-8 produces chromosome separation at diakinesis (Pasierbek et al., 2001).

To determine if REC-8 is removed from chromosomes in *cul-2(RNAi)* zygotes, we studied REC-8 localization using immunofluorescence with anti-REC-8 antibody (Pasierbek et al., 2001). We found that the anti-REC-8 staining pattern in *cul-2(RNAi)* zygotes was similar to that in wild type. For both wild type and *cul-2(RNAi)* zygotes, REC-8 is located along the axes of sister chromatids during metaphase I, and is located at the junction of the sister chromatids during metaphase II (Fig. 3.2 A) (Pasierbek et al., 2001). In wild type, REC-8 is completely lost from the separating wild-type chromatids during anaphase II (Fig. 3.2 A). In *cul-2(RNAi)* zygotes, although chromosomes remain in a metaphase II pentagonal array for an extended period, the majority of metaphase chromosomes do not have anti-REC-8 staining (70%, n = 26) (Fig. 3.2 A). When *cul-2(RNAi)* zygotes are in the later stages of the extended meiosis II, the meiotic spindle often wanders away from the anterior pole of the egg. None of these late stage meiosis II zygotes were observed to have anti-REC8 staining (data not shown).

The lack of REC-8 staining suggests that the chromosomes in *cul-2(RNAi)* zygotes are not bound together. Indeed, we occasionally observed separated sister chromatids during the extended metaphase II of *cul-2* mutant zygotes (Fig. 3.1 C). In 1/11 *cul-2(RNAi)* and 1/ 7 *cul-2(ek1)* mutants, approximately 12 individual chromatids were observed at the metaphase II plate rather than the normal six joined sister chromatids, indicating that cohesion had been lost

between the sister chromatids although chromosome segregation did not occur. A similar separation of sister chromatids during metaphase II is observed in *zyg-11(mn40)* mutant embryos (data not shown).

A further indication that a defect in chromosome cohesion was not responsible for the CUL-2 meiotic defects was obtained from experiments in which zygotes were depleted of REC-8. Inactivation of REC-8 produces a loss of chromatid cohesion from the meiotic diakinesis stage onwards (Pasierbek et al., 2001). In both *rec-8(RNAi)* and *cul-2*; *rec-8* double RNAi zygotes, chromosomes segregate during anaphase I (Davis et al., 2002). However, in both zygotes we observed that chromosomes failed to segregate during meiosis II. Nevertheless, *rec-8(RNAi)* zygotes had normal meiosis II timing (16.1 ± 0.7 min, n = 9) (Fig. 3.2 B). In contrast, *cul-2*; *rec-8* double RNAi zygotes had a meiosis II delay comparable to that observed in *cul-2(RNAi)* zygotes (55.2 ± 6.5 min, n = 4), indicating that the *cul-2* meiotic delay was not rescued by removing REC-8 (Fig. 3.2 B).

An interesting observation was that in the majority of *rec-8(RNAi)* zygotes (7/8), a monopoleward movement of chromosomes toward the cortex was observed at the time when the second polar body would be extruded in wild type (Fig. 3.2 B). The mechanistic basis of this monopoleward chromosome movement is not known, but it is similar to the chromosome behavior reported in *air-2(RNAi)* zygotes, which have a failure to remove REC-8 from meiotic chromosomes (Rogers et al., 2002). Interestingly, *cul-2*; *rec-8* double RNAi zygotes did not have the monopoleward chromosome movement (n = 9), indicating that this aspect of meiotic chromosome movement was also defective (Fig. 3.2 B).

Cyclin B1 is not degraded during meiosis in *cul-2(RNAi)* zygotes

The cyclin B/CDK1 complex is essential for entry and completion of mitosis and meiosis (Nebreda and Ferby, 2000). A failure to degrade cyclin B1 blocks the metaphase to anaphase transition in mitotically-dividing mammalian cells and is required for meiotic homolog disjunction in mice (Stemmann et al., 2001; Hagting et al., 2002; Chang et al., 2003; Herbert et al., 2003). To analyze whether the degradation of cyclin B1, CYB-1, was normal in *cul-2(RNAi)* embryos, we used the *pie-1* promoter to express CYB-1::GFP in the germline. In wild type, CYB-1::GFP fluorescence was detected in mature oocytes, but rapidly disappeared during meiosis I and II following fertilization (Fig. 3.3 A,B). In contrast, in *cul-2(RNAi)* embryos, CYB-1::GFP signal decreased only modestly during meiosis and remained at elevated levels in mitotic-stage embryos (Fig. 3.3 A,B). Elevated levels of CYB-1 were also detected in *cul-2(RNAi)* embryos with an anti-CYB-1 antibody kindly provided by Sander van den Heuvel (data not shown). A similar defect in CYB-1::GFP degradation was observed in *zyg-11(RNAi)* embryos (Fig. 3.3 A).

Given the requirement for cyclin B1 degradation for entry into anaphase in mammals, we tested whether the failure to degrade cyclin B1 was responsible for the *cul-2* metaphase II arrest phenotype. RNAi depletion of *cyb-1* does not affect the timing of meiosis II (Fig. 3.3 C). If the elevated level of CYB-1 in *cul-2* mutants was solely responsible for the metaphase arrest then depletion of CYB-1 would be expected to allow *cul-2* mutants to proceed through anaphase. However, this is not the case, as chromosome segregation was not observed in 6/12 of the *cul-2(ek1); cyb-1(RNAi)* embryos, a ratio similar to what was observed in *cul-2* mutants alone. Interestingly, in *cul-2(ek1)* homozygous embryos depleted for *cyb-1*, chromosomes were observed to split in 3 directions at anaphase I in 3 of 12 embryos, and in all 12 embryos

examined chromosomes did not form a pentagonal array in meiosis II (data not shown). This latter result is surprising as pentagonal arrays form in both *cyb-1(RNAi)* and *cul-2(ek1)* homozygous meiosis II-stage embryos (Fig. 3.1 A; data not shown). Although the anaphase defect was not rescued, *cyb-1* RNAi did produce a partial rescue of the *cul-2* meiotic delay phenotype. In seven of 12 *cul-2(ek1); cyb-1(RNAi)* embryos, meiosis II length was similar to *cul-2(ek1)* alone, however, the remaining five embryos had significantly shorter meiosis II timings, three of which were indistinguishable from wild type (Fig. 3.3 C).

The anaphase-promoting complex/cyclosome (APC/C) ubiquitin ligase promotes cyclin B degradation during mitosis in yeast and metazoa (Peters, 2002). APC/C also promotes cyclin B degradation during meiosis in *Xenopus* and mouse (Peter et al., 2001, Nixon et al., 2002). In *C. elegans*, loss of APC/C produces a one-cell embryonic arrest at metaphase of meiosis I (Furuta et al., 2000; Davis et al., 2002). Levels of CYB-1::GFP were stabilized in *apc-11(RNAi)* embryos (Fig. 3.3 B), suggesting that both CUL-2 and APC/C are required for CYB-1 degradation.

The meiotic spindle maintains normal morphology for an extended period in *cul-2(RNAi)* zygotes

We studied the morphology and dynamics of the meiotic spindle in *cul-2(RNAi)* zygotes by both anti-α-tubulin antibody staining and live β-tubulin::GFP movies. In meiosis I, the meiotic spindles of *cul-2(RNAi)* and wild type embryos were indistinguishable (data not shown). Meiosis II spindles in *cul-2(RNAi)* embryos maintained a normal barrel-shaped structure for an extended period of time (Fig. 3.4 A). Eventually, the *cul-2(RNAi)* meiotic spindle shrunk and lost its barrel structure. On average, the *cul-2(RNAi)* meiosis II spindle lasted three times as long as in wild type (36.2 ± 2.5 vs. 12.2 ± 0.7 minutes, n = 6 for each) (Fig. 4A). Meiotic spindle

morphology characteristic of anaphase II (Fig. 3.4 B) was never observed in *cul-2(RNAi)* embryos.

Perdurance of the Meiosis II spindle is associated with polarity reversal

In wild-type embryos after meiosis, PAR-3 and PAR-6 are expelled from the posterior cortex near the sperm asters, and concomitantly, PAR-2 stably accumulates on the posterior cortex (Hung and Kemphues, 1999; Boyd et al., 1996) (Fig. 3.5 A). In contrast to wild type, *cul-2(RNAi)* zygotes stably accumulate cortical PAR-2 while still in meiosis II. We analyzed the PAR-2 localization pattern in meiosis II-stage *cul-2(RNAi)* zygotes using immunofluorescence with anti-PAR-2 antibodies. In the majority of meiosis II-stage *cul-2(RNAi)* embryos (76%, 50/67), strong cortical PAR-2 staining was observed on the anterior cortex, a reversal of the wild-type pattern (Fig. 3.5 A; Table 3.1). *zyg-11(RNAi)* embryos similarly had a high percentage of anterior-localized PAR-2 (Fig. 3.5 C; Table 3.1). PAR-3 and PAR-6 localizations were also reversed, with exclusion of both proteins from the anterior cortex in the majority of *cul-2(RNAi)* embryos (23/33 and 8/10, respectively) (Fig. 3.5 A).

We analyzed whether downstream aspects of polarity were reversed in *cul-2(RNAi)* embryos. After meiosis is completed in wild type, dispersed P granules move toward the posterior and are completely in the posterior half by the pronuclei meeting stage (Strome and Wood, 1983) (Fig. 3.5 D). In *cul-2(RNAi)* zygotes, P granules can localize to the anterior, posterior, center, or lateral cytoplasm. The abnormal localization is coupled to the altered placement of PAR-2, as P granules co-localize with anterior or lateral cortical PAR-2 in the majority of mitotic *cul-2(RNAi)* embryos (10/11) (Fig. 3.5 D).

In wild type, maternal pronuclei migrate from the anterior to meet the sperm pronucleus in the posterior (Fig. 3.5 E). This aspect of polarity is also reversed in *cul-2(RNAi)* embryos. In the majority of *cul-2(RNAi)* embryos (8/10), the sperm pronucleus migrates further than the maternal pronucleus (Fig. 3.5 E). Pronuclei often meet in the anterior of the embryo rather than in the posterior, and the anterior daughter cell is smaller than the posterior cell in over half of *cul-2(RNAi)* embryos (16/31) (Fig. 3.5 B). Similar polarity defects were observed in *elc-1* and *rbx-1* RNAi embryos (Fig. 3.5 B; data not shown).

To study if the polarity reversal correlated with the extended meiosis II delay in *cul-2(RNAi)* zygotes, we varied the penetrance of *cul-2* RNAi depletion by altering the length of time adult hermaphrodites were exposed to *cul-2* dsRNA prior to fertilization. The partial *cul-2* RNAi treatment produced meiosis II timing ranging from that of wild type to delays similar to that of *cul-2(ek1)* null mutants (Table 3.2). In wild type, meiosis II lasted 16.2 ± 1.3 minutes and PAR-2 accumulated on the posterior cortex approximately 2 minutes after the completion of meiosis II (18.4 ± 0.9 minutes after meiosis I) (Table 3.2). In two of five wild-type zygotes, transient, weak, anterior cortical PAR-2 was observed during meiosis II, similar to previous reports (Boyd et al., 1996; Cuenca et al., 2003) (Table 3.2). Transient, weak, anterior PAR-2 localizations were also observed in two *cul-2(RNAi)* embryos that had meiosis II timing similar to wild type (Table 3.2). *cul-2(RNAi)* zygotes with meiosis II timing of ≥ 28 minutes developed intense, stable PAR-2 patches on anterior or lateral cortexes (Table 3.2). An extended meiotic delay coupled with an anterior PAR-2 patch was associated with a reversal in the longitudinal placement of the mitotic spindle, so that the first division produced a posterior cell larger than the anterior cell (Table 3.2).

Ectopic lateral PAR-2 localization is associated with loss of CUL-2

We were intrigued by the observation in *cul-2(RNAi)* zygotes of PAR-2 patches (8/67 embryos) and exclusions of PAR-3 (3/33) and PAR-6 (2/10) on the lateral cortex that were often distant from both the meiotic spindle and the SPCC (Fig. 3.5A; Table 3.1). As microtubule (MT) organizing foci have been implicated in PAR-2 localization (O'Connell et al., 2000; Wallenfang and Seydoux, 2000), we sought to determine if the lateral PAR-2 arose from prior transient association of the meiotic spindle or SPCC with the lateral cortex. To address this, we followed the initiation of cortical PAR-2 in living embryos expressing either a combination of PAR-2::GFP and β-tubulin::GFP (to visualize the meiotic spindle) or PAR-2::GFP and histone H2B::GFP (to visualize oocyte and sperm DNA). In the two strains, PAR-2 patches appeared to initiate distant from the meiotic spindle or distant from both oocyte and sperm DNA (5/20 and 3/10 embryos, respectively) (Fig. 3.6 A). With the PAR-2::GFP strains, we observed a higher percentage of lateral accumulations of PAR-2 upon *cul-2* RNAi than was observed for *cul-2(RNAi)* embryos probed with anti-PAR-2 antibodies (Table 3.1). In particular, we observed a substantial percentage of embryos in which PAR-2::GFP spread extensively on the cortex to form a circular band around the embryo (Fig. 3.6 B; Table 3.1). One third of the circular PAR-2 patterns were observed distant from the meiotic spindle (Fig. 3.6 B; Table 3.1). These observations of PAR-2 accumulation distant from the meiotic spindle suggest that in *cul-2(RNAi)* embryos, the initiation or spreading of cortical PAR-2 is under less stringent control.

In wild-type zygotes, PAR-2 and PAR-6 cortical localizations are mutually antagonistic (Watts et al., 1996; Hung and Kemphues, 1999; Cuenca et al., 2003). It has been proposed that the normal accumulation of PAR-2 on the posterior cortex occurs after the exclusion of PAR-6 (Cuenca et al., 2003). With a combination of anti-PAR-6 antibodies and PAR-2::GFP, we

observed that ten of twelve lateral or circular PAR-2 patches that were distant from the meiotic spindle had overlapping cortical PAR-6, suggesting that the lateral PAR-2 localization can occur without the prior removal of PAR-6 (Fig. 3.6 C).

Interestingly, the percentage of lateral and circular PAR-2 was significantly lower in *zyg-11(RNAi)* embryos with no examples of PAR-2 patches distant from the meiotic spindle observed (Table 3.1). While this may reflect a reduced effectiveness of the RNAi procedure in depleting ZYG-11 relative to CUL-2, it nevertheless suggests that the lateral accumulation of PAR-2 does not arise directly from the meiotic delay, as RNAi of both genes gave comparable meiotic lengths but only *cul-2(RNAi)* embryos had lateral patches distant from the meiotic spindle.

To further test if the accumulation of PAR-2 distant from the meiotic spindle was a secondary consequence of the meiotic delay or reflected the loss of a separable CUL-2 function, we analyzed PAR-2 localization in an *emb-30* mutant background. *emb-30* encodes the APC/C component APC-4 (Furuta et al., 2000). At the restrictive temperature of 24°C, *emb-30(tn377*ts*)* embryos arrest at the metaphase I stage of meiosis (Furuta et al., 2000). As described above, CUL-2 is not required for progression through meiosis I; and *emb-30(tn377); cul-2(RNAi)* embryos have the same metaphase I-arrest phenotype and spindle morphology as *emb-30(tn377)* embryos (Fig. 3.6 E; data not shown). Therefore, any differences in PAR-2 localization between the two strains should reflect the loss of CUL-2 functions that are independent of its role in meiotic progression. As expected from previous work on *emb-30* by Wallenfang and Seydoux, 2000, we observed that a high percentage of both *emb-30(tn377)* and *emb-30(tn377); cul-2(RNAi*) embryos had anterior PAR-2 (89%, n = 54; and 83%, n= 47, respectively). In *emb-30(tn377)* zygotes, only a small minority of embryos had lateral or posterior PAR-2 patches

(3.7%, 2/54) (Fig. 3.6 E), also as observed by Wallenfang and Seydoux. In *emb-30(tn377); cul-2(RNAi*) zygotes, however, the percentage of embryos with lateral or posterior PAR-2 patches was significantly higher (23%, 11/47; $P < 0.01$); most of these embryos also had anterior PAR-2 patches (Fig. 3.6 E). Similarly, 27% of *emb-30(tn377); cul-2(RNAi*) zygotes (n = 56) had exclusion of PAR-6 on lateral or posterior cortexes compared to 4% of *emb-30(tn377)* zygotes (n = 28) (significance of $P < 0.05$) (Fig. 3.6 E). There was no difference in the MT distributions observed in *emb-30(tn377)* and *emb-30(tn377); cul-2(RNAi)* embryos, both of which had disorganized spindles at comparable percentages (43% and 33%, respectively). These results provide evidence that CUL-2 has a separable function to prevent the ectopic initiation or spreading of cortical PAR-2.

Our observations suggested that the lateral PAR-2 patches could occur distant from the meiotic spindle or sperm DNA. To rigorously test whether PAR-2 can localize to the cortex in the absence of the meiotic spindle in *cul-2(RNAi)* embryos, we disrupted MTs by depleting the β-tubulin gene *tbb-2*, which had the effect of eliminating the meiotic spindle and visible MTs during meiosis. The elimination of MTs made distinguishing the two meiotic stages problematic because of the loss of chromosome and spindle dynamics. Therefore, all meiotic embryos were analyzed rather than just those in meiosis II, the stage in which ectopic PAR-2 localization generally occurs. We observed that in *tbb-2*; *cul-2* double RNAi embryos, the overall percentage of cortical PAR-2 was markedly reduced, particularly in the anterior where PAR-2 is normally associated with the meiotic spindle (Table 3.1). However, discrete PAR-2 patches were still observed in 11.2% of meiotic embryos, most of which was localized to the lateral cortex (Fig. 3.6 D; Table 3.1). Wild type embryos subjected to *tbb-2* RNAi had no meiotic PAR-2 staining (Table 3.1). These results indicate that PAR-2 localization can occur in *cul-2(RNAi)* embryos in

the absence of the meiotic spindle. However, the reduction in the percentage of lateral PAR-2 localization in *tbb-2*; *cul-2* RNAi embryos relative to *cul-2(RNAi)* embryos, suggests that the presence of MTs potentiates the ectopic PAR-2 localization.

Interestingly, depletion of *tbb-2* alone produced a high percentage of post-meiotic embryos with condensed mitotic prometaphase chromosomes and cortical PAR-2 localized in the same half of the embryo. In 13 of 15 of these embryos, α-tubulin staining was observed in one or two small circles of approximately 0.3 μm diameter near the condensed chromosomes, presumably the centrosomes. For *tbb-2*, *cul-2* RNAi embryos with mitotic prometaphase chromosomes, 8 of 12 had one or two similar small α-tubulin circles, with PAR-2 either localized on the cortical half of the embryo with the chromosomes and α-tubulin circles (9/12) or on lateral cortexes distant from α-tubulin circles (3/12). The observation of α-tubulin at the centrosome suggests that even though visible MT filaments were eliminated after *tbb-2* RNAi, a residual capacity for tubulin to be organized into the centrosome still exists and potentially this structure is capable of localizing PAR-2. Therefore, while our results demonstrate that the loss of CUL-2 during meiosis can localize cortical PAR-2 in the absence of the meiotic spindle, we cannot conclude that the PAR-2 localization is independent of all MT activity.

DISCUSSION

CUL-2 and ZYG-11 are required for the initiation of anaphase II and meiotic progression

In zygotes devoid of CUL-2, anaphase II either fails to occur or is severely delayed, and meiosis II lasts three to four times longer than in wild type. The delay in meiotic exit may be more than just a secondary effect of the failure of anaphase II, as *air-2(RNAi)* and *rec-8(RNAi)*

zygotes have normal meiotic timing even though the former lacks anaphase I and II, and the latter lacks anaphase II (Rogers et al., 2002; this study).

Three lines of evidence indicate that the meiosis II defects in *cul-2* mutants do not arise from a failure of chromosome separation. First, the cohesin REC-8, which is required to hold sister chromatids together (Pasierbek et al., 2001), dissociates from metaphase II chromosomes in *cul-2* mutants. Second, a small percentage of *cul-2* mutant zygotes are observed in which sister chromatids separate during meiosis II but still fail to move to the spindle poles. And third, in *cul-2(RNAi); rec-8(RNAi)* zygotes, all chromatids separate from each other, yet exit from meiosis II is still delayed.

Mitotic anaphase chromosome movement has been extensively analyzed. Both MT spindle dynamics and MT motors are required for mitotic anaphase poleward force generation (Wittmann et al., 2001). In contrast, meiotic anaphase has not been extensively studied, and it is unclear to what extent similar mechanisms will function to move chromosomes during meiosis. Interestingly, the morphology and dynamics of the *C. elegans* meiotic spindle are quite different from the mitotic spindle. The mitotic spindle is composed of long polar MTs and relatively short midzone MTs. Ablation of the mitotic midzone MTs increases the velocity and distance of chromosome separation, suggesting that they are not required to "push" chromosomes apart but instead function to limit the speed and/or extent of chromosome movement (Grill et al., 2001). In contrast, during meiotic anaphase, the MTs near the meiotic spindle poles appear to depolymerize, while the amount of midzone MTs between the separating chromosomes increases dramatically (Albertson and Thomson, 1993) (Fig. 3.4 B). During late anaphase, all MTs appear to be located between the separating chromosomes (Fig. 3.4 B). The reorganization of MTs to the midzone that occurs during meiotic anaphase suggests that meiotic chromosomes are

"pushed" apart by MT polymerization between the chromosomes rather than being "pulled" to the spindle poles as occurs during mitosis. In *cul-2* mutants, the meiotic spindle maintains its normal size and shape for an extended period of time during metaphase II, indicating a defect in the initiation of MT depolymerization at the spindle poles and polymerization between sister chromatids. CUL-2 therefore appears to function upstream of the dramatic MT rearrangements that occur during meiotic chromatid segregation.

CUL-2 and ZYG-11 are required for the degradation of Cyclin B1 during meiosis

Using a CYB-1::GFP reporter, we observed that maternally-provided cyclin B1 is degraded upon fertilization. In both *cul-2(RNAi)* and *zyg-11(RNAi)* embryos, CYB-1::GFP is stabilized during both meiosis I and II. This is not a secondary consequence of the meiosis II arrest, as the failure to degrade CYB-1::GFP precedes the arrest. Surprisingly, depletion of CYB-1 by RNAi in *cul-2(ek1)* mutants produced a synthetic phenotype of loss of the pentagonal chromosome array in meiosis II, indicating that *cul-2* mutant zygotes have additional meiotic defect(s) that are exacerbated by loss of CYB-1. The depletion of CYB-1 partially rescued the meiosis II delay of *cul-2(ek1)* embryos, suggesting that the failure to degrade CYB-1 may be contributing to the meiotic delay.

The APC/C ubiquitin ligase promotes cyclin B degradation during mitosis in yeast and metazoa (Peters, 2002). APC/C has also been shown to promote meiotic cyclin B degradation in budding yeast, fission yeast, *Xenopus,* and mouse (Cooper et al., 2000; Blanco et al., 2001; Peter et al., 2001; Nixon et al., 2002). In *C. elegans,* inactivation of the APC component *apc-11* also stabilized cyclin B1 levels. Further research will be required to assess the roles of CUL-2 and APC/C in regulating cyclin B1 levels.

The spindle dynamics of anaphase I and II appear similar to each other in wild type (Albertson and Thomson, 1993). Therefore it is surprising that in *cul-2(ek1)* embryos, anaphase I is normal but anaphase II is severely delayed or abolished. This is not due to the perdurance of *cul-2* maternal product through meiosis I because these embryos arose from *cul-2(ek1)* homozygous hermaphrodite parents; and further, *cul-2(ek1)* embryos completely lack anti-CUL-2 staining (Feng et al., 1999). The initiation of the metaphase to anaphase transition in the two meiotic stages therefore appears to be differentially regulated.

CUL-2 ubiquitin ligase complex components share meiotic and polarity functions

In mammals, elongin C has been shown to interact only with CUL2 and CUL5 but not with other cullins (Pause et al., 1999; Kamura et al., 2001). CUL2 and CUL5 share homology in the N-terminal region, which is required for elongin C binding (Pause et al., 1999; Pintard et al., 2003b). Inactivation of CUL-5 in *C. elegans* does not produce visible phenotypes (Kamath et al., 2003), suggesting that it is not involved in the meiotic or polarity defects described in this work. RNAi depletion of *elc-1* phenocopies all visible *cul-2* mutant phenotypes including the G1 arrest of germ cells (Hui Feng and E.T.K., unpublished data), as well as the degradation of embryonic CCCH proteins (DeRenzo et al., 2003), suggesting that ELC-1 participates in all known CUL-2 functions. RBX-1 depletion in *C. elegans* phenocopies multiple cullins (Sasagawa et al., 2003; data not shown), consistent with its interaction with multiple cullins in mammals (Ohta et al., 1999). The observation of meiotic and polarity defects upon inactivation of homologs of both core CUL-2 complex components suggests that CUL-2 functions in the context of a conserved ubiquitin ligase complex.

A substrate recognition component (SRC) is required for the core CUL-2 complex to bind substrates. A number of mammalian CUL2 SRCs have been identified that function in distinct CUL2 E3 complexes, including the von Hippel-Lindau tumor suppressor protein (VHL) (Kim and Kaelin, 2003; Kamizono et al., 2001; Brower et al., 2002). Inactivation of the *C. elegans* VHL ortholog produces no embryonic phenotypes (Epstein et al., 2001), indicating that SRCs other than VHL are required for the CUL-2 meiotic and embryonic functions.

Currently, the only genes in *C. elegans* known to specifically affect the meiosis II metaphase-to-anaphase transition are CUL-2 complex components and *zyg-11*. Combining homozygous null alleles of both *cul-2* and *zyg-11* in the same embryo did not enhance the meiotic phenotype, which is consistent with both genes functioning in the same pathway. Both genes also share other embryonic phenotypes, including multiple nuclei, cytoplasmic extensions, and embryonic arrest with approximately 24 cells (Kemphues et al., 1986; Feng et al., 1999; data not shown). ZYG-11 is a leucine-rich repeat protein and this protein-interaction motif is found in a number of SRCs for CUL-1-based SCF E3 complexes (Tyers and Jorgensen, 2000). It is therefore possible that ZYG-11 functions as an SRC in one of the CUL-2-based E3 complexes to promote meiosis; although our data suggests that ZYG-11 does not function with CUL-2 to promote germ cell proliferation. As the localization of PAR-2 independently of MT-foci was not observed in *zyg-11(RNAi)* embryos, currently there is no evidence that ZYG-11 functions to restrain PAR-2 localization in regions distant from MT-organizing centers.

Meiotic timing and A-P polarity

During the extended meiosis II in *cul-2* mutants, the majority of embryos accumulate stable PAR-2 on the anterior cortex near the meiotic spindle. It has been shown that in APC/C mutant

zygotes arrested in meiosis I, the meiotic spindle can initiate the localization of PAR-2 onto the anterior cortex (Wallenfang and Seydoux, 2000). The disorganized 'frayed' appearance of the meiotic spindle observed in older meiosis I-arrested embryos was proposed to initiate the PAR-2 reversal (Wallenfang and Seydoux, 2000). In contrast, our study found that stable anterior PAR-2 localizations occur with meiosis II spindles of normal morphology and with timing similar to the appearance of PAR-2 on the posterior cortex in wild type. In addition, we observed that P granules segregate toward the mislocalized PAR-2; the SPCC migrates further than the meiotic pronucleus; and the cell division plane is often asymmetrically positioned to produce a reversal in daughter cell size. None of these downstream polarity changes are observed in meiosis I-arrested APC/C mutants (Wallenfang and Seydoux, 2000), suggesting either that the meiosis II spindle is fundamentally different than the meiosis I spindle in effecting polarity or that these changes can only manifest upon entry into interphase.

Transient and weak PAR-2 patches occasionally arise on the anterior cortex during meiosis II in wild-type zygotes, which suggests that the intact meiosis II spindle has an intrinsic ability to direct PAR-2 localization (Table 3.2) (Boyd et al., 1996; Cuenca et al., 2003). We observed that the longer *cul-2(RNAi)* zygotes remained in meiosis, the more stabilized the anterior PAR-2 became and the less likely that a posterior PAR-2 patch would form. With only a modest meiosis II delay, a full reversal of PAR localization was observed with PAR-2 exclusively on the anterior and the asymmetric cleavage of the zygote reversed (Table 3.2). The failure of PAR-2 to localize to the posterior in these *cul-2(RNAi)* embryos may derive in part from the aberrant migration of the SPCC to the anterior, which begins during meiosis (Fig. 3.5 E). In *cul-2(RNAi)* embryos, sperm asters generally form during meiosis but are very small until meiosis is completed, presumably due to the effect of the MT-severing katanin MEI-1, which is degraded

after meiosis (Pintard et al., 2003a). Therefore, the failure of the SPCC to form full mitotic asters while in the posterior may contribute to the lack of PAR-2 in that region. In total, our results suggest that only a short window of meiotic timing is compatible with the proper placement of the A-P axis.

CUL-2 limits the inappropriate localization of PAR-2

The establishment of A-P polarity in the *C. elegans* zygote has been proposed to be a MT-directed process (O'Connell et al., 2000; Wallenfang and Seydoux, 2000). In *cul-2(RNAi)* embryos, PAR-2 was observed to initiate cortical localization distant from the meiotic spindle or sperm DNA. Upon elimination of the meiotic spindle by RNAi depletion of the β-tubulin TBB-2, lateral cortical PAR-2 was still observed in *cul-2(RNAi)* embryos at significant although somewhat reduced levels. This suggests that the aberrant PAR-2 localization is not dependent on the presence of a MT organizing center, although MTs may potentiate the localization. The ectopic PAR-2 localization in *cul-2* mutants does not appear to arise as a secondary consequence of the meiosis II delay, as the depletion of CUL-2 produces a significant increase in ectopic PAR-2 localization even in an *emb-30* mutant background in which embryos are arrested in metaphase I. Furthermore, although ZYG-11 is also required for meiotic progression, the localization of PAR-2 distant from the meiotic spindle was not observed in *zyg-11(RNAi)* embryos. We propose that CUL-2 has a separate function to restrain ectopic PAR-2 association with the cortex during meiosis. In combination with the recently described role for CUL-2 in degrading germ cell determinants in anterior cells of the early embryo (DeRenzo et al., 2003), our results indicate that CUL-2 promotes the initiation of A-P polarity through multiple mechanisms.

ACKNOWLEDGEMENTS

We thank Yuji Kohara for cDNA clones; the *Caenorhabditis* Genetics Center for strains, Hui Feng, Vikas Dhingra, Kenneth Kemphues, Susan Strome, Geraldine Seydoux, and Sander van den Heuvel for reagents; and S. van den Heuvel for comments on the manuscript. This work was supported by a grant from the American Cancer Society (RSG-01-251-01-DDC) to ETK.

REFERENCES

Albertson, D. G. and Thomson, J. N. (1993). Segregation of holocentric chromosomes at meiosis in the nematode, *Caenorhabditis elegans*. *Chromosome Res.* **1**, 15-26.

Blanco, M. A., Pelloquin, L. and Moreno, S. (2001). Fission yeast mfr1 activates APC and coordinates meiotic nuclear division with sporulation. *J. Cell Sci.* **114**, 2135-43.

Boyd, L., Guo, S., Levitan, D., Stinchcomb, D. T. and Kemphues, K. J. (1996). PAR-2 is asymmetrically distributed and promotes association of P granules and PAR-1 with the cortex in *C. elegans* embryos. *Development* **122**, 3075-84.

Brenner, S. (1974). The Genetics of *Caenorhabditis elegans*. *Genetics* **77**, 71-94.

Brower, C. S., Sato, S., Tomomori-Sato, C., Kamura, T., Pause, A., Stearman, R., Klausner, R. D., Malik, S., Lane, W. S., Sorokina, I. et al. (2002). Mammalian mediator subunit mMED8 is an Elongin BC-interacting protein that can assemble with Cul2 and Rbx1 to reconstitute a ubiquitin ligase. *Proc. Natl. Acad. Sci. USA* **99**, 10353-8.

Buonomo, S. B., Clyne, R. K., Fuchs, J., Loidl, J., Uhlmann, F. and Nasmyth, K. (2000). Disjunction of homologous chromosomes in meiosis I depends on proteolytic cleavage of the meiotic cohesin Rec8 by separin. *Cell* **103**, 387-98.

Chang, D. C., Xu, N. and Luo, K. Q. (2003). Degradation of cyclin B is required for the onset of anaphase in mammalian cells. *J. Biol. Chem.* **278**, 37865-37873.

Cooper, K. F., Mallory, M. J., Egeland, D. B., Jarnik, M. and Strich, R. (2000). Ama1p is a meiosis-specific regulator of the anaphase promoting complex/cyclosome in yeast. *Proc. Natl. Acad. Sci. USA* **97**, 14548-53.

Cuenca, A. A., Schetter, A., Aceto, D., Kemphues, K. and Seydoux, G. (2003). Polarization of the *C. elegans* zygote proceeds via distinct establishment and maintenance phases. *Development* **130**, 1255-65.

Davis, E. S., Wille, L., Chestnut, B. A., Sadler, P. L., Shakes, D. C. and Golden, A. (2002). Multiple subunits of the *Caenorhabditis elegans* anaphase-promoting complex are required for chromosome segregation during meiosis I. *Genetics* **160**, 805-13.

DeRenzo, C., Reese, K. J. and Seydoux, G. (2003). Exclusion of germ plasm proteins from somatic lineages by cullin-dependent degradation. *Nature* **424**, 685-9.

Epstein, A. C., Gleadle, J. M., McNeill, L. A., Hewitson, K. S., O'Rourke, J., Mole, D. R., Mukherji, M., Metzen, E., Wilson, M. I., Dhanda, A. et al. (2001). *C. elegans* EGL-9 and mammalian homologs define a family of dioxygenases that regulate HIF by prolyl hydroxylation. *Cell* **107**, 43-54.

Feng, H., Zhong, W., Punkosdy, G., Gu, S., Zhou, L., Seabolt, E. K. and Kipreos, E. T. (1999). CUL-2 is required for the G1-to-S phase transition and mitotic chromosome condensation in *Caenorhabditis elegans*. *Nat. Cell. Biol.* **1**, 486-492.

Fire, A., Xu, S., Montgomery, M. K., Kostas, S. A., Driver, S. E. and Mello, C. C. (1998). Potent and specific genetic interference by double-stranded RNA in *Caenorhabditis elegans*. *Nature* **391**, 806-11.

Furuta, T., Tuck, S., Kirchner, J., Koch, B., Auty, R., Kitagawa, R., Rose, A. M. and Greenstein, D. (2000). EMB-30: an APC4 homologue required for metaphase-to-anaphase transitions during meiosis and mitosis in *Caenorhabditis elegans*. *Mol. Biol. Cell* **11**, 1401-19.

Goldstein, B. and Hird, S. N. (1996). Specification of the anteroposterior axis in *Caenorhabditis elegans*. *Development* **122**, 1467-74.

Grill, S. W., Gonczy, P., Stelzer, E. H. and Hyman, A. A. (2001). Polarity controls forces governing asymmetric spindle positioning in the *Caenorhabditis elegans* embryo. *Nature* **409**, 630-3.

Hagting, A., den Elzen, N., Vodermaier, H. C., Waizenegger, I. C., Peters, J. M. and Pines, J. (2002). Human securin proteolysis is controlled by the spindle checkpoint and reveals when the APC/C switches from activation by Cdc20 to Cdh1. *J. Cell Biol.* **157**, 1125-1137.

Herbert, M., Levasseur, M., Homer, H., Yallop, K., Murdoch, A. and McDougall, A. (2003). Homologue disjunction in mouse oocytes requires proteolysis of securin and cyclin B1. *Nat. Cell. Biol.* **5**, 1023-1025.

Hung, T. J. and Kemphues, K. J. (1999). PAR-6 is a conserved PDZ domain-containing protein that colocalizes with PAR-3 in *Caenorhabditis elegans* embryos. *Development* **126**, 127-35.

Joberty, G., Petersen, C., Gao, L. and Macara, I. G. (2000). The cell-polarity protein Par6 links Par3 and atypical protein kinase C to Cdc42. *Nat. Cell. Biol.* **2**, 531-9.

Kamath, R. S., Fraser, A. G., Dong, Y., Poulin, G., Durbin, R., Gotta, M., Kanapin, A., Le Bot, N., Moreno, S., Sohrmann, M. et al. (2003). Systematic functional analysis of the *Caenorhabditis elegans* genome using RNAi. *Nature* **421**, 231-7.

Kamizono, S., Hanada, T., Yasukawa, H., Minoguchi, S., Kato, R., Minoguchi, M., Hattori, K., Hatakeyama, S., Yada, M., Morita, S. et al. (2001). The SOCS box of SOCS-1 accelerates ubiquitin-dependent proteolysis of TEL-JAK2. *J. Biol. Chem.* **276**, 12530-8.

Kamura, T., Burian, D., Yan, Q., Schmidt, S. L., Lane, W. S., Querido, E., Branton, P. E., Shilatifard, A., Conaway, R. C. and Conaway, J. W. (2001). Muf1, a novel Elongin BC-interacting leucine-rich repeat protein that can assemble with Cul5 and Rbx1 to reconstitute a ubiquitin ligase. *J. Biol. Chem.* **276**, 29748-53.

Kemphues, K. J., Wolf, N., Wood, W. B. and Hirsh, D. (1986). Two loci required for cytoplasmic organization in early embryos of *Caenorhabditis elegans*. *Dev. Biol.* **113**, 449-460.

Kim, W. and Kaelin, W. G., Jr. (2003). The von Hippel-Lindau tumor suppressor protein: new insights into oxygen sensing and cancer. *Curr. Opin. Genet. Dev.* **13**, 55-60.

Kitajima, T. S., Miyazaki, S., Yamamoto, A. and Watanabe, Y. (2003). Rec8 cleavage by separase is required for meiotic nuclear divisions in fission yeast. *EMBO J.* **22**, 5643-5653.

Nebreda, A. R. and Ferby, I. (2000). Regulation of the meiotic cell cycle in oocytes. *Curr. Opin. Cell Biol.* **12**, 666-75.

Nixon, V. L., Levasseur, M., McDougall, A. and Jones, K. T. (2002). Ca(2+) oscillations promote APC/C-dependent cyclin B1 degradation during metaphase arrest and completion of meiosis in fertilizing mouse eggs. *Curr. Biol.* **12**, 746-50.

O'Connell, K. F., Maxwell, K. N. and White, J. G. (2000). The *spd-2* gene is required for polarization of the anteroposterior axis and formation of the sperm asters in the *Caenorhabditis elegans* zygote. *Dev. Biol.* **222**, 55-70.

Ohta, T., Michel, J. J., Schottelius, A. J. and Xiong, Y. (1999). ROC1, a homolog of APC11, represents a family of cullin partners with an associated ubiquitin ligase activity. *Mol. Cell* **3**, 535-541.

Pasierbek, P., Jantsch, M., Melcher, M., Schleiffer, A., Schweizer, D. and Loidl, J. (2001). A *Caenorhabditis elegans* cohesion protein with functions in meiotic chromosome pairing and disjunction. *Genes Dev.* **15**, 1349-60.

Pause, A., Peterson, B., Schaffar, G., Stearman, R. and Klausner, R. D. (1999). Studying interactions of four proteins in the yeast two-hybrid system: structural resemblance of the pVHL/elongin BC/hCUL-2 complex with the ubiquitin ligase complex SKP1/cullin/F-box protein. *Proc. Natl. Acad. Sci. USA* **96**, 9533-8.

Pellettieri, J. and Seydoux, G. (2002). Anterior-posterior polarity in *C. elegans* and *Drosophila*-PARallels and differences. *Science* **298**, 1946-50.

Peter, M., Castro, A., Lorca, T., Le Peuch, C., Magnaghi-Jaulin, L., Doree, M. and Labbe, J. C. (2001). The APC is dispensable for first meiotic anaphase in *Xenopus* oocytes. *Nat. Cell. Biol.* **3**, 83-7.

Peters, J. M. (2002). The anaphase-promoting complex: proteolysis in mitosis and beyond. *Mol. Cell* **9**, 931-43.

Petronczki, M., Siomos, M. F. and Nasmyth, K. (2003). Un Menage a Quatre. The Molecular Biology of Chromosome Segregation in Meiosis. *Cell* **112**, 423-40.

Pickart, C. M. (2001). Mechanisms underlying ubiquitination. *Annu. Rev. Biochem.* **70**, 503-33.

Pintard, L., Kurz, T., Glaser, S., Willis, J. H., Peter, M. and Bowerman, B. (2003a). Neddylation and deneddylation of CUL-3 is required to target MEI-1/Katanin for degradation at the meiosis-to-mitosis transition in *C. elegans*. *Curr. Biol.* **13**, 911-21.

Pintard, L., Willis, J. H., Willems, A., Johnson, J. L., Srayko, M., Kurz, T., Glaser, S., Mains, P. E., Tyers, M., Bowerman, B. et al. (2003b). The BTB protein MEL-26 is a substrate-specific adaptor of the CUL-3 ubiquitin-ligase. *Nature* **425**, 311-6.

Rogers, E., Bishop, J. D., Waddle, J. A., Schumacher, J. M. and Lin, R. (2002). The aurora kinase AIR-2 functions in the release of chromosome cohesion in *Caenorhabditis elegans* meiosis. *J. Cell Biol.* **157**, 219-29.

Sasagawa, Y., Urano, T., Kohara, Y., Takahashi, H. and Higashitani, A. (2003). *Caenorhabditis elegans* RBX1 is essential for meiosis, mitotic chromosomal condensation and segregation, and cytokinesis. *Genes Cells* **8**, 857-72.

Schneider, S. Q. and Bowerman, B. (2003). Cell polarity and the cytoskeleton in the *Caenorhabditis elegans* zygote. *Annu. Rev. Genet.* **37**, 221-49.

Shelton, C. A. and Bowerman, B. (1996). Time-dependent responses to *glp-1*-mediated inductions in early *C. elegans* embryos. *Development* **122**, 2043-50.

Siomos, M. F., Badrinath, A., Pasierbek, P., Livingstone, D., White, J., Glotzer, M. and Nasmyth, K. (2001). Separase is required for chromosome segregation during meiosis I in *Caenorhabditis elegans*. *Curr. Biol.* **11**, 1825-35.

Stemmann, O., Zou, H., Gerber, S. A., Gygi, S. P. and Kirschner, M. W. (2001). Dual inhibition of sister chromatid separation at metaphase. *Cell* **107**, 715-26.

Strome, S. and Wood, W. B. (1982). Immunofluorescence visualization of germ-line-specific cytoplasmic granules in embryos, larvae, and adults of *Caenorhabditis elegans*. *Proc. Natl. Acad. Sci. USA* **79**, 1558-62.

Strome, S. and Wood, W. B. (1983). Generation of asymmetry and segregation of germ-line granules in early *C. elegans* embryos. *Cell* **35**, 15-25.

Tabuse, Y., Izumi, Y., Piano, F., Kemphues, K. J., Miwa, J. and Ohno, S. (1998). Atypical protein kinase C cooperates with PAR-3 to establish embryonic polarity in *Caenorhabditis elegans*. *Development* **125**, 3607-14.

Timmons, L., Court, D. L. and Fire, A. (2001). Ingestion of bacterially expressed dsRNAs can produce specific and potent genetic interference in *Caenorhabditis elegans*. *Gene* **263**, 103-12.

Tyers, M. and Jorgensen, P. (2000). Proteolysis and the cell cycle: with this RING I do thee destroy. *Curr. Opin. Genet. Dev.* **10**, 54-64.

Uhlmann, F., Wernic, D., Poupart, M. A., Koonin, E. V. and Nasmyth, K. (2000). Cleavage of cohesin by the CD clan protease separin triggers anaphase in yeast. *Cell* **103**, 375-86.

Wallenfang, M. R. and Seydoux, G. (2000). Polarization of the anterior-posterior axis of *C. elegans* is a microtubule-directed process. *Nature* **408**, 89-92.

Watts, J. L., Etemad-Moghadam, B., Guo, S., Boyd, L., Draper, B. W., Mello, C. C., Priess, J. R. and Kemphues, K. J. (1996). *par-6*, a gene involved in the establishment of asymmetry in early *C. elegans* embryos, mediates the asymmetric localization of PAR-3. *Development* **122**, 3133-40.

Wittmann, T., Hyman, A. and Desai, A. (2001). The spindle: a dynamic assembly of microtubules and motors. *Nat. Cell. Biol.* **3**, E28-34.

FIGURE LEGENDS

Fig. 3.1. CUL-2 complex components and ZYG-11 are required for progression into meiotic anaphase II. (A) Histone H2B::GFP epifluorescence movie sequences of live zygotes of the indicated genotype. Time post-fertilization is indicated in the upper left corner (hours:minutes). Interphase denotes the initiation of chromosome decondensation after meiotic exit. The

metaphase images are generally transverse views to show the pentagonal array except for the *elc-1* (00:01) and *zyg-11(mn40)* (00:25), which are side views showing paired homologous chromosomes and sister chromatids, respectively. Arrowheads denote polar bodies. (B) The duration of meiosis I post-fertilization (left) and meiosis II (right) derived from histone H2B::GFP movies. See the materials and methods section for the number of embryos analyzed. (C) Histone H2B::GFP images of separated metaphase II chromosomes in *cul-2(RNAi)* and *cul-2(ek1)* embryos. Scale bars, 5 μm.

Fig. 3.2. The *cul-2* meiotic phenotypes are not caused by a failure to remove the cohesin REC-8 from sister chromatids. (A) Immunofluorescence images of REC-8 in wild type and *cul-2(RNAi)* embryos. Images of wild type (top) and *cul-2(RNAi)* zygotes (bottom) stained with DAPI and anti-REC-8 antibody at the indicated meiotic stages. Note that in late metaphase II *cul-2(RNAi)* zygotes, REC-8 is not detected but chromosomes fail to segregate. (B) Depletion of *rec-8* by RNAi does not rescue the meiotic delay in *cul-2(RNAi)* zygotes. Histone H2B::GFP fluorescence movie sequences in *rec-8(RNAi)* or *cul-2(RNAi)*; *rec-8(RNAi)* double RNAi embryos. In the *rec-8(RNAi)* zygote, chromosomes compress and rapidly move to the cell cortex between time points 00:17 and 00:22. Time from fertilization (hours:minutes) is in the upper left corner of images. Stars denote meiotic chromosomes or interphase pronuclei. Dashed lines denote the egg boundary. Arrowheads denote polar bodies. Scale bars, 5 μm.

Fig. 3.3. Cyclin B1 is not degraded during meiosis in *cul-2(RNAi)* embryos. (A) DIC (top) and epifluorescence (bottom) images of wild type and *cul-2(RNAi)* gravid adults expressing a

cyb-1::GFP transgene. Embryo stages are labeled. Note that CYB-1::GFP signal is absent in the wild-type pronuclei stage embryo (immediately after meiosis) but perdures in *cul-2(RNAi)* embryos. Intestine autofluorescence is observed above the oocyte and eggs. Scale bar, 10 μm. (B) Graph of CYB-1::GFP epifluorescence intensity at times post-fertilization. Data was collected under the same conditions for each embryo and is presented in equivalent arbitrary units. The completion of meiosis is denoted by a thick striped bar. (C) Meiosis II timing for individual embryos of the strains listed, derived from histone H2B::GFP movies.

Fig. 3.4. The meiosis II spindle in *cul-2(RNAi)* zygotes maintains a normal morphology for an extended period. (A) β-tubulin::GFP epifluorescence movie sequences of live wild type (upper) and *cul-2(RNAi)* (lower) zygotes to show meiotic II spindle dynamics. Time post-anaphase I is indicated in the upper left corner of images (hours:minutes). (B) Overlaid epifluorescence images of anti-α-tubulin (green) and DAPI (red) staining of meiosis II spindles for wild type (right) and *cul-2(RNAi)* (left) zygotes. The stage of meiosis is indicated above the image. Scale bars, 5 μm.

Fig. 3.5. Polarity defects in *cul-2*, *elc-1*, *rbx-1*, and *zyg-11* RNAi embryos. (A) Overlaid epifluorescence images of anti-PAR-2 (green, upper panel), anti-PAR-6 (green, middle panel), anti-PAR-3 (green, lower panel), anti-α-tubulin (red), and DAPI (blue) staining in wild type (left) and *cul-2(RNAi)* (middle and right) zygotes. The wild type zygotes are in interphase, while the *cul-2(RNAi)* zygotes are in meiosis II. Red stars denote meiotic spindles; red arrows, sperm asters; ‘o’, maternal pronuclei; ‘s’, sperm DNA; white arrowheads, polar bodies; and white arrows, regions of the cortex lacking PAR-6 or PAR-3 staining. (B) Matched DIC and PAR-

2::GFP or PAR-6::GFP images of two-cell stage wild type, *cul-2(RNAi)*, *elc-1(RNAi)*, and *rbx-1(RNAi)* embryos. (C) Overlaid epifluorescence images of anti-PAR-2 (green), anti-α-tubulin (red), and DAPI (blue) staining in *zyg-11(RNAi)* one-cell (left) and two-cell stage (right) embryos. (D) P granule localization in mitotic *cul-2(RNAi)* embryos; PAR-2::GFP (green); anti-P granule (red); and DAPI (blue). White arrowheads denote polar bodies. (E) Diagram of migration of spindles and pronuclei in wild type (left) and *cul-2(RNAi)* zygotes (middle and right) derived from β-tubulin::GFP/DIC movies. Timing begins with the initial observation of sperm asters and ends at pronuclei meeting. In five of five *cul-2(RNAi)* embryos, the sperm asters formed during meiosis, although they were very small relative to their size after meiosis. Anterior is to the left. Scale bars, 10 μm.

Fig. 3.6. Ectopic lateral PAR-2 in *cul-2(RNAi)* embryos. (A) The initial localization of lateral PAR-2 as monitored in epifluorescence movies of *cul-2(RNAi)* embryos expressing PAR-2::GFP and β-tubulin::GFP (top) and PAR-2::GFP and histone H2B::GFP (bottom). Green arrows denote cortical PAR-2. The cortical PAR-2::GFP signals were observed in regions that were distal to the meiotic spindle (top) or oocyte and sperm DNAs (bottom) during the entire time period post-fertilization. (B) Epifluorescence (top) and confocal three-dimensional reconstruction of *cul-2(RNAi)* embryo showing circular PAR-2 pattern; PAR-2::GFP (green); anti-α-tubulin (red); and DAPI (blue). Note that the confocal reconstruction is only of the embryo and excludes the surrounding germ cell DAPI signal. In the bottom image, anterior is in front. (C) Simultaneous localization of PAR-2 and PAR-6 in meiosis II-stage *cul-2(RNAi)* embryos. Left images, anterior and lateral PAR-2::GFP (top) with uniform anti-PAR-6 staining (bottom). Right images, anterior anti-PAR-2 with anterior exclusion of PAR-6::GFP. (D) PAR-

2::GFP localization in *tbb-2(RNAi)* and *tbb-2; cul-2* double RNAi meiotic embryos. Epifluorescence images of PAR-2::GFP (green, top), DAPI (blue, top), and anti-α-tubulin (red, bottom); 'o', marks the location of maternal DNA; 's', marks the location of sperm DNA. The middle *tbb-2; cul-2* double RNAi embryo has a lateral PAR-2::GFP patch, while the right embryo has PAR-2::GFP on the end of the embryo near both the maternal and condensed sperm DNAs. (E) *emb-30(tn377)* (left) and *emb-30(tn377); cul-2(RNAi)* (right) zygotes were stained with anti-α-tubulin (red) and either anti-PAR-2 (green, upper panel) or anti-PAR-6 (green, lower panel). For each genotype: the left panels show anterior PAR-2 localization (top) or PAR-6 exclusion (bottom); the right panels show lateral/posterior PAR-2 localization (top) or PAR-6 exclusion (bottom). White arrows denote regions of the cortex lacking PAR-6 staining. Anterior is to the left. Scale bars, 10 μm.

Table 3.1. PAR-2 localization in *cul-2*, *zyg-11*, and *tbb-2* RNAi embryos.

condition	n	PAR-2 localization in meiosis II embryos (%)					
		anterior	lateral*	circular*	faint all around	none	posterior
cul-2(RNAi); PAR-2 antibody	67	76.1	12.1 (7.5)	0	0	9.0	3.0
zyg-11(RNAi); PAR-2 antibody	58	69.0	3.4 (0)	0	3.4	19.0	5.2
cul-2(RNAi); PAR-2::GFP	54	44.4	13.0 (3.7)	29.6 (9.3)	13	0	0
zyg-11(RNAi); PAR-2::GFP	47	59.6	6.4 (0)	12.8 (0)	21.3	0	0
tbb-2; cul-2 RNAi; PAR-2::GFP†	36	0‡	5.6 (5.6)	2.8 (0)	13.9	77.8	2.8‡
tbb-2(RNAi); PAR-2::GFP†	11	0	0	0	0	100	0
PAR-2::GFP	13	7.7 (faint)	0	0	23.1	69.2	0

*Numbers in parentheses denote the percentage of embryos in which the lateral or circular PAR-2 is distant from the meiotic spindle.

†*tbb-2(RNAi)* embryos do not undergo meiosis I, so *tbb-2(RNAi)* numbers represent all embryos in meiosis, rather than just meiosis II embryos.

‡One *cul-2* RNAi; PAR-2::GFP embryo had an ambiguous localization with both meiotic DNA and condensed sperm DNA in the same end with cortical PAR-2::GFP (Fig. 6 E, right). We have assigned the localization to the posterior because the sperm DNA generally remains in one end of the embryo in *tbb-2(RNAi)* embryos while the meiotic DNA location is much more variable.

Table 3.2. Cortical PAR-2 localization and division pattern upon titration of *cul-2* RNAi.

Genotype/ treatment	Meiosis II duration (minutes)	Initiation of anterior or lateral PAR-2 (minutes after start of meiosis II)	Initiation of posterior PAR-2 (minutes)	Cell size in 2-cell stage embryo	PAR-2 localization in 2-cell stage
wild type	17	–	19	AB > P_1	P_1
wild type	14	–	19.	AB > P_1	P_1
wild type	16	3 transient, weak Ant.†	19	AB > P_1	P_1
wild type	17	–	17	AB > P_1	P_1
wild type	17	11 transient, weak Ant.†	18	AB > P_1	P_1
cul-2(RNAi)	16	9 transient, weak Ant.†	20	AB > P_1	P_1
cul-2(RNAi)	16	–	21	AB > P_1	P_1
cul-2(RNAi)	17	–	18	AB > P_1	P_1
cul-2(RNAi)	23	11 transient, weak Ant.†	19	AB > P_1	P_1
cul-2(RNAi)	28	12 Anterior	44	AB > P_1	P_1
cul-2(RNAi)	30	16 Anterior	28	AB > P_1	AB and P_1
cul-2(RNAi)	32	16 Lateral*	35	AB > P_1	P_1
cul-2(RNAi)	37	24 Lateral*	49	AB > P_1	AB and P_1
cul-2(RNAi)	42	29 Anterior	58	AB > P_1	AB and P_1
cul-2(RNAi)	42	21 Lateral*	–	AB = P_1	AB and P_1
cul-2(RNAi)	48	16 Anterior	–	AB < P_1	AB
cul-2(RNAi)	51	33 Anterior	–	AB < P_1	AB

These experiments were performed with a wild-type strain expressing PAR-2::GFP and β-tubulin::GFP (JH1473). All times are from the end of meiotic anaphase I. No occurrence is denoted by dash (–).

*lateral PAR-2 patches arose distant from the meiotic spindle.

†transient and weak anterior PAR-2 patches were of lower intensity than the general interior cytoplasmic PAR-2::GFP signal.

Fig. 3.1.

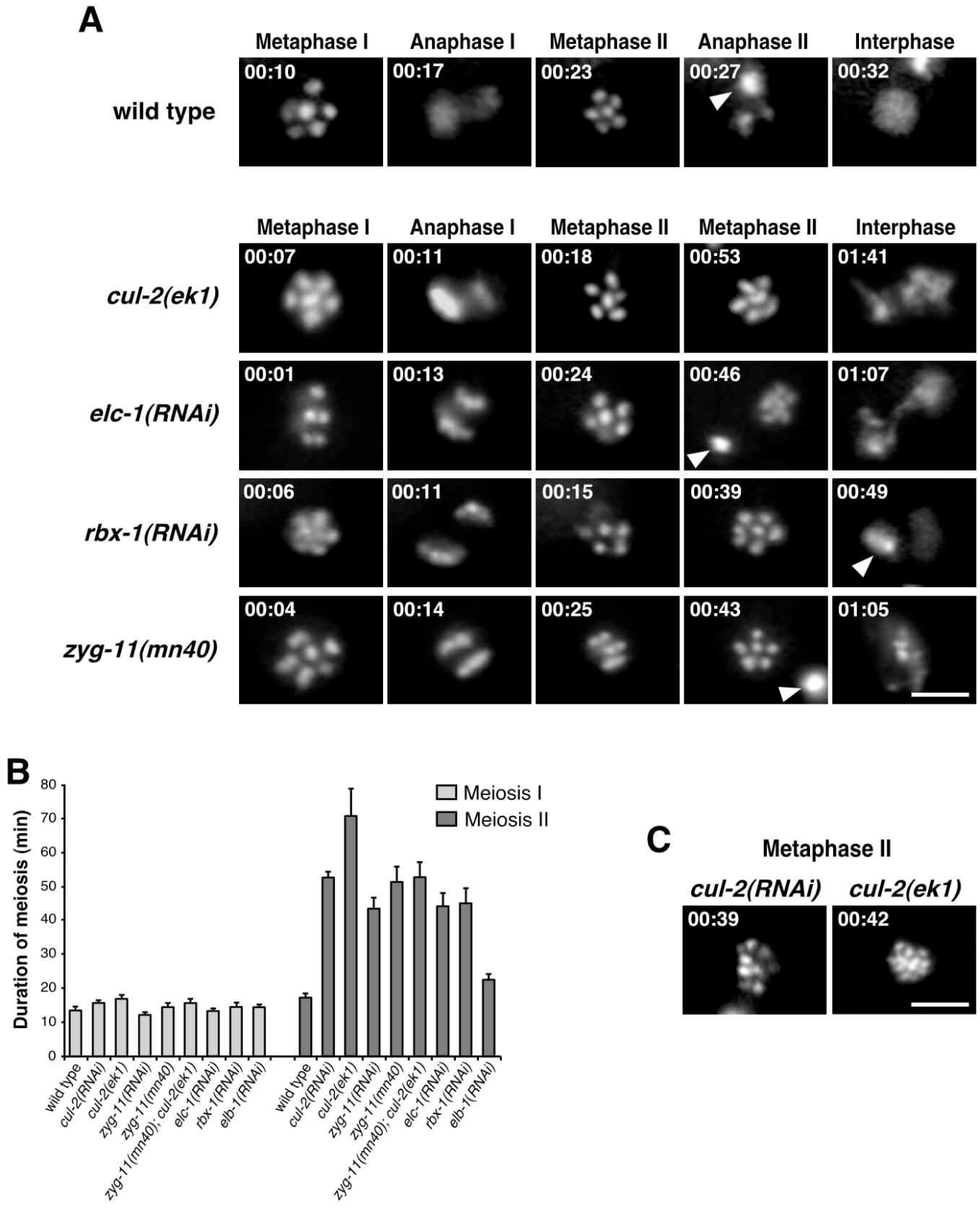
A
Metaphase I
Anaphase I
Metaphase II
Anaphase II
Interphase
wild type
00:10
00:17
00:23
00:27
00:32
Metaphase I
Anaphase I
Metaphase II
Metaphase II
Interphase
cul-2(ek1)
00:07
00:11
00:18
00:53
01:41
elc-1(RNAi)
00:01
00:13
00:24
00:46
01:07
rbx-1(RNAi)
00:06
00:11
00:15
00:39
00:49
zyg-11(mn40)
00:04
00:14
00:25
00:43
01:05
B
Duration of meiosis (min)
Meiosis I
Meiosis II
wild type
cul-2(RNAi)
cul-2(ek1)
zyg-11(RNAi)
zyg-11(mn40)
zyg-11(mn40); cul-2(ek1)
elc-1(RNAi)
rbx-1(RNAi)
elb-1(RNAi)
C
Metaphase II
cul-2(RNAi)
cul-2(ek1)
00:39
00:42

Fig. 3.2.

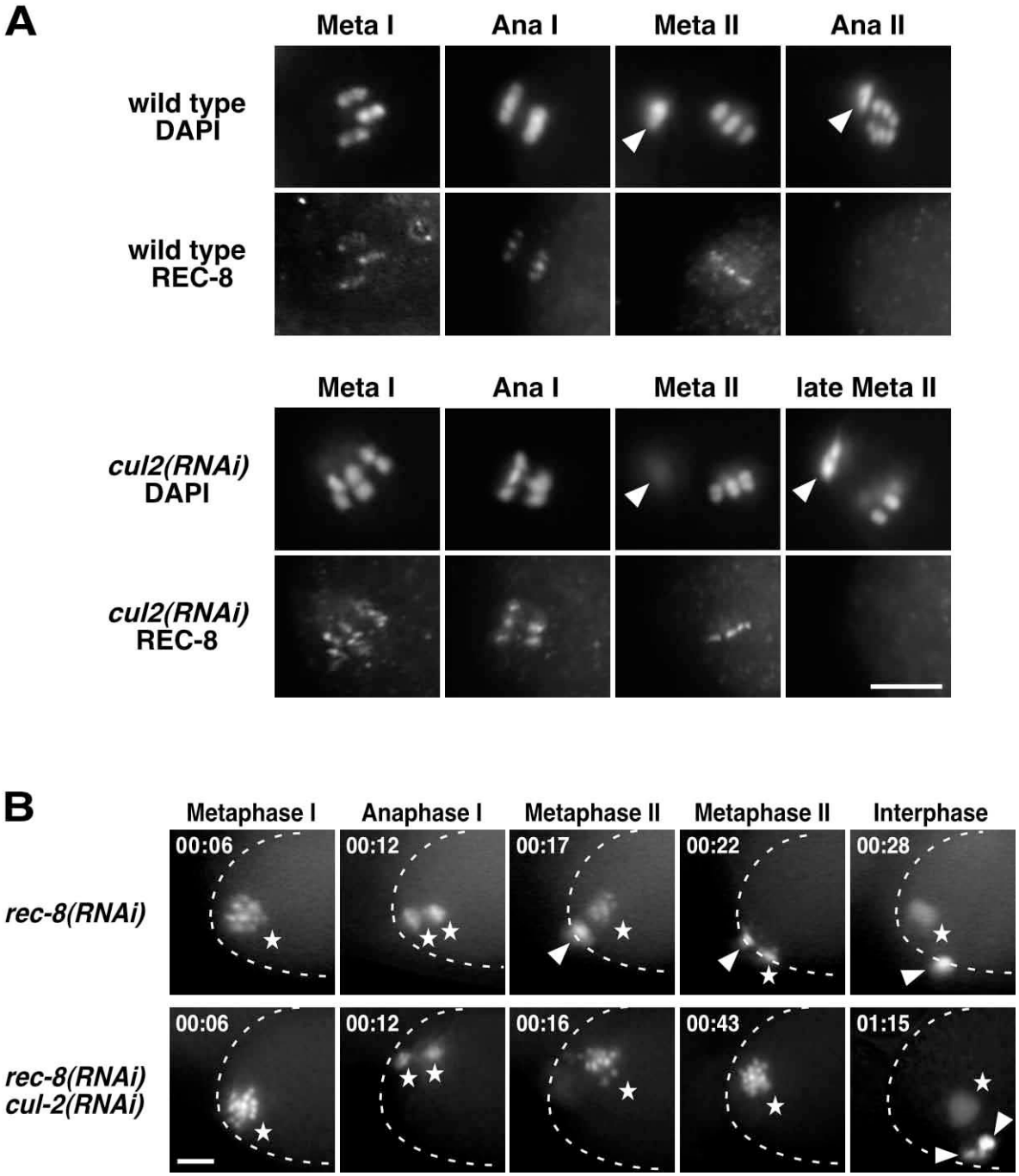
A
Meta I
Ana I
Meta II
Ana II
wild type DAPI
wild type REC-8
Meta I
Ana I
Meta II
late Meta II
cul2(RNAi) DAPI
cul2(RNAi) REC-8
B
Metaphase I
Anaphase I
Metaphase II
Metaphase II
Interphase
rec-8(RNAi)
00:06
00:12
00:17
00:22
00:28
rec-8(RNAi) cul-2(RNAi)
00:06
00:12
00:16
00:43
01:15

Fig. 3.3.

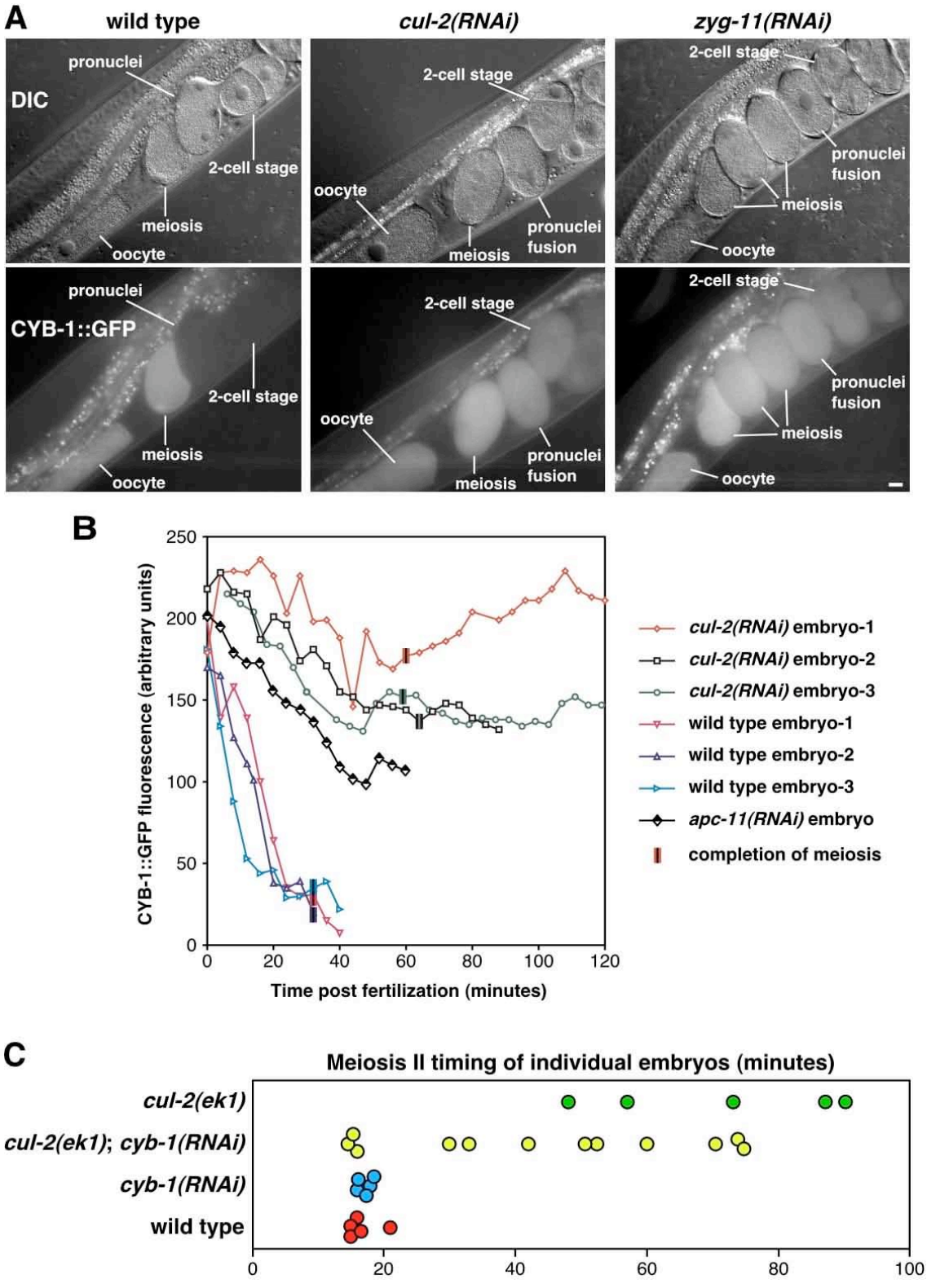
A
wild type
cul-2(RNAi)
zyg-11(RNAi)
DIC
CYB-1::GFP
pronuclei
2-cell stage
meiosis
oocyte
pronuclei fusion
B
CYB-1::GFP fluorescence (arbitrary units)
Time post fertilization (minutes)
cul-2(RNAi) embryo-1
cul-2(RNAi) embryo-2
cul-2(RNAi) embryo-3
wild type embryo-1
wild type embryo-2
wild type embryo-3
apc-11(RNAi) embryo
completion of meiosis
C
Meiosis II timing of individual embryos (minutes)
cul-2(ek1)
cul-2(ek1); cyb-1(RNAi)
cyb-1(RNAi)
wild type

Fig. 3.4.

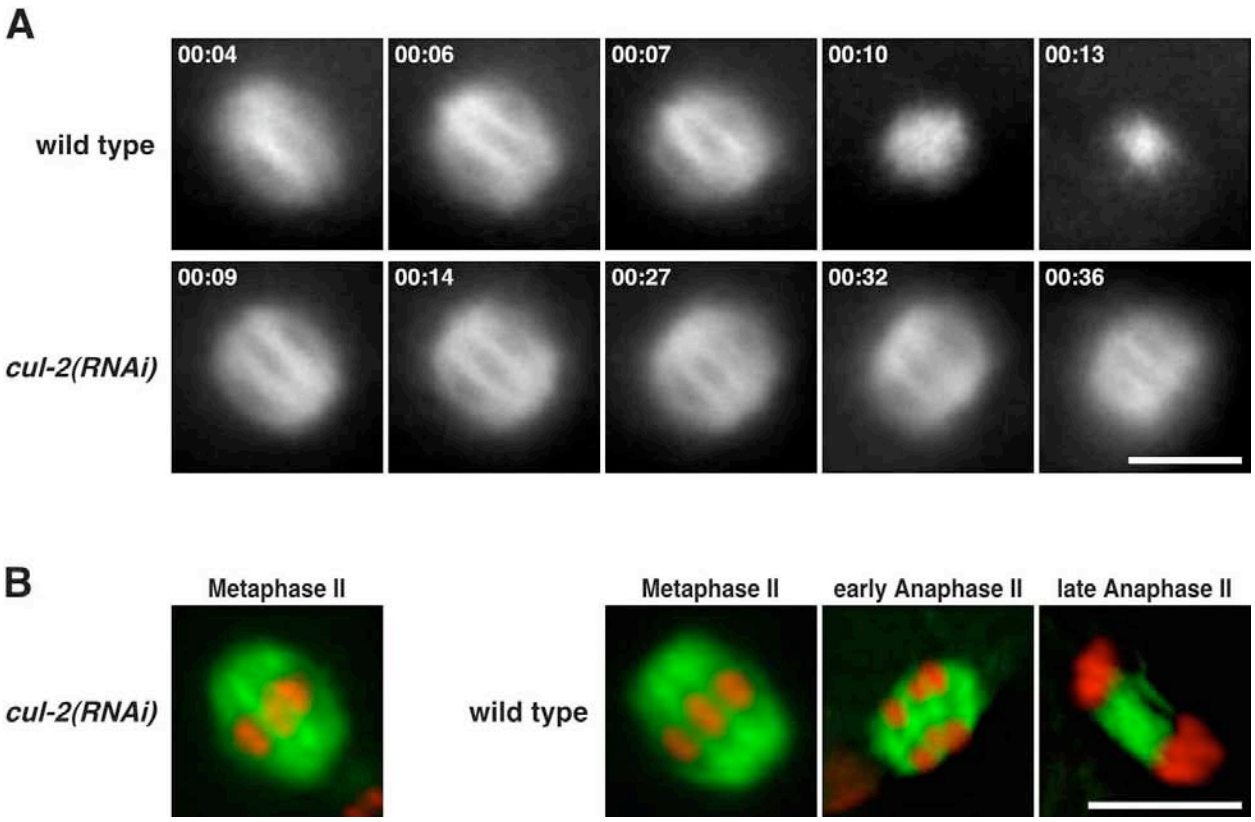
A
wild type
00:04
00:06
00:07
00:10
00:13
cul-2(RNAi)
00:09
00:14
00:27
00:32
00:36
B
Metaphase II
cul-2(RNAi)
wild type
Metaphase II
early Anaphase II
late Anaphase II

Fig. 3.5.

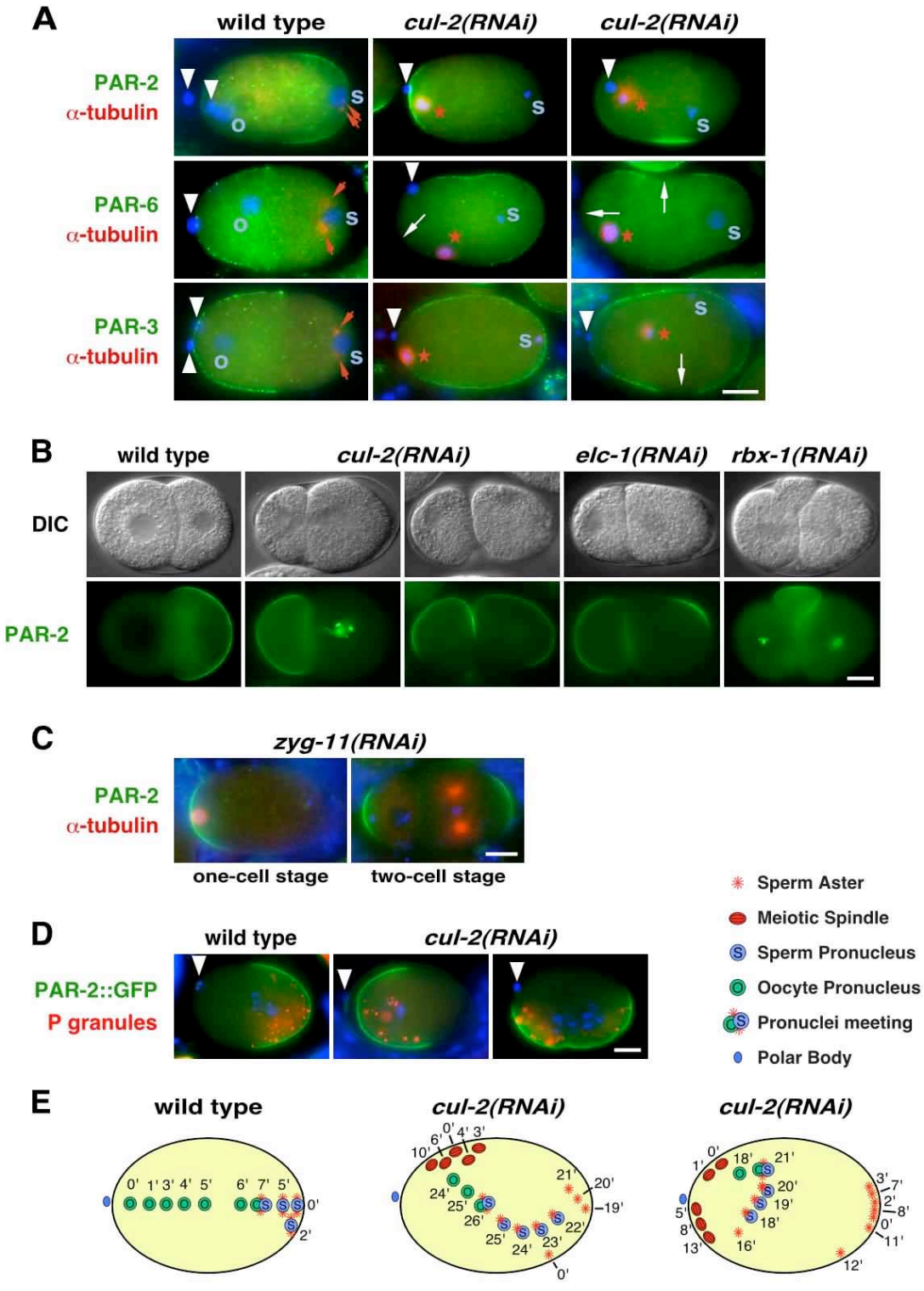
A
wild type
cul-2(RNAi)
cul-2(RNAi)
PAR-2
α-tubulin
PAR-6
α-tubulin
PAR-3
α-tubulin
B
wild type
cul-2(RNAi)
elc-1(RNAi)
rbx-1(RNAi)
DIC
PAR-2
C
zyg-11(RNAi)
PAR-2
α-tubulin
one-cell stage
two-cell stage
D
wild type
cul-2(RNAi)
PAR-2::GFP
P granules
Sperm Aster
Meiotic Spindle
Sperm Pronucleus
Oocyte Pronucleus
Pronuclei meeting
Polar Body
E
wild type
cul-2(RNAi)
cul-2(RNAi)

Fig. 3.6.

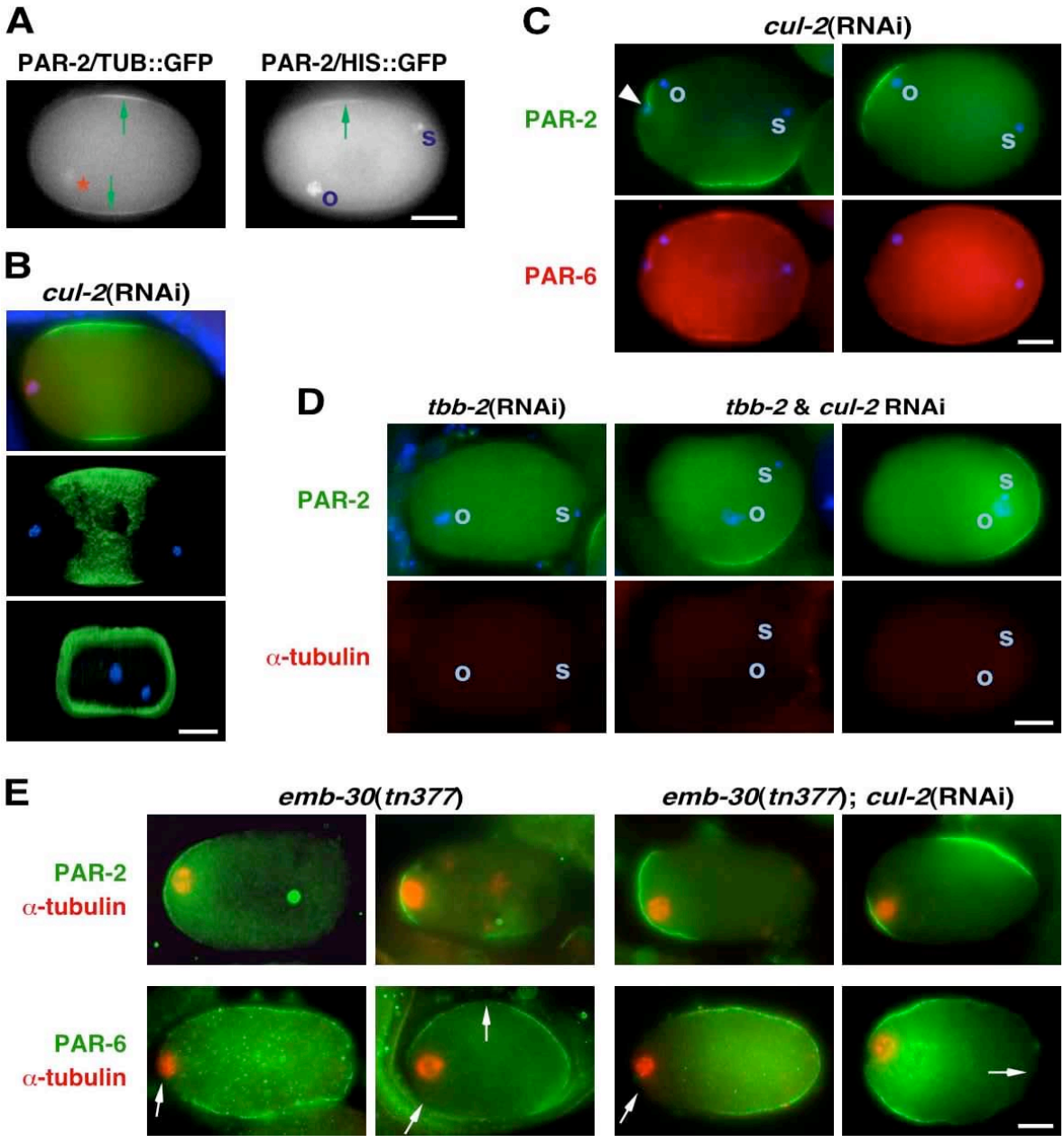
A
PAR-2/TUB::GFP
PAR-2/HIS::GFP
B
cul-2(RNAi)
C
cul-2(RNAi)
PAR-2
PAR-6
D
tbb-2(RNAi)
tbb-2 & cul-2 RNAi
PAR-2
α-tubulin
E
emb-30(tn377)
emb-30(tn377); cul-2(RNAi)
PAR-2
α-tubulin
PAR-6
α-tubulin

CHAPTER 4

THE *C. elegans* CELL CYCLE REGULATOR ZYG-11 DEFINES A CONSERVED FAMILY OF CUL-2 COMPLEX COMPONENTS[2]

[2] **Srividya Vasudevan, Natalia G. Starostina and Edward T. Kipreos.**
EMBO Rep. 2007 Mar;8(3): 279-86
Reprinted here with the permission of the publisher.

ABSTRACT

CUL-2 is a central component of a subclass of multisubunit cullin-RING ubiquitin ligases. The specificity of CUL-2 based complexes is provided by variable substrate-recognition subunits that bind specific substrates. In *C. elegans*, CUL-2 regulates a number of key processes in cell division and embryonic development, including meiotic progression, anterior-posterior polarity, and mitotic chromatin condensation. However, the substrate-recognition subunit(s) that work in these CUL-2-dependent processes were unknown. Here we present evidence that ZYG-11 is the substrate-recognition subunit for a CUL-2-based complex that regulates these functions. We observe that ZYG-11 interacts with CUL-2 *in vivo* and binds to the complex adaptor protein Elongin C using a nematode-variant of the VHL-box motif. We show that the ZYG11 gene family encompasses two major branches within metazoa, and provide evidence that members of the extended ZYG11 family in nematodes and humans are conserved components of CUL2-based ubiquitin ligases.

INTRODUCTION

Members of the cullin-RING family of ubiquitin ligases (E3s) function in a wide-range of dynamic cellular processes, including the cell cycle, signal transduction, and transcription (Petroski and Deshaies, 2005). Ubiquitin ligases facilitate the transfer of ubiquitin from a ubiquitin-conjugating enzyme (E2) to the substrate. The cullin CUL2 is a central component of multisubunit E3 complexes (designated CBC) that include the adaptor protein Elongin C, a ubiquitin like protein Elongin B, the RING finger protein Rbx1/Roc1 and a variable substrate recognition subunit (SRS) (Petroski and Deshaies, 2005). In mammals, three CBC complex SRSs have been identified: the von Hippel-Lindau tumor suppressor (VHL), which degrades hypoxia-inducible factor-α (HIF-α) under normoxic conditions; LRR-1, which suppresses 4-1-BB receptor signaling in $CD4^+$ and $CD8^+$ T cells; and FEM1b, which regulates glucose-stimulated insulin secretion (Jang et al., 2001; Kamura et al., 2004; Kim and Kaelin, 2004; Lu et al., 2005).

Genetic studies of CUL2 complexes in mammals have been limited to analysis of individual SRSs, while the loss of core components, which would inactivate all CBC complexes, has not been analyzed. In *C. elegans*, analysis of *cul-2* mutants has revealed roles for CUL-2 in important cell cycle and developmental processes. In germ cells, CUL-2 is required for the negative regulation of the CDK-inhibitor CKI-1 to allow cell cycle progression from G1 to S phase (Feng et al., 1999). CUL-2 is also required for a number of processes in the early embryo: the meiosis II metaphase-to-anaphase transition; establishment of anterior-posterior polarity; cyclin B degradation; chromosome condensation; mitotic progression; proper cytoplasmic organization; and the degradation of CCCH-finger polarity proteins (DeRenzo et al., 2003; Feng et al., 1999; Liu et al., 2004; Sonneville and Gonczy, 2004). Significantly, RNAi and mutant

analysis of the *C. elegans* homologs of the known mammalian SRSs indicates that they do not function in these processes (Epstein et al., 2001; data not shown). An additional SRS, ZIF-1, has been identified, and it is required for the degradation of CCCH polarity proteins, but not for the other known CUL-2 phenotypes (DeRenzo et al., 2003). Therefore, the SRSs for the CBC complexes that execute the majority of known CUL-2 functions have not been identified.

In this work, we identify ZYG-11 as the SRS for a CBC^{ZYG-11} complex that is responsible for the majority of known CUL-2 functions. We show that ZYG-11 binds to the CUL-2 complex *in vivo* through direct interaction with Elongin C (ELC-1). ZYG-11 binds ELC-1 using a nematode-variant of the VHL-box motif. Phylogenetic analysis identifies two branches of *zyg-11* homologs in diverse metazoa: the ZYG11 and ZER1 subfamilies. We provide evidence that *C. elegans* ZER-1 and human ZYG11B and ZYG11BL associate with CUL-2 *in vivo* through direct interaction with Elongin C. Our work therefore suggests that members of the extended metazoan ZYG11 family function as conserved SRS components for CUL-2 ubiquitin ligase complexes.

RESULTS AND DISCUSSION

ZYG-11 interacts with the CBC complex through VHL-box-mediated binding to ELC-1

zyg-11 was identified as a mutant that disrupted *C. elegans* zygote development (Kemphues et al., 1986). *zyg-11* mutant phenotypes are similar to a subset of phenotypes observed in *cul-2* mutants, including a prolonged delay in meiosis II, a failure to degrade cyclin B, defects in anterior-posterior polarity, and defects in chromatin condensation (Table 4.1). Here we extend the analysis of *cul-2* and *zyg-11* phenotypes. Both *cul-2* and *zyg-11* mutant zygotes enter an extended period of arrest in metaphase II (Liu et al., 2004; Sonneville and Gonczy, 2004). After the meiosis II delay, *zyg-11(mn40)* null mutants complete anaphase (8/8 embryos), although DNA bridges are observed between the separating DNA strands, and the second polar body is

generally not extruded (7/8 embryos). In contrast, *cul-2(ek1)* null mutants either have no discernable anaphase II (3/5 embryos) or have aberrant splitting of DNA after decondensation has started (2/5 embryos). In both *zyg-11* and *cul-2* mutant zygotes, maternal pronuclei subsequently enter mitosis with the paternal pronucleus.

During meiosis II, *cul-2* mutants have one or more large cytoplasmic regions devoid of granules, similar to *zyg-11* mutants (Fig. 4.1 A; Kemphues et al., 1986). In both mutants, these granule-free regions are temporally restricted to the extended meiosis II period (Fig. 4.1 B). The underlying cause of the cleared regions is unknown; and they do not arise from an accumulation of tubulin or actin-based cytoskeleton (Suppl. Fig. 4.1). We observe that the length of mitosis is extended in both *cul-2* and *zyg-11* mutant embryos, however, mitotic timing is significantly longer for *cul-2* than for *zyg-11* (Fig. 4.1C). *cul-2* mutants also exhibit some phenotypes that are not observed in *zyg-11* mutants. *cul-2* mutant embryos undergo an early embryonic arrest with fewer cells (~24) and more uneven DNA distribution than is generally observed for arrested *zyg-11* mutant embryos (Fig. 4.1D). Germ cells in *cul-2* mutants undergo a G1 phase arrest so that there are fewer, larger cells, while *zyg-11* germ cells exhibit normal proliferation (Fig. 4.1E).

The substantial overlap of *cul-2* and *zyg-11* mutant phenotypes suggests that the two proteins might function together. We affinity purified transgenic FLAG-tagged CUL-2 from gravid adults to identify associated proteins. We observed that ZYG-11 co-purified with CUL-2-FLAG using both western blot and mass spectrometry, indicating physical association *in vivo* (Fig. 4.2A; data not shown).

The observation that *zyg-11* mutants exhibit a subset of *cul-2* mutant phenotypes led to the proposal that ZYG-11 may function as an SRS (Liu et al., 2004; Sonneville and Gonczy, 2004), as individual SRSs govern only a subset of CUL-2 functions. SRSs are expected to

physically interact with the adaptor Elongin C (ELC-1) (Stebbins et al., 1999). We asked whether ZYG-11 interacts with ELC-1 using three systems. First, in the yeast two-hybrid system, we observed that ZYG-11 interacted specifically with ELC-1 but not with the related protein SKR-1, which serves as an adaptor for CUL-1 complexes (Nayak et al., 2002; Yamanaka et al., 2002) (Fig. 4.2C). SRSs do not interact independently with the cullin, and consistently, we did not observe interaction between ZYG-11 and CUL-2 (Fig. 4.2C). Second, *in vitro* translated ^{35}S-labeled ZYG-11 interacted with recombinant GST-ELC-1 (Fig. 4.2B). Finally, RNAi depletion of *elc-1* in *C. elegans* reduced the amount of ZYG-11 that co-precipitated with CUL-2-FLAG, suggesting that ELC-1 is required for the association of ZYG-11 with CUL-2 *in vivo* (Fig. 4.2A). The *elc-1* RNAi appeared to be impenetrant because ~15% of *elc-1(RNAi)* embryos hatched, while 100% of *cul-2(RNAi)* and *zyg-11(RNAi)* embryos arrest.

The ZYG-11 protein contains four variant leucine rich repeat (vLRR) motifs and an Armadillo-like helical domain (ARM-like) (Suppl. Fig. 4.2). The regions of ZYG-11 that interact with ELC-1 were mapped using deletion constructs in the two-hybrid system (Fig. 4.3A). The N-terminal region of ZYG-11, which does not contain the vLRR or ARM-like domains, is sufficient for interaction with ELC-1. Mammalian SRSs bind to Elongin C via a three α-helix structure called the VHL box (Kamura et al., 2004), and we identified a divergent VHL-box motif within the N-terminus of ZYG-11 (Fig. 4.3B).

The *C. elegans* VHL-box motif is notably different from that in humans. In particular, there is an aliphatic amino acid rather than a cysteine in the conserved eighth position, and the residues LP in the distal region. The LP corresponds to the LPXP sequence of the mammalian SOCS-box motif, which is related to the VHL-box motif but binds CUL5 complexes rather than CUL2 complexes (Kamura et al., 2004). In humans, the LPXP sequence is in the CUL5-box

region of the SOCS box, and the terminal proline is required for interaction with CUL5 (Kamura et al., 2004). However, the LPXP sequence does not appear to be specific for CUL-5 binding in *C. elegans*, as we observed that a protein that contains the LPXP sequence, ZER-1, physically associates with CUL-2 *in vivo* (Fig. 4.5A).

To determine whether the interaction of ZYG-11 with ELC-1 is dependent on the VHL-box motif, we generated full-length ZYG-11 with missense mutations in the VHL box. When either leucine 18 or leucine 21 of the VHL box were replaced with serines, the interaction of ZYG-11 with ELC-1 was abolished (Fig. 4.3C). The second half of the VHL-box motif is the CUL2-box region, which is required for binding to CUL2 but not Elongin C (Kamura et al., 2004). Consistently, mutation of the proline of the LP motif located within the CUL2 box did not disrupt ZYG-11 binding to ELC-1. Thus, our results indicate that ZYG-11 interaction with ELC-1 utilizes the VHL box.

In total, several lines of evidence support ZYG-11 as an SRS of a new CBC complex. ZYG-11 physically associates with CUL-2 *in vivo*. ZYG-11 binds to the CBC complex adaptor ELC-1; and this association is required for the interaction of ZYG-11 with CUL-2 *in vivo*. ZYG-11 and ELC-1 interaction requires the VHL-box motif of ZYG-11, as expected for a CBC-complex SRS. The phenotypic overlap suggests that a CBC^{ZYG-11} complex is required for promoting: the meiosis II metaphase-to-anaphase transition; the degradation of maternal cyclin B; mitotic chromosome condensation; proper localization of the PAR-2 polarity protein; and cytoplasmic organization (Table 4.1).

Five genes have been identified as interactors of ZYG-11 in the two-hybrid assay: *pal-1*, *mut-2/rde-3*, *ftt-2*, *him-3*, and *W03D8.9* (Li et al., 2004). We asked whether RNAi depletion of any of these genes could specifically enhance or suppress the viability of the temperature

sensitive *zyg-11(b2ts)* mutant. *pal-1* RNAi produces 100% arrested embryos (Gonczy et al., 2000), and therefore could not be analyzed for its effect on viability. RNAi depletions of *mut-2/rde-3, ftt-2,* and *W03D8.9* did not affect *zyg-11(b2ts)* viability (Suppl. Table 4.1). In contrast, *him-3* RNAi increased the percentage of *zyg-11(b2ts)* mutant progeny that hatched at the non-permissive temperature of 25°C [5.6% viability for *zyg-11(b2ts)* alone vs. 11.8% viability for *zyg-11(b2ts), him-3(RNAi)*; $p < 0.01$] (Suppl. Table 4.1). HIM-3 is required for synapsis and chiasma formation as well as chromosome segregation during meiosis (Zetka et al., 1999). RNAi depletion of *him-3* does not significantly affect the timing of meiosis II in *zyg-11(mn40)* mutant zygotes (data not shown). However, *him-3* RNAi promotes the anaphase II extrusion of polar bodies in *zyg-11(b2ts)* mutants; a higher percentage of *zyg-11(b2ts)* embryos grown at 25°C have two polar bodies upon *him-3* RNAi treatment (57%; 12/21) than with no RNAi treatment (30%; 9/30), $p < 0.01$. We analyzed an integrated GFP::*him-3* strain and found that GFP::HIM-3 localized to the region between meiosis I chromosomes during metaphase I but was not present on chromosomes during anaphase I or meiosis II, similar to what has been reported for anti-HIM-3 staining (Zetka et al., 1999). *zyg-11* RNAi treatment did not change the meiotic localization pattern of GFP::HIM-3, suggesting that ZYG-11 does not regulate this event (Suppl. Fig. 4.3).

ZYG-11 homologs

C. elegans has two ZYG11 family members, ZYG-11 and ZER-1; *Drosophila* has a single homolog; sea urchin has two; and mice and humans have three each. All of the ZYG11 family members contain an ARM-like helical domain and at least three vLRR motifs (Fig. 4.4A; Suppl. Fig. 4.2). Phylogenetic analysis shows two major clades within the ZYG11 family that are

supported by a 100% bootstrap score: 1) a ZYG11 clade that contains sea urchin ZYG11B, mammalian ZYG11A and ZYG11B; and 2) a ZER1 clade that contains sea urchin ZYG11BL, *Drosophila* ZYG11BL, and mammalian ZYG11BL (Fig. 4.4B). We have been unable to detect homologs in prokaryotes, protozoa, plants, or fungi, suggesting that ZYG-11 homologs are restricted to metazoa.

The phylogeny implies that the last common ancestor of both Ecdysozoa (which includes insects and nematodes) and Deuterostomes (which includes vertebrates and sea urchin) contained both ZYG11 and ZER1 ancestral genes. The absence of a ZYG11 family member in flies and mosquitoes suggests that the ancestral ZYG11 gene was lost in the insect lineage. In mammals, ZYG11A and ZYG11B appear to have arisen by a recent duplication, and are tandemly adjacent to each other in the mouse and human genomes.

C. elegans and human ZYG-11 homologs interact with the CBC complex via Elongin C

ZER-1 was identified by mass spectrometry among proteins that co-purified with CUL-2-FLAG from *C. elegans* lysate, indicating that ZER-1 associates with CUL-2 *in vivo* (Fig. 4.5A). ZER-1 contains a putative VHL box (Fig. 4.3B) and interacts with ELC-1 in the two-hybrid system, as would be expected for an SRS (Fig. 4.5B). The function of ZER-1 is currently unknown; *zer-1* RNAi depletion does not produce overt phenotypes in either wild-type or *zyg-11* (*mn40*) genetic backgrounds, although *zer-1* RNAi modestly increases the lethality of the temperature sensitive *zyg-11(b2ts)* allele (65% lethality, 96/146, at 20°C with *zer-1* RNAi vs. 45% lethality, 53/118, without RNAi, $p = 0.001$ chi-squares test) (Gonczy et al., 2000; our data).

Human ZYG11B and ZYG11BL have predicted VHL-box motifs in their N-termini (Fig. 4.3B). The largest open reading frame in the human *ZYG11A* cDNA lacks the N-terminal region

containing the VHL box. The 5' region of the human *ZYG11A* cDNA could encode an N-terminal ZYG11 polypeptide but frameshift mutations prevent its inclusion with the larger open reading frame (data not shown). In contrast, the murine *ZYG11A* cDNA has a full, intact coding region. It is possible that human *ZYG11A* is an expressed pseudogene.

In the two-hybrid system, human ZYG11B interacts with Elongin C alone, whereas interaction of human ZYG11BL with Elongin C requires co-expression of Elongin B (Fig. 4.6A), similar to what is observed with human VHL (Pause et al., 1999). Mutation of the VHL box of ZYG11B and ZYG11BL by substituting a conserved leucine residue with a serine significantly reduced or abolished interaction with Elongin C, indicating that the interactions are VHL-box-dependent (Fig. 4.6A). To determine if ZYG11B and ZYG11BL interact with the endogenous CUL2 protein *in vivo*, we transfected human 293T cells with vectors expressing VSV-G-tagged ZYG11B or ZYG11BL. Immunoprecipitation of ZYG11B-VSV-G and ZYG11BL-VSV-G co-precipitated endogenous CUL2, demonstrating that the human ZYG-11 homologs physically associate with CUL2 *in vivo* (Fig. 4.6B). Interestingly, ZYG11B-VSV-G protein accumulated only upon treatment with the proteasome inhibitor LLnL, indicating that the expressed protein is subjected to proteasome-mediated degradation.

In humans, the ZER-1-family member ZYG11BL has high levels of expression in skeletal muscle and the testes, where it is expressed in late pachytene spermatocytes and spermatids (Feral et al., 2001). However, the functions of mammalian ZYG-11 homologs have not been explored. We propose that the ZYG11 family arose within the metazoan lineage specifically to function as SRSs in CBC E3 complexes. Given the multiple essential functions carried out by *C. elegans* ZYG-11, other ZYG11 homologs are anticipated to function in important CUL2-dependent cellular processes.

METHODS

ZYG-11 Antibody

Rabbit polyclonal anti-ZYG-11 antibody was raised against the C-terminal peptide CHSLSSSPVRLVRRV conjugated to KLH (Imject Conjugation kit, Pierce). The antiserum was affinity purified by binding to a HIS-tagged ZYG-11 protein (residues 55 to 799), and precleared by incubation with PVDF membrane containing *zyg-11(RNAi)* lysate.

CUL-2-FLAG affinity purification

Frozen gravid adults expressing CUL-2-FLAG or control vector were ground in liquid nitrogen, then suspended in Lysis buffer (50mM HEPES, pH 7.8, 300 mM NaCl, 10% glycerol, 0.2% Triton X-100, 2 mM DTT, 1 mM EDTA, Roche protease inhibitor cocktail). Lysate was clarified by high-speed (100,000xg 40 min) centrifugation. Extracts were incubated with anti-FLAG M2 antibody-agarose beads (Sigma) in Lysis Buffer with 200 mM NaCl. After washing in the same buffer, CUL-2-FLAG was eluted by incubation with 0.4 mg/ml FLAG peptide, Sigma). CUL-2-FLAG and associated proteins were separated by SDS-PAGE. Gels were stained with Coomassie R-250 (Sigma). Protein bands were in-gel digested with trypsin and analyzed by MALDI-TOF

MS at the University of Georgia Proteomics Center.

ACKNOWLEDGEMENTS

We thank Chris Dowd for technical assistance; Hui Feng for creating the CUL-2-FLAG strain; Yuji Kohara for cDNA clones; the *Caenorhabditis* Genetics Center for strains; and members of the Kipreos laboratory for comments on the manuscript. This work was supported by American Cancer Society grant RSG-01-251-01-DDC.

REFERENCES

DeRenzo, C., Reese, K.J. and Seydoux, G. (2003) Exclusion of germ plasm proteins from somatic lineages by cullin-dependent degradation. *Nature*, **424**, 685-689.

Epstein, A.C., et al. (2001) *C. elegans* EGL-9 and mammalian homologs define a family of dioxygenases that regulate HIF by prolyl hydroxylation. *Cell*, **107**, 43-54.

Feng, H., Zhong, W., Punkosdy, G., Gu, S., Zhou, L., Seabolt, E.K. and Kipreos, E.T. (1999) CUL-2 is required for the G1-to-S-phase transition and mitotic chromosome condensation in *Caenorhabditis elegans*. *Nat Cell Biol*, **1**, 486-492.

Feral, C., Wu, Y.Q., Pawlak, A. and Guellaen, G. (2001) Meiotic human sperm cells express a leucine-rich homologue of *Caenorhabditis elegans* early embryogenesis gene, Zyg-11. *Mol Hum Reprod*, **7**, 1115-1122.

Gonczy, P., et al. (2000) Functional genomic analysis of cell division in *C. elegans* using RNAi of genes on chromosome III. *Nature*, **408**, 331-336.

Jang, L.K., Lee, Z.H., Kim, H.H., Hill, J.M., Kim, J.D. and Kwon, B.S. (2001) A novel leucine-rich repeat protein (LRR-1): potential involvement in 4-1BB-mediated signal transduction. *Mol Cells*, **12**, 304-312.

Kamura, T., Maenaka, K., Kotoshiba, S., Matsumoto, M., Kohda, D., Conaway, R.C., Conaway, J.W. and Nakayama, K.I. (2004) VHL-box and SOCS-box domains determine binding specificity for Cul2-Rbx1 and Cul5-Rbx2 modules of ubiquitin ligases. *Genes Dev*, **18**, 3055-3065.

Kemphues, K.J., Wolf, N., Wood, W.B. and Hirsh, D. (1986) Two loci required for cytoplasmic organization in early embryos of *Caenorhabditis elegans*. *Dev Biol*, **113**, 449-460.

Kim, W.Y. and Kaelin, W.G. (2004) Role of VHL gene mutation in human cancer. *J Clin Oncol*, **22**, 4991-5004.

Li, S., et al. (2004) A map of the interactome network of the metazoan *C. elegans*. *Science*, **303**, 540-543.

Liu, J., Vasudevan, S. and Kipreos, E.T. (2004) CUL-2 and ZYG-11 promote meiotic anaphase II and the proper placement of the anterior-posterior axis in *C. elegans*. *Development*, **131**, 3513-3525.

Lu, D., Ventura-Holman, T., Li, J., McMurray, R.W., Subauste, J.S. and Maher, J.F. (2005) Abnormal glucose homeostasis and pancreatic islet function in mice with inactivation of the Fem1b gene. *Mol Cell Biol*, **25**, 6570-6577.

Nayak, S., Santiago, F.E., Jin, H., Lin, D., Schedl, T. and Kipreos, E.T. (2002) The *Caenorhabditis elegans* Skp1-related gene family: diverse functions in cell proliferation, morphogenesis, and meiosis. *Curr Biol*, **12**, 277-287.

Pause, A., Peterson, B., Schaffar, G., Stearman, R. and Klausner, R.D. (1999) Studying interactions of four proteins in the yeast two-hybrid system: structural resemblance of the pVHL/elongin BC/hCUL-2 complex with the ubiquitin ligase complex SKP1/cullin/F-box protein. *Proc Natl Acad Sci U S A*, **96**, 9533-9538.

Petroski, M.D. and Deshaies, R.J. (2005) Function and regulation of cullin-RING ubiquitin ligases. *Nat Rev Mol Cell Biol,* **6**, 9-20.

Sonneville, R. and Gonczy, P. (2004) *zyg-11* and *cul-2* regulate progression through meiosis II and polarity establishment in *C. elegans*. *Development,* **131**, 3527-3543.

Stebbins, C.E., Kaelin, W.G., Jr. and Pavletich, N.P. (1999) Structure of the VHL-ElonginC-ElonginB complex: implications for VHL tumor suppressor function. *Science,* **284**, 455-461.

Yamanaka, A., Yada, M., Imaki, H., Koga, M., Ohshima, Y. and Nakayama, K. (2002) Multiple Skp1-related proteins in *Caenorhabditis elegans*: diverse patterns of interaction with Cullins and F-box proteins. *Curr Biol,* **12**, 267-275.

Zetka, M.C., Kawasaki, I., Strome, S. and Muller, F. (1999) Synapsis and chiasma formation in *Caenorhabditis elegans* require HIM-3, a meiotic chromosome core component that functions in chromosome segregation. *Genes Dev,* **13**, 2258-2270.

FIGURE LEGENDS

Figure 4.1. *cul-2* and *zyg-11* phenotypes.

(A) DIC and histone H2B::GFP epifluorescence images of *in utero* metaphase II wild-type, *zyg-11(mn40),* and *cul-2(ek4)* zygotes. "m", meiotic spindle region. White arrowheads, first polar body (out-of-focus in the *cul-2* image). Black arrows, granule free areas. **(B)** Graphical representation of the timing of meiotic divisions and the appearance of granule free areas (red boxes) for wild-type, *cul-2(ek1),* and *zyg-11(mn40)* embryos. Anaphase I, blue box; anaphase II, green box. **(C)** Graph of timing of the first mitosis in wild-type, *zyg-11(mn40),* and *cul-2(ek4)* embryos. Mitotic timing was calculated from nuclear envelope breakdown to nuclear envelope

reformation. Error bars, standard error of the mean. Statistical significance: wild type vs. *cul-2*, $p < 1 \times 10^{-6}$; wild type vs. *zyg-11*, $p < 0.05$; *cul-2* vs. *zyg-11*, $p < 0.005$. **(D)** DIC and Histone H2B::GFP images of an early-stage wild-type embryo, and *cul-2* and *zyg-11* arrested embryos collected 24 hrs after being laid. Note that the *cul-2* mutant embryo has a more unequal DNA distribution between cells than wild-type or *zyg-11* mutant embryos. **(E)** DIC micrograph of wild-type, *zyg-11(mn40)*, and *cul-2(ek4)* L4-stage gonad arms. Arrowhead, the distal tip cell. Scale bars, 10 μm.

Figure 4.2. ZYG-11 interacts with CBC components *in vivo* and *in vitro*.

(A) ZYG-11 interacts with CUL-2 *in vivo*. Anti-FLAG affinity purification from animals expressing no transgenes (lane 1), or a CUL-2::FLAG transgene without RNAi treatment (lane 2), with *zyg-11* RNAi (lane 3), or with *elc-1* RNAi (lane 4) were analyzed by western blot with anti-ZYG-11 (top) and anti-FLAG (bottom) antibodies. **(B)** ZYG-11 interacts with GST-ELC-1 *in vitro*. ^{35}S-labeled *in vitro* translated CUL-2 (left panel), ZYG-11 (middle panel), or human p53 (right panel) were incubated with GST or GST-ELC-1. GST-associated proteins were precipitated, separated by SDS-PAGE and analyzed by autoradiography (top) or Coomassie Blue staining (bottom). Input denotes 100% of the *in vitro* translated protein used for the binding reactions. **(C)** ZYG-11 interacts with ELC-1 in the two-hybrid system. Yeast expressing the indicated two-hybrid fusion proteins were streaked on nonselective media (Leu^-, Trp^-) or selective medias (Leu^-, Trp^-, Ade^-; and Leu^-, Trp^-, His^- with 2 mM 3-AT, 3-amino-1,2,4-triazole). VHL-1, a predicted SRS, is included as a positive control.

Figure 4.3. ZYG-11 binds ELC-1 through a VHL box sequence.

(A) Schematic representation of ZYG-11 deletion mutants (top) and two-hybrid interactions with ELC-1 (bottom). The ZYG-11 132-260 amino acid region interacted with ELC-1 under adenine-deficient selection, but not the more stringent histidine-deficient + 2 mM 3-AT selection. **(B)** Alignment of VHL-box sequences of *C. elegans* ZYG-11, VHL-1 and ZER-1, and human VHL, FEM1B, LRR-1, ZYG11B and ZYG11BL. Amino acids that are conserved in over half of the aligned sequences are highlighted: dark green (Ser or Thr), red (Leu), purple (Pro), yellow (Ala), light green (Cys), and orange (aliphatic residues). A consensus is provided above the alignment; ϕ = aliphatic amino acid. Human VHL-box features: α-helices (h); residues that make contact with CUL2 (C); and major (E) or minor (e) contacts with Elongin C (Kamura et al., 2004; Stebbins et al., 1999). **(C)** The ZYG-11 VHL-box sequence and residues mutated to Ser (blue highlight) (top). Interactions of ELC-1 with the ZYG-11 VHL-box mutant constructs in the two-hybrid system (bottom).

Figure 4.4. Evolution of the ZYG11 family.

(A) Schematic of *C. elegans* and human ZYG-11 homologs showing the locations of the VHL box (red), vLRR (green), and Armadillo-like domains (purple). **(B)** Neighbor-Joining phylogeny of *C. elegans*, *S. purpuratus*, *D. melanogaster*, *M. musculus* and *H. sapiens* ZYG11 family members. Bootstrap support values above 50% are listed. Scale bar, amino acid substitutions per site.

Fig. 4.5. ZER-1 interacts with CBC components *in vivo* and *in vitro*.

(A) Coomassie-stained gel of CUL-2-FLAG affinity purification. ZER-1 and CUL-2 were identified by mass spectrometry in the marked protein bands of the CUL-2-FLAG affinity purification, but not from gel slices taken from the equivalent positions of the control purification lane. **(B)** Two-hybrid analysis of interaction of ZER-1 with ELC-1, SKR-1, and CUL-2.

Figure 4.6. Human ZYG11B and ZYG11BL associate with Elongin C and CUL2.

(A) The VHL-box sequences of human ZYG11B and ZYG11BL with residues mutated to Ser shown with blue highlight. Two-hybrid analysis of interaction of ZYG11B and ZYG11BL wild type and Ser mutants with Elongin C in the presence or absence of Elongin B (upper and lower panels, respectively). **(B)** ZYG11B and ZYG11BL associate with endogenous human CUL2 *in vivo*. Expression constructs that were transfected into 293T cells and LLnL pretreatment are noted above the lanes. Immunoprecipitation (IP) was performed with anti-VSV-G antibody. Lysate and IP were analyzed by western blotting with anti-VSV-G (top) and anti-human CUL2 (bottom) antibodies. The asterisk marks antibody heavy chain.

Table 4.1 Comparison of mutant phenotypes of *cul-2* and SRS genes

cul-2	***zyg-11***	***zif-1***	***vhl-1***
Meiotic metaphase II delay[2]	**YES**[2]	NO[5]	NO[4,6]
Failure to degrade maternal cyclin B1 and cyclin B3 [2]	**YES**[2]	ND	ND
Ectopic localization of PAR-2 [2]	**YES**[2]	NO[5]	ND
Cytoplasmic extensions[1]	**YES**[3]	NO[5]	NO[4]
Granule-free areas in zygote[4]	**YES**[3]	NO[5]	NO[4]
Failure of chromosome condensation[1]	**YES**[3]	NO[5]	NO[4,6]
Early embryonic developmental arrest[1]	Partial[3,4]	NO[5]	NO[4,6]
Mitotic delay[1]	Partial[4]	NO[5]	NO[4]
Germ cell arrest in G1 phase, accumulation of CKI-1[1]	NO[4]	NO[5]	NO[4,6]
Failure to degrade CCCH polarity proteins[5]	NO[4]	**YES**[5]	ND

1: (Feng et al., 1999); 2: (Liu et al., 2004; Sonneville and Gonczy, 2004); 3: (Kemphues et al., 1986); 4: our observations; 5: (DeRenzo et al., 2003); 6: (Epstein et al., 2001); ND: not done.

Fig. 4.1.

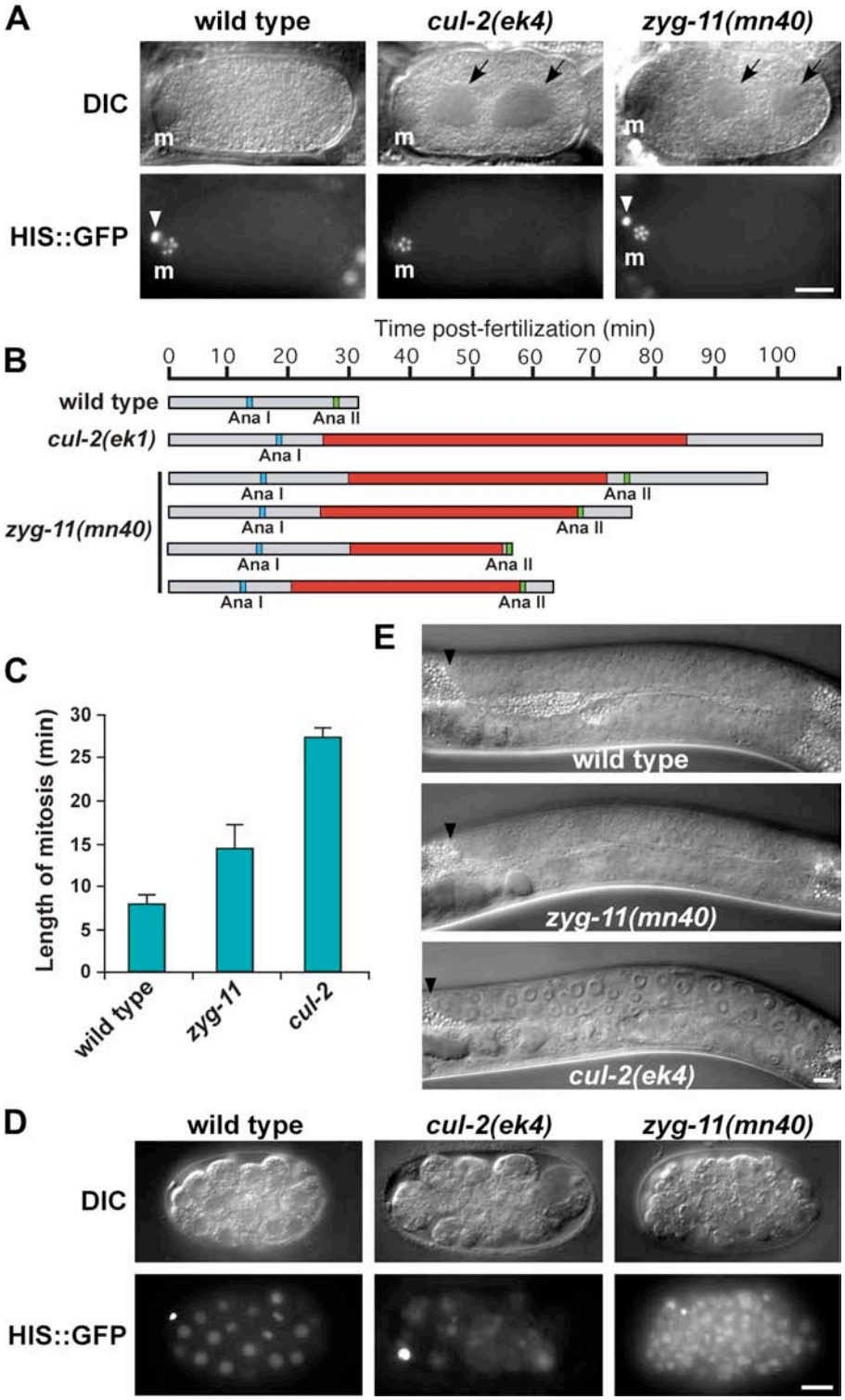
A
wild type
cul-2(ek4)
zyg-11(mn40)
DIC
HIS::GFP
m
B
Time post-fertilization (min)
0 10 20 30 40 50 60 70 80 90 100
wild type
cul-2(ek1)
zyg-11(mn40)
Ana I
Ana II
C
Length of mitosis (min)
0 5 10 15 20 25 30
wild type
zyg-11
cul-2
D
wild type
cul-2(ek4)
zyg-11(mn40)
DIC
HIS::GFP
E
wild type
zyg-11(mn40)
cul-2(ek4)

Fig. 4.2.

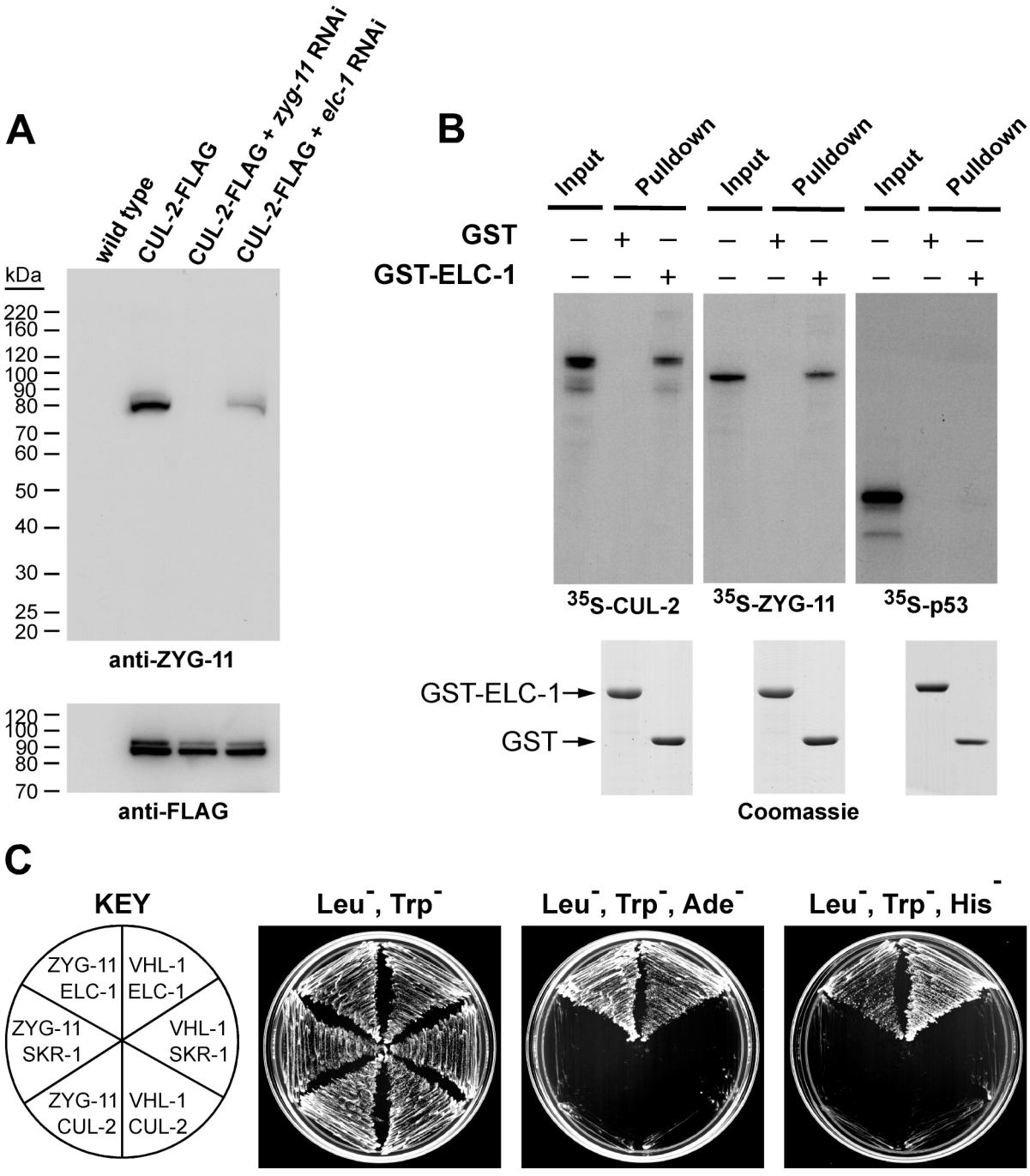
A
wild type
CUL-2-FLAG
CUL-2-FLAG + zyg-11 RNAi
CUL-2-FLAG + elc-1 RNAi
kDa
220
160
120
100
90
80
70
60
50
40
30
25
20
anti-ZYG-11
120
100
90
80
70
anti-FLAG
B
Input
Pulldown
Input
Pulldown
Input
Pulldown
GST
GST-ELC-1
35S-CUL-2
35S-ZYG-11
35S-p53
GST-ELC-1
GST
Coomassie
C
KEY
ZYG-11 ELC-1
VHL-1 ELC-1
ZYG-11 SKR-1
VHL-1 SKR-1
ZYG-11 CUL-2
VHL-1 CUL-2
Leu-, Trp-
Leu-, Trp-, Ade-
Leu-, Trp-, His-

Fig. 4.3.

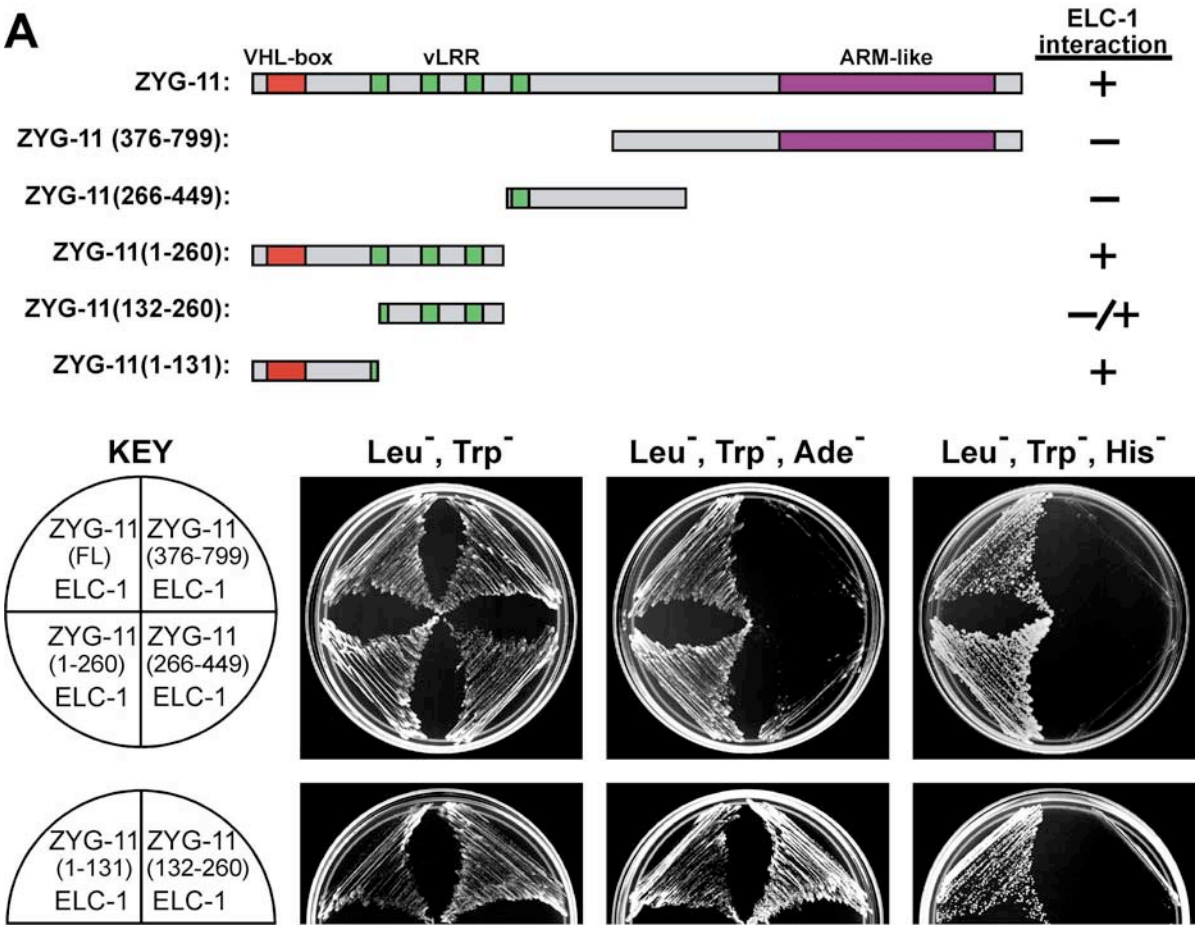
A
VHL-box
vLRR
ARM-like
ELC-1 interaction
ZYG-11:
+
ZYG-11 (376-799):
–
ZYG-11(266-449):
–
ZYG-11(1-260):
+
ZYG-11(132-260):
–/+
ZYG-11(1-131):
+
KEY
ZYG-11 (FL) ELC-1
ZYG-11 (376-799) ELC-1
ZYG-11 (1-260) ELC-1
ZYG-11 (266-449) ELC-1
ZYG-11 (1-131) ELC-1
ZYG-11 (132-260) ELC-1
Leu-, Trp-
Leu-, Trp-, Ade-
Leu-, Trp-, His-

Fig. 4.3.

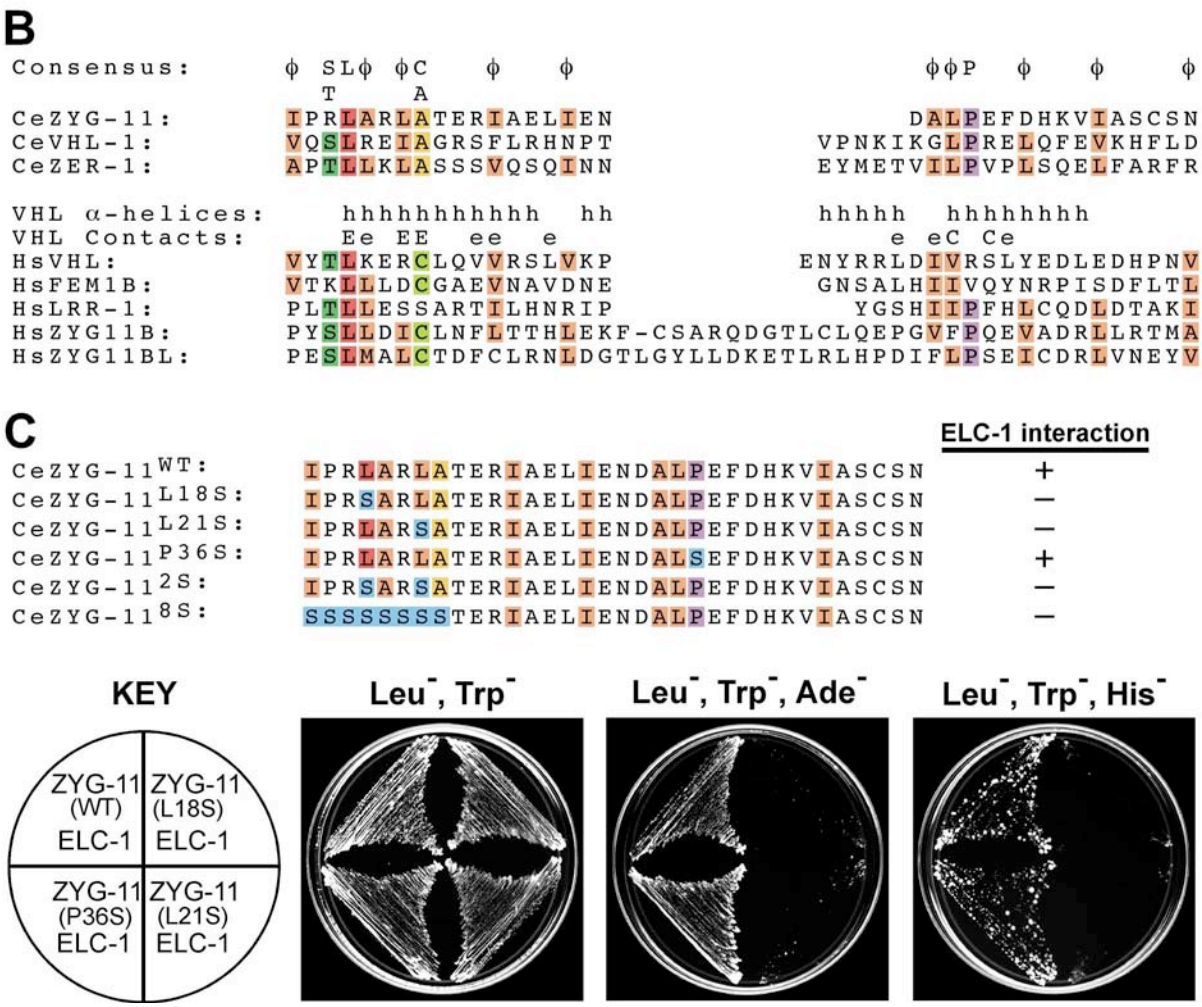
B
Consensus: ϕ SLϕ ϕC ϕ ϕ ϕϕP ϕ ϕ ϕ
T A
CeZYG-11: IPRLARLATERIAELIEN DALPEFDHKVIASCSN
CeVHL-1: VQSLREIAGRSFLRHNPT VPNKIKGLPRELQFEVKHFLD
CeZER-1: APTLLKLASSSVQSQINN EYMETVILPVPLSQELFARFR
VHL α-helices: hhhhhhhhhh hh hhhhh hhhhhhhh
VHL Contacts: Ee EE ee e e eC Ce
HsVHL: VYTLKERCLQVVRSLVKP ENYRRLDIVRSLYEDLEDHPNV
HsFEM1B: VTKLLLDCGAEVNAVDNE GNSALHIIVQYNRPISDFLTL
HsLRR-1: PLTLLESSARTILHNRIP YGSHIIPFHLCQDLDTAKI
HsZYG11B: PYSLLDICLNFLTTHLEKF-CSARQDGTLCLQEPGVFPQEVADRLLRTMA
HsZYG11BL: PESLMALCTDFCLRNLDGTLGYLLDKETLRLHPDIFLPSEICDRLVNEYV
C
ELC-1 interaction
CeZYG-11WT: IPRLARLATERIAELIENDALPEFDHKVIASCSN +
CeZYG-11L18S: IPRSARLATERIAELIENDALPEFDHKVIASCSN –
CeZYG-11L21S: IPRLARSATERIAELIENDALPEFDHKVIASCSN –
CeZYG-11P36S: IPRLARLATERIAELIENDALSEFDHKVIASCSN +
CeZYG-112S: IPRSARSATERIAELIENDALPEFDHKVIASCSN –
CeZYG-118S: SSSSSSSSTERIAELIENDALPEFDHKVIASCSN –
KEY
ZYG-11 (WT) ELC-1
ZYG-11 (L18S) ELC-1
ZYG-11 (P36S) ELC-1
ZYG-11 (L21S) ELC-1
Leu-, Trp-
Leu-, Trp-, Ade-
Leu-, Trp-, His-

Fig. 4.4.

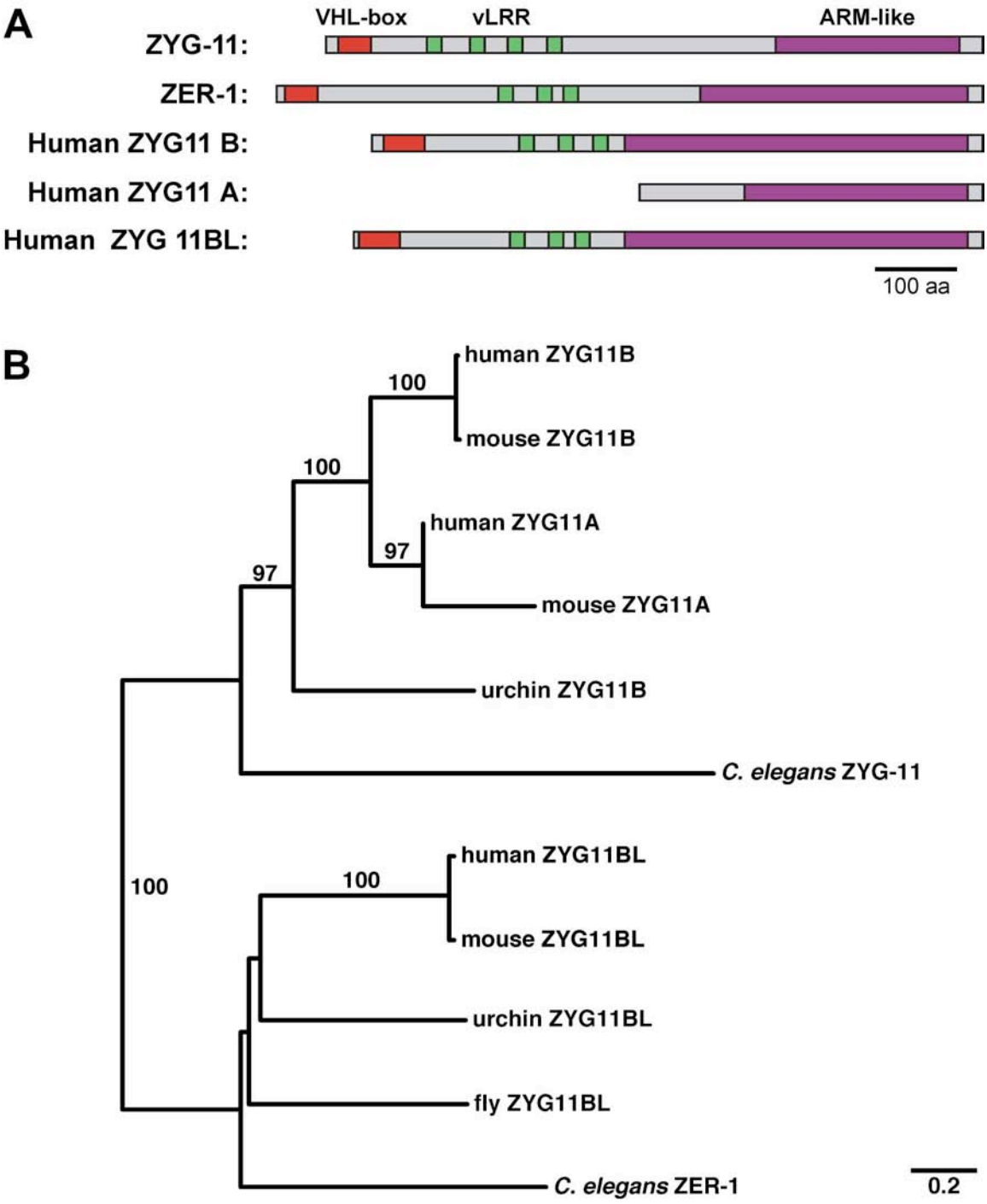
A
VHL-box
vLRR
ARM-like
ZYG-11:
ZER-1:
Human ZYG11 B:
Human ZYG11 A:
Human ZYG 11BL:
100 aa
B
human ZYG11B
mouse ZYG11B
human ZYG11A
mouse ZYG11A
urchin ZYG11B
C. elegans ZYG-11
human ZYG11BL
mouse ZYG11BL
urchin ZYG11BL
fly ZYG11BL
C. elegans ZER-1
100
100
97
97
100
100
0.2

Fig. 4.5.

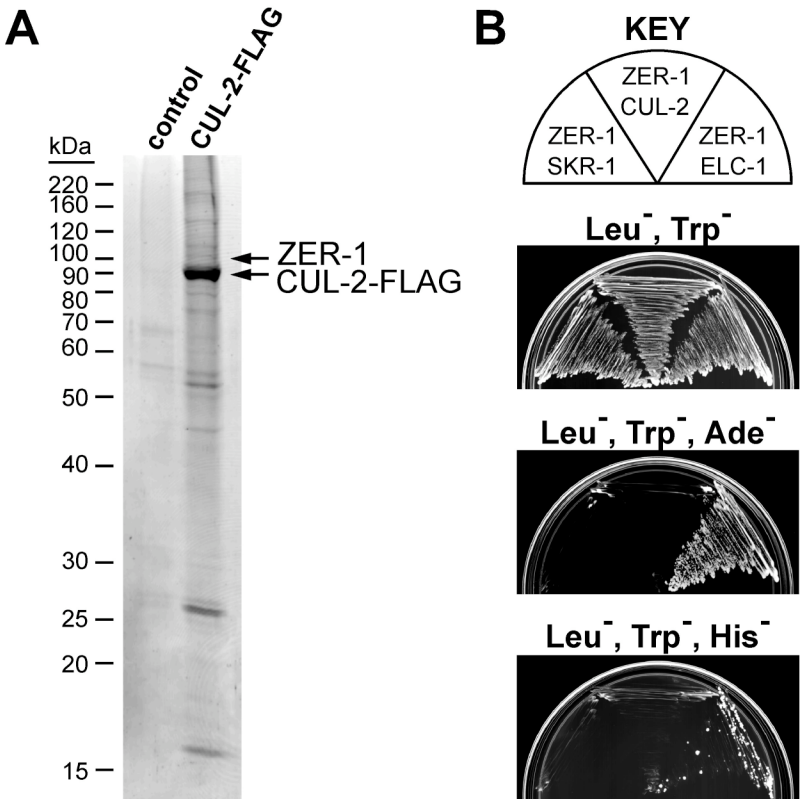
A
control
CUL-2-FLAG
kDa
220
160
120
100
90
80
70
60
50
40
30
25
20
15
ZER-1
CUL-2-FLAG
B
KEY
ZER-1
CUL-2
ZER-1
SKR-1
ZER-1
ELC-1
Leu-, Trp-
Leu-, Trp-, Ade-
Leu-, Trp-, His-

Fig. 4.6.

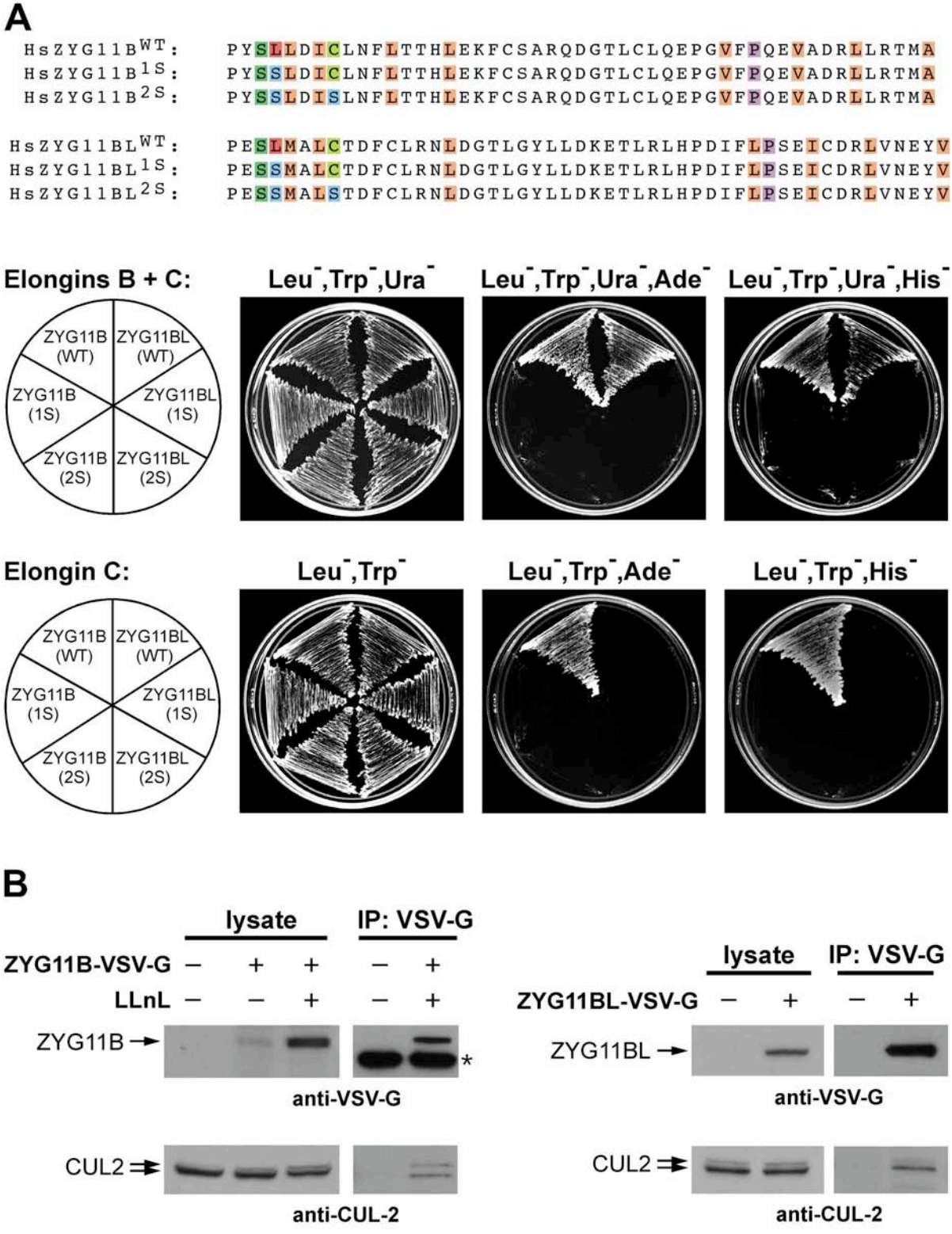
A
HsZYG11B^WT: PYSLLDICLNFLTTHLEKFCSARQDGTLCLQEPGVFPQEVADRLLRTMA
HsZYG11B^1S: PYSSLDICLNFLTTHLEKFCSARQDGTLCLQEPGVFPQEVADRLLRTMA
HsZYG11B^2S: PYSSLDISLNFLTTHLEKFCSARQDGTLCLQEPGVFPQEVADRLLRTMA
HsZYG11BL^WT: PESLMALCTDFCLRNLDGTLGYLLDKETLRLHPDIFLPSEICDRLVNEYV
HsZYG11BL^1S: PESSMALCTDFCLRNLDGTLGYLLDKETLRLHPDIFLPSEICDRLVNEYV
HsZYG11BL^2S: PESSMALSTDFCLRNLDGTLGYLLDKETLRLHPDIFLPSEICDRLVNEYV
Elongins B + C:
Leu-,Trp-,Ura-
Leu-,Trp-,Ura-,Ade-
Leu-,Trp-,Ura-,His-
ZYG11B (WT)
ZYG11BL (WT)
ZYG11B (1S)
ZYG11BL (1S)
ZYG11B (2S)
ZYG11BL (2S)
Elongin C:
Leu-,Trp-
Leu-,Trp-,Ade-
Leu-,Trp-,His-
ZYG11B (WT)
ZYG11BL (WT)
ZYG11B (1S)
ZYG11BL (1S)
ZYG11B (2S)
ZYG11BL (2S)
B
lysate
IP: VSV-G
ZYG11B-VSV-G – + + – +
LLnL – – + – +
ZYG11B
*
anti-VSV-G
CUL2
anti-CUL-2
lysate
IP: VSV-G
ZYG11BL-VSV-G – + – +
ZYG11BL
anti-VSV-G
CUL2
anti-CUL-2

SUPPLEMENTARY METHODS

Nematode strains and analysis

C. elegans strains were maintained according to standard procedures (Brenner, 1974). Strains used were: N2, wild type; ET134, *cul-2(ek4) unc-64(e246)/bli-5(e518)*; ET65, *cul-2(ek1)/unc-64(e246)*; *him-1(e879)*; SP152, *zyg-11(mn40) unc-4(e120)*/*mnC1* (Kemphues et al., 1986); DH2, *zyg-11(b2ts)* (Kemphues et al., 1986); AZ244, *unc-119(ed3)*; *ruIs57* (*unc-119(+), pie-1* promoter::GFP::β-tubulin); AZ212, *unc-119(ed3)*; *ruIs32* (*unc-119(+), pie-1* promoter::GFP:: histone H2B) (Praitis et al., 2001); ET259, *unc-119(ed3)*; *ekIs8* (*unc-119(+), pie-1* promoter:: GFP::*him-3*); and ET099, *cul-2(ek1)/unc-64(e246), ekEx19* (genomic *cul-2(+)* with FLAG-tag sequence inserted before the Stop codon, pRF4 *rol-6(su1006)* plasmid, and N2 genomic DNA). The *cul-2(ek4)* allele carries a mutation within intron 4 near the 5' splice site: a G-to-A transition in nucleotide position 13,172 of cosmid ZK520 that changes the sequence gtgaGtttgcgac to gtgaAtttgcgac. The *cul-2(ek4)* allele is a molecular null, as homozygotes fail to express CUL-2 protein when analyzed by immunofluorescence (data not shown).

RNAi was performed using the feeding protocol with bacterial strain HT115, as described (Timmons and Fire, 1995). Double-T7 expression constructs used to produce dsRNA in bacteria were obtained from the Ahringer library (Kamath et al., 2003), for the following genes: *zyg-11*, *pal-1*, *mut-1/rde-3*, *ftt-2*, *him-3*, and *W03D8.9*.

C. elegans phenotypic analysis was performed with a Zeiss Axioplan microscope equipped with a Hamamatsu ORCA-ER CCD camera, connected to a computer running Openlab 4.0.2 software (Improvision). Polar body numbers were analyzed by freeze-fracture of early-stage embryos from gravid adults (Miller and Shakes, 1995), which were stained with 1 μg/ml DAPI (4,6-diamidino-2-phenylindole) and analyzed by epifluorescence and DIC

microscopy. Statistical significance was determined with the 2-tailed, unpaired Student's t-test or the chi-squares test.

Molecular analysis

The *C. elegans zyg-11* gene was amplified from the RB1 library (Barstead and Waterston, 1989). Human IMAGE clone cDNAs were obtained from Open Biosystems and Invitrogen: *ZYG11A* (Clone ID 610325); *ZYG11B* (30345285); *ZYG11BL* (4373769), *Elongin B* (5609063), and *Elongin C* (3923736). The *ZYG11B* cDNA used in these studies has a coding region that is 179 residues shorter than another cDNA reported in GenBank (gi: 12698005) due to alternative splicing. We have deposited this sequence in GenBank (acc. no. DQ646393).

zyg-11, *zer-1*, *vhl-1*, *ZYG11B*, and *ZYG11BL* cDNAs were cloned into the two-hybrid GAL4 DNA-binding domain vector pAS1-CYH2. *elc-1*, *skr-1*, *cul-2*, and human *Elongin C* cDNAs were cloned into the GAL4 activation domain vector pACT2 (Clontech). Human *Elongin B* cDNA was cloned into the pYES2 vector (Invitrogen). Human *ZYG11B* and *ZYG11BL* cDNAs were cloned into the pVSV-G-N1 vector, which is a derivative of pEGFP-N1 (Clontech) with a C-terminal VSV-G tag. Amino acid substitutions were generated using the QuikChange kit (Stratagene) or a two-step PCR method, and confirmed by sequencing. Two-hybrid analysis was performed with the yeast strain *PJ69-4A* (James et al., 1996) as described (Janssen, 1995).

In addition to anti-ZYG-11, the following primary antibodies were used: anti-VSV-G (Sigma); anti-FLAG (M2, Sigma); anti-CUL-2 (Feng et al., 1999); anti-human CUL2 (Zymed); anti-α-tubulin (DM1A, Sigma); and anti-actin (C4, ICN). Westerns were performed with the ECL Advance kit (Amersham)

***in vitro* binding assay**

Recombinant GST-ELC-1 protein was expressed from the pGEX-2T vector (Smith and Johnson, 1988) in *E. coli BL21(DE3)*, and purified with Glutathione Sepharose 4 Fast Flow (Amersham) according to the manufacturer's instructions. ^{35}S-methionine-labeled ZYG-11 was produced using the TNT Rabbit Reticulocyte Lysate System (Promega). 5 μl of *in vitro* translated product was mixed with 10 μg of GST or GST-ELC-1, and incubated with Glutathione Sepharose beads in Binding buffer (50 mM HEPES pH 7.8, 150 mM NaCl, 5 mM $MgCl_2$, 0.1 mM DTT, 0.01% Tween-20, Roche protease inhibitor cocktail). After incubation for 2 hrs at room temperature, beads were washed with 1x PBS, and boiled in 1x SDS sample buffer. Half of the samples were used for gel autoradiography and half for Coomassie staining.

Phylogenetic analysis

Protein sequences were aligned using Clustal X version 1.8 software (Thompson et al., 1994) and manually refined. Regions with extensive insertions/deletions (gaps) were excluded from the phylogenetic analysis (see Supplemental Fig. 1). The phylogeny was created with the Neighbor-Joining method using PHYLIP 3.65 software employing the JTT distance matrix. Bootstrap analysis was performed with 1000 data sets.

Proteins used in the alignment and phylogeny: *C. elegans* ZYG-11 (gi: 17538167) and ZER-1 (gi: 82654527); *D. melanogaster* ZYG11BL homolog (CG12084; gi: 24655224); *Strongylocentrotus purpuratus* (sea urchin) ZYG11B homolog (72128970) and ZYG11BL homolog (72103839); *M. musculus* ZYG11B (74141507), ZYG11BL (34784554), and ZYG11A (94373543); and *H. sapiens* ZYG11B (12698005), ZYG11BL (33589814), and ZYG11A (33286861).

Tissue culture and immunoprecipitation

Human 293T cells were transiently transfected with pVSV-G-N1/ZYG11B and pVSV-G-N1/ZYG11BL expression constructs using Lipofectamine-2000 (Invitrogen) according to the manufacturer's instructions. Cells expressing ZYG11B-VSV-G were treated with 50 μM LLnL for 24 hrs prior to harvest. Cells were harvested 60-72 hrs after transfection and lysed in NP-40 buffer (1% NP-40, 150 mM NaCl, 10 mM Sodium Phosphate pH 7.2, 2 mM EDTA, protease inhibitor cocktail, and 50 μM LLnL). Cell extracts were centrifuged at 13,000 rpm for 30 min at 4°C and the supernatant was precleared with protein G Sepharose. ZYG11B-VSV-G (treated with and without LLnL) and ZYG11BL-VSV-G were immunoprecipitated from lysate (2 mg of total protein) with 8 μg of mouse anti-VSV-G antibodies (Sigma), captured on Protein G Sepharose beads. Washed beads were resuspended in SDS-PAGE sample buffer and boiled for 5 min. Half of the boiled samples were used for westerns with mouse anti-VSV-G and the other half for a western with polyclonal anti-hCUL2 (Zymed).

SUPPLEMENTARY REFERENCES

Barstead, R.J. and Waterston, R.H. (1989) The basal component of the nematode dense-body is vinculin. *J Biol Chem*, **264**, 10177-10185.

Brenner, S. (1974) The genetics of *Caenorhabditis elegans*. *Genetics*, **77**, 71-94.

Feng, H., Zhong, W., Punkosdy, G., Gu, S., Zhou, L., Seabolt, E.K. and Kipreos, E.T. (1999) CUL-2 is required for the G1-to-S-phase transition and mitotic chromosome condensation in *Caenorhabditis elegans*. *Nat Cell Biol*, **1**, 486-492.

James, P., Halladay, J. and Craig, E.A. (1996) Genomic libraries and a host strain designed for highly efficient two-hybrid selection in yeast. *Genetics*, **144**, 1425-1436.

Janssen, K. (1995) Current Protocols in Molecular Biology. John Wiley & Sons, Boston, MA.

Kajava, A.V. and Kobe, B. (2002) Assessment of the ability to model proteins with leucine-rich repeats in light of the latest structural information. *Protein Sci*, **11**, 1082-1090.

Kamath, R.S., et al. (2003) Systematic functional analysis of the *Caenorhabditis elegans* genome using RNAi. *Nature*, **421**, 231-237.

Kemphues, K.J., Wolf, N., Wood, W.B. and Hirsh, D. (1986) Two loci required for cytoplasmic organization in early embryos of *Caenorhabditis elegans*. *Dev Biol*, **113**, 449-460.

Kobe, B. and Kajava, A.V. (2001) The leucine-rich repeat as a protein recognition motif. *Curr Opin Struct Biol*, **11**, 725-732.

Miller, D.M. and Shakes,D.C. (1995) Immunofluorescence microscopy. *Methods Cell Biol* **48**, 365-394.

Praitis, V., Casey, E., Collar, D. and Austin, J. (2001) Creation of low-copy integrated transgenic lines in *Caenorhabditis elegans*. *Genetics*, **157**, 1217-1226.

Smith, D.B. and Johnson, K.S. (1988) Single-step purification of polypeptides expressed in *Escherichia coli* as fusions with glutathione S-transferase. *Gene,* **67**, 31-40.

Thompson, J.D., Higgins, D.G. and Gibson, T.J. (1994) CLUSTAL W: improving the sensitivity of progressive multiple sequence alignment through sequence weighting, position-specific gap penalties and weight matrix choice. *Nucleic Acids Res,* **22**, 4673-4680.

Timmons, L. and Fire, A. (1998). Specific interference by ingested dsRNA. *Nature* **395**, 854.

Suppl. Fig. 4.1.

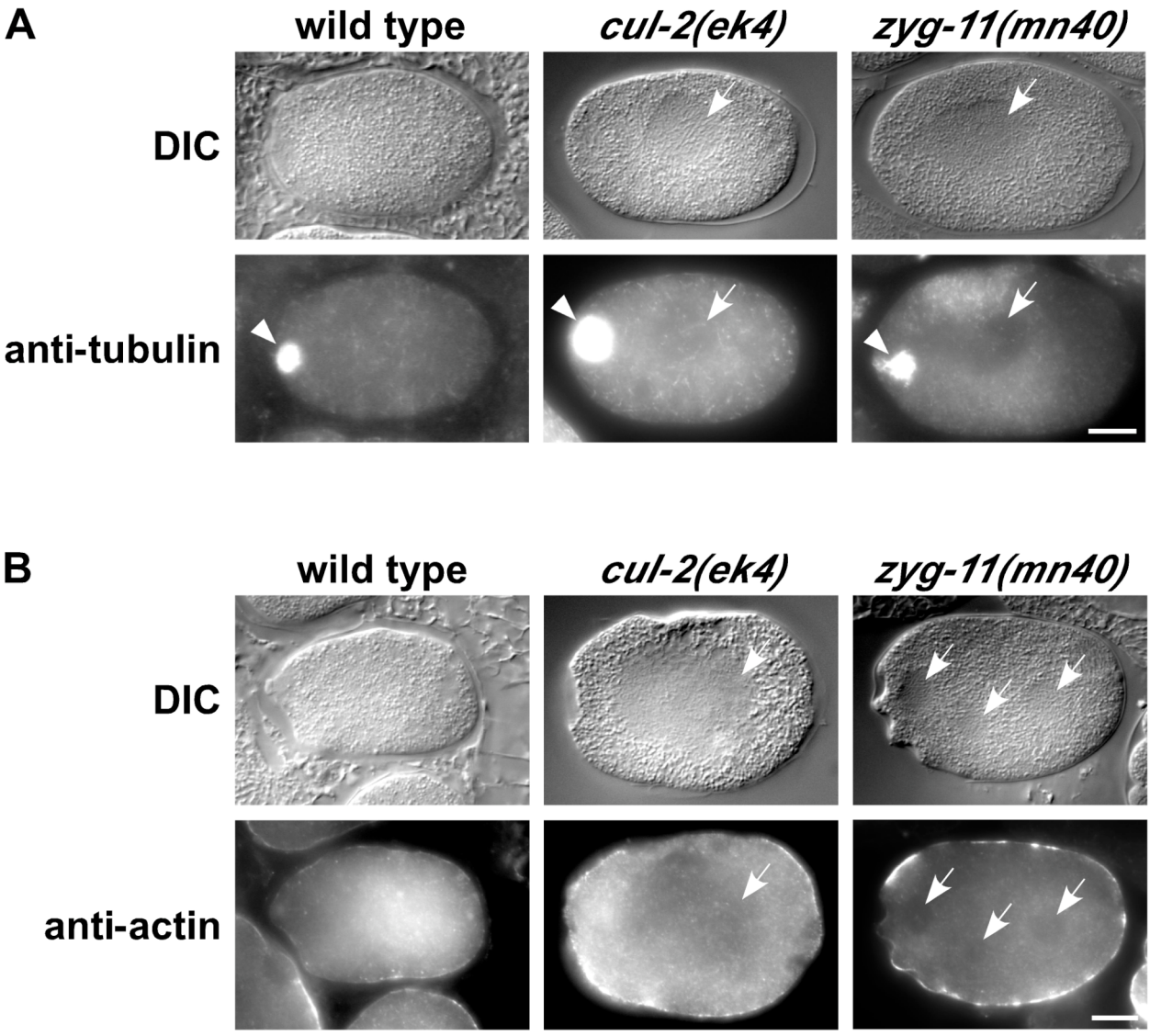

Supplementary Figure 1. Tubulin and actin do not accumulate in the granule-free cytoplasmic regions of *zyg-11* and *cul-2* mutants. Fixed wild-type, *cul-2*, and *zyg-11* mutant zygotes observed by DIC and either anti-α-tubulin (top panel) or anti-actin (bottom panel) immunofluorescence. White arrows denote granule-free regions. White arrowheads denote meiotic spindles. Scale bars, 10 μm.

Suppl. Fig. 4.2.

Suppl. Fig. 4.3.

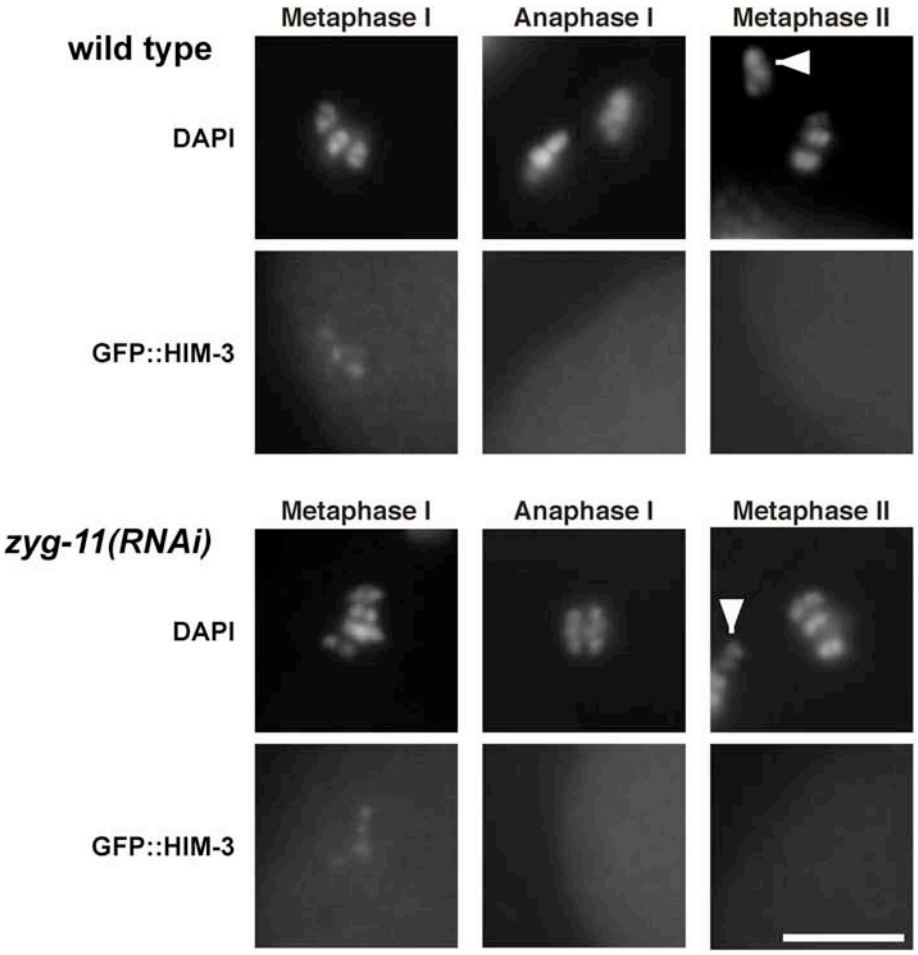

Supplementary Figure 3. GFP::HIM-3 localization on meiotic chromosomes in wild-type (top) and *zyg-11(RNAi)* (bottom) zygotes. DAPI and anti-GFP immunofluorescence images are presented for metaphase I (left), anaphase I (middle), and metaphase II (right). Arrowheads denote polar bodies. Note that GFP::HIM-3 staining visible between chromosome homologs in metaphase I is not visible on chromosomes during anaphase I or metaphase II. Scale bar, 10 μm.

CHAPTER 5

A GENETIC SCREEN TO IDENTIFY SUPPRESSORS OF *zyg-11*[3]

[3] **Srividya Vasudevan and Edward T. Kipreos**
To be submitted.

ABSTRACT

ZYG-11 is the substrate recognition subunit for the CUL-2 ubiquitin ligase complex. Mutations in the *zyg-11* gene cause a host of phenotypes including a meiosis II delay, defects in the establishment of anterior-posterior polarity, defects in the degradation of cyclin B and defects in the maintenance of the cytoskeleton. We have undertaken a temperature sensitive *zyg-11* suppressor screen to identify the targets and regulators of the CUL-2-ZYG-11 complex. Upon screening 100,000 F2 worms we have identified 19 extragenic suppressors of *zyg-11*. We have obtained both semi-dominant and recessive suppressors and have mapped six of the suppressors to chromosomes.

INTRODUCTION

In *C. elegans* the CBC^{ZYG-11} complex regulates a number of critical cell cycle and developmental processes such as meiotic II progression, establishment of anterior-posterior polarity, and cyclin B1 degradation (Liu et al., 2004; Sonneville and Gonczy, 2004). ZYG-11 is the substrate recognition subunit for CUL-2, however the substrates that are not degraded resulting in the meiosis II delay, reversal in polarity and failure in the degradation of cyclin B1 in *cul-2* and *zyg-11* mutants are not known (Vasudevan et al., 2007).

To identify substrates and regulators of the CBC^{ZYG-11} complex we performed a suppressor screen using a *zyg-11* temperature sensitive mutant. In this study we have recovered 19 *zyg-11* suppressors. All of the suppressors are extragenic and are viable at the restrictive temperature. Six of the suppressors are recessive, nine are semidominant, and the dominance of the remaining suppressors have not been determined. We have mapped four of these suppressors to a sub chromosomal region.

MATERIALS AND METHODS

Suppressor Screen: The temperature sensitive *zyg-11* hermaphrodites were synchronized by the bleaching method and grown to L4 stage at 16°C. The worms were mutagenized either with 50 mM ethyl methanesulfonate (EMS) or with 0.3-1mM N-ethyl-N-nitrosourea (ENU) and grown to gravid adults (Brenner, 1974; De Stasio and Dorman, 2001). Synchronized F1 progeny were grown at 16°C and the F2 L1 larvae were transferred to 25°C. Each F2 plate was seeded with approximately 25 F2 larvae and incubated at 25°C for three weeks. 1xNGM plates that contained suppressors starved out and were devoid of any bacterial lawn. Each suppressor was outcrossed by mating with the *zyg-11 (ax491), unc-4 (e120)*.

Strains: The mapping strain was made by backcrossing the *zyg-1l* or the *zyg-11, unc-4* strain with the CB4856 Hawaiian strain six times.

Genetic Mapping: Suppressors were mapped to a chromosome by mating *zyg-11 (ax491) unc-4; suppressor* hermaphrodites to the CB4856 – *zyg-11 (ax491)* males or by mating *zyg-11 (ax491); suppressor* males to the CB4856 – *zyg-11 (ax491), unc-4* hermaphrodites at 20°C. Twenty non-unc-4 F1 progeny were picked and grown on individual plates at 20°C. From each F1 plate, ten F2 progeny were picked and grown on individual plates at 25°C. After 4 days at 25°C the plates were segregated into suppressed and unsuppressed populations. 30 suppressed and 30 unsuppressed worms were picked into individual tubes and mapped to chromosomal regions as described (Davis et al., 2005).

Embryonic Hatching: To determine embryonic hatching ten L4 stage hermaphrodites were shifted to the restrictive temperature for 24 hours. The hermaphrodites were removed after 6 hours of egg laying. The embryos were allowed to develop for an additional 24 hours. At that time unhatched embryos and larvae were counted and the total percentage of hatched progeny was calculated.

Dominance: Each suppressor was determined to be dominant or recessive by mating *zyg-11 (ax491); him-8* males into *zyg-11 (ax491) unc-4; suppressor* hermaphrodites. Five non- unc-4 L4 hermaphrodites were shifted to the restrictive temperature (25°) and the percentage of embryos hatching was determined. When the number of viable progeny produced by the heterozygotes were similar to that of *zyg-11*, the suppressors were considered to be recessive. When the

heterozygotes produced more progeny than *zyg-11* but less that the homozygotes, then they were classified as semi-dominant. When the suppressor heterozygotes produced same or more progeny than the homozygotes then they were classified as dominant suppressors.

RESULTS

Isolation and characterization of suppressors:

To identify the substrates and regulators of the CBC^{ZYG-11} complex, I performed a suppressor screen using the temperature sensitive *zyg-11 (ax491)* allele. The *zyg-11 (ax491)* allele carries a point mutation at the C-terminus of the protein whereby glycine at position 632 has been changed to glutamic acid (Fig. 5.1A). At the permissive temperatures of 16°C and 20°C *zyg-11 (ax491)* produced viable progeny, however at restrictive temperature of 25°the embryos fail to hatch (Table 5.1). I examined the meiotic chromosome dynamics using time-lapse movies of *zyg-11 (ax491)* expressing transgenic H2B::GFP (Fig. 5.1B). In wild-type worms the time taken to complete meiosis I and II are the same, which is about 14 min. I observed in *zyg-11 (ax491)* that while meiosis I ranged from 13-17 min, meiosis II was delayed ranging from 27- 40 min at the restrictive temperature (n = 5). The *zyg-11 (ax491)* allele also has a high-incidence-of-male phenotype. At 20°C, the percentage of males observed in *zyg-11 (ax491)* allele is 3.86% whereas the wild-type worms produce males at the rate of 0.3% at 24° (Stein et al., 2007).

Upon screening 100,000 F2 progeny we obtained 19 suppressors of *zyg-11* (Fig. 5.2). The percentage of embryos hatching in the *zyg-11 (ax491)* allele is 0.06% at the restrictive temperature while in the suppressors the percentage hatching embryos ranged from 9-86% (Table 5.1).

I was able to outcross the suppressors into a *zyg-11(ax491)* allele whereby the *zyg-11* gene is linked to *unc-4,* suggesting that the suppressors are extragenic suppressors of *zyg-11*. The suppression was specific for the *zyg-11(ax491)* allele and failed to suppress *zyg-11(RNAi)* or *cul-2 (RNAi)* phenotypes. I also observed that all suppressors had no visible phenotype in the *zyg-11(ax491)* background at the restrictive or permissive temperature except for *ek10* and *ek12* which were medium dumpy. The dominance test revealed that suppressors *ek9, ek10, ek12, ek13, ek18* and *ek24* were recessive, suppressors *ek6, ek7, ek14, ek15, ek20, ek21 and ek22* were semi-dominant and suppressors *ek5* and *ek19* were dominant (Table 5.2).

Suppressor Mapping:

As all the suppressors do not have a phenotype of their own, mapping strains containing the original *zyg-11* mutation was essential. The suppressor mutations were assigned to a chromosome based on modifications of the principle of bulk segregant analysis described by Wicks et al. (Davis et al., 2005) (Table 5.3 and Fig. 5.3).

DISCUSSION

I have isolated suppressor mutations that restore embryonic viability in the temperature sensitive *zyg-11* mutants. ZYG-11 is the substrate recognition subunit for the CUL-2 ubiquitin ligase and regulates progression through meiosis II, establishment of anterior posterior polarity and degradation of cyclin B1. Through this genetic screen I hope to recover loss of function mutations in genes that could serve as substrates of the CBC^{ZYG-11} complex.

After screening 100,000 F2 progeny I have identified 19 suppressors. At present I have mapped five of the suppressors to chromosomes I, II, III and V. *ek13* and *ek14* map to

chromosome V. However they are not alleles of each other as *ek13* maps towards the left end of the chromosome while *ek14* maps to the center of the chromosome.

Temperature sensitive mutations in subunits of the anaphase-promoting complex arrest at metaphase of meiosis I at the restrictive temperature. A genetic suppressor screen with a weak allele of the APC subunit, *apc-8* whose defects are specific to meiosis has led to the recovery of 27 suppressors. These suppressors map to the APC co-activator *fzy-1* and spindle checkpoint genes that are orthologs of Mad1, Mad2 and Mad3 (Stein et al., 2007). Thus in addition to regulators and substrates we also expect to recover mutations in the spindle checkpoint genes.

ACKNOWLEDGEMENTS

We thank Geraldine Seydoux for the *zyg-11 (ax491)* allele; the *Caenorhabditis* Genetics Center for strains; and members of the Kipreos laboratory for comments on the manuscript.

REFERENCES

Brenner, S. (1974). The genetics of Caenorhabditis elegans. Genetics *77*, 71-94.

Davis, M.W., Hammarlund, M., Harrach, T., Hullett, P., Olsen, S., and Jorgensen, E.M. (2005). Rapid single nucleotide polymorphism mapping in C. elegans. BMC Genomics *6*, 118.

De Stasio, E.A., and Dorman, S. (2001). Optimization of ENU mutagenesis of Caenorhabditis elegans. Mutat Res *495*, 81-88.

Liu, J., Vasudevan, S., and Kipreos, E.T. (2004). CUL-2 and ZYG-11 promote meiotic anaphase II and the proper placement of the anterior-posterior axis in C. elegans. Development *131*, 3513-3525.

Sonneville, R., and Gonczy, P. (2004). Zyg-11 and cul-2 regulate progression through meiosis II and polarity establishment in C. elegans. Development *131*, 3527-3543.

Stein, K.K., Davis, E.S., Hays, T., and Golden, A. (2007). Components of the spindle assembly checkpoint regulate the anaphase-promoting complex during meiosis in Caenorhabditis elegans. Genetics *175*, 107-123.

Vasudevan, S., Starostina, N.G., and Kipreos, E.T. (2007). The Caenorhabditis elegans cell-cycle regulator ZYG-11 defines a conserved family of CUL-2 complex components. EMBO reports *8*, 279-286.

FIGURE LEGENDS

Figure 5.1.

(A) Schematic of the ZYG-11 protein showing the location of the mutation. The ZYG-11 protein contains a VHL box motif (Red), leucine rich repeats (Green) and Armadillo domain (Purple) (B) Movie sequences of histone H2B::GFP epifluorescence demonstrating chromosome dynamics in *zyg-11 (ax491)* zygotes.

Figure 5.2.

Schematic of the temperature sensitive *zyg-11* suppressor screen.

The P0 population were mutagenized with EMS/ENU and the F1 progeny were grown to adulthood at 16°C. 25 F2 larvae were seeded on 1X NGM plates containing a bacterial lawn and transferred to the restrictive temperature of 25°C. After incubation for three weeks, plates that no longer contained the bacterial lawn as a result of increase in population were scored as suppressors.

Figure 5.3.

Schematic showing the chromosomal locations of various suppressors.

The suppressors *ek5, ek7, ek13, ek14* and *ek22* were mapped to various chromosomes. (r)-Recessive, (sd)- Semidominant and (d)- Dominant suppressors. Scale Bar: 5 map units.

Table 5.1

Embryonic viability in *zyg-11 (ax491); suppressor* strains.

Strain	Hatching (%)
zyg-11(ax491)	0.06
zyg-11(ax491); ek5	10
zyg-11(ax491); ek6	32
zyg-11(ax491); ek7	40
zyg-11(ax491); ek8	20
zyg-11(ax491); ek9	35
zyg-11(ax491); ek10	19
zyg-11(ax491); ek11	9
zyg-11(ax491); ek12	13
zyg-11(ax491); ek13	17
zyg-11(ax491); ek14	75
zyg-11(ax491); ek15	25
zyg-11(ax491); ek16	18
zyg-11(ax491); ek18	48
zyg-11(ax491); ek19	12
zyg-11(ax491); ek20	72
zyg-11(ax491); ek21	27
zyg-11(ax491);ek22	13
zyg-11(ax491); ek23	86
zyg-11(ax491); ek24	31

Table 5.2

Determination of dominance.

Strain	% hatching in homozygotes (n=5)	% hatching in heterozygotes (n=5)	Dominance
zyg-11(ax491)	0.8-2.52		
zyg-11(ax491); ek5	2.09	5.16	Dominant
zyg-11(ax491); ek6	6.05	5.68	Semidominant
zyg-11(ax491); ek7	18.314	9.042	Semidominant
zyg-11(ax491); ek8	ND	ND	ND
zyg-11(ax491); ek9	2.02	1.82	Recessive
zyg-11(ax491); ek10	20.56	2.89	Recessive
zyg-11(ax491); ek11	ND	ND	ND
zyg-11(ax491); ek12	12.95	0.87	Recessive
zyg-11(ax491); ek13	18.27	0.43	Recessive
zyg-11(ax491); ek14	57.24	5.92	Semidominant
zyg-11(ax491); ek15	12.5	5.90	Semidominant
zyg-11(ax491); ek16	ND	ND	ND
zyg-11(ax491); ek18	8.9	2.02	Recessive
zyg-11(ax491); ek19	4.21	5.63	Dominant
zyg-11(ax491); ek20	68.57	5.95	Semidominant
zyg-11(ax491); ek21	9.15	3.22	Semidominant
zyg-11(ax491);ek22	9.29	4.35	Semidominant

zyg-11(ax491); ek23	3.12	ND	ND
zyg-11(ax491); ek24	4.18	1.93	Recessive

Table 5.3.

Chromosomal location of the *zyg-11* suppressors.

Strain	Chromosomal location
zyg-11(ax491)	II, center
zyg-11(ax491); ek5	III, left
zyg-11(ax491); ek7	II, left
zyg-11(ax491); ek13	V, left
zyg-11(ax491); ek14	V, center
zyg-11(ax491);ek22	I, center

Fig. 5.1.

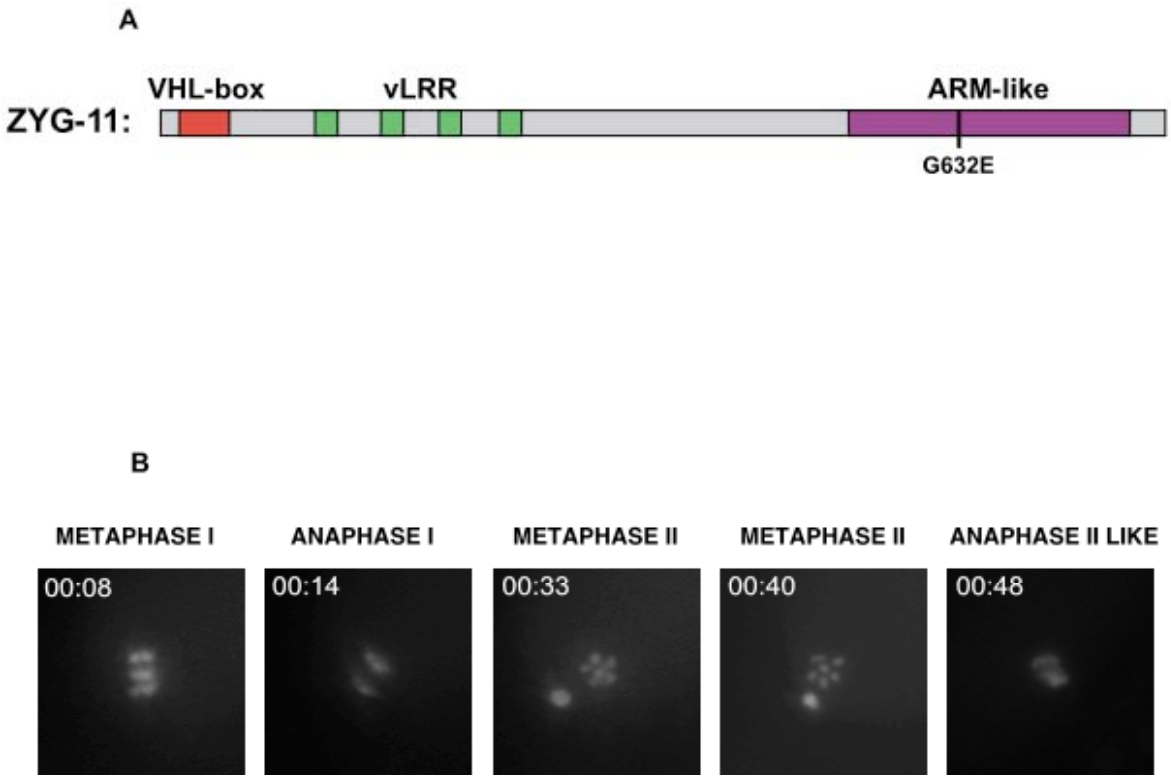
A
VHL-box
vLRR
ARM-like
ZYG-11:
G632E
B
METAPHASE I
ANAPHASE I
METAPHASE II
METAPHASE II
ANAPHASE II LIKE
00:08
00:14
00:33
00:40
00:48

Fig. 5.2.

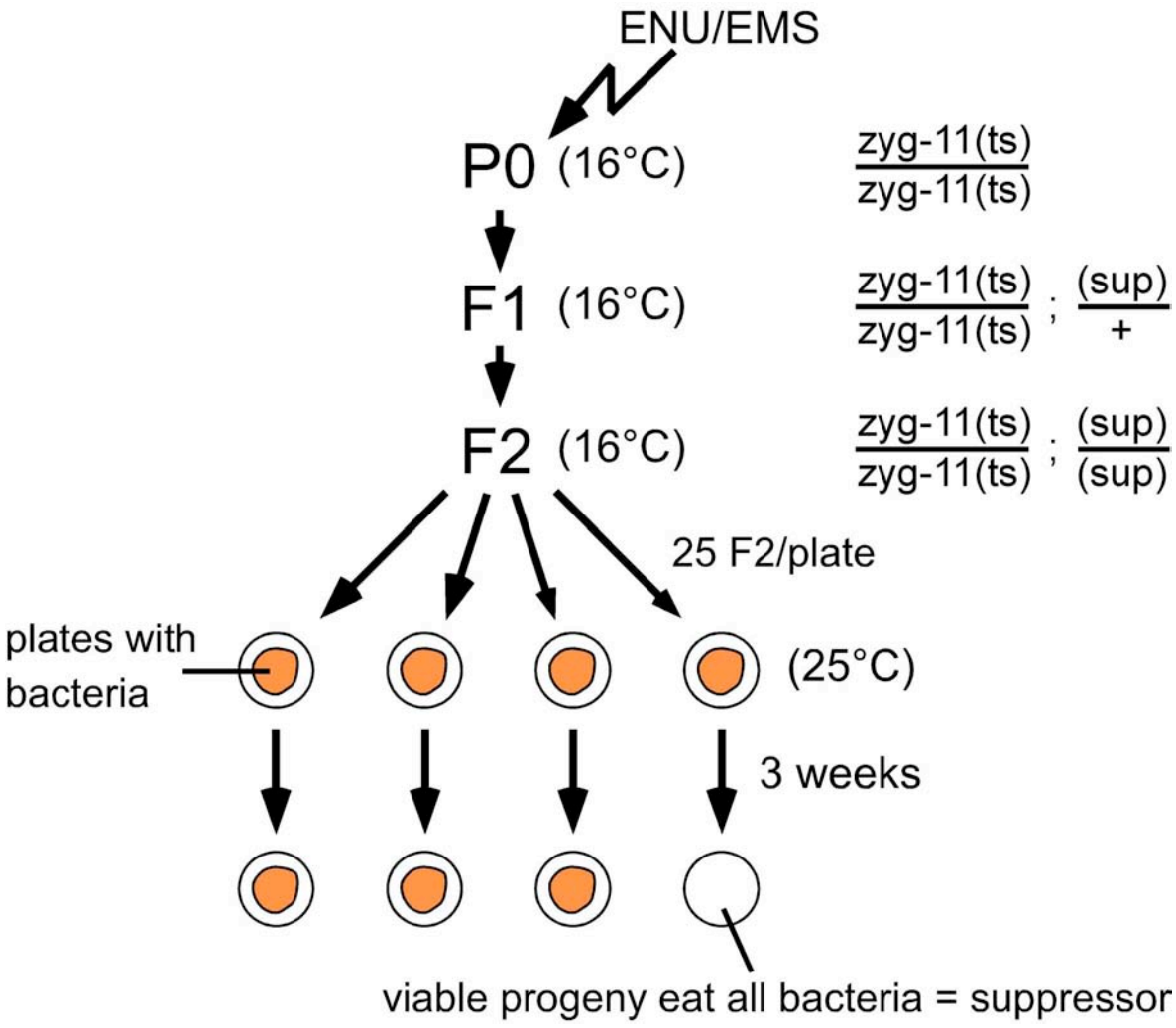
ENU/EMS
P0 (16°C)
zyg-11(ts) / zyg-11(ts)
F1 (16°C)
zyg-11(ts) / zyg-11(ts) ; (sup) / +
F2 (16°C)
zyg-11(ts) / zyg-11(ts) ; (sup) / (sup)
25 F2/plate
plates with bacteria
(25°C)
3 weeks
viable progeny eat all bacteria = suppressor

Fig. 5.3.

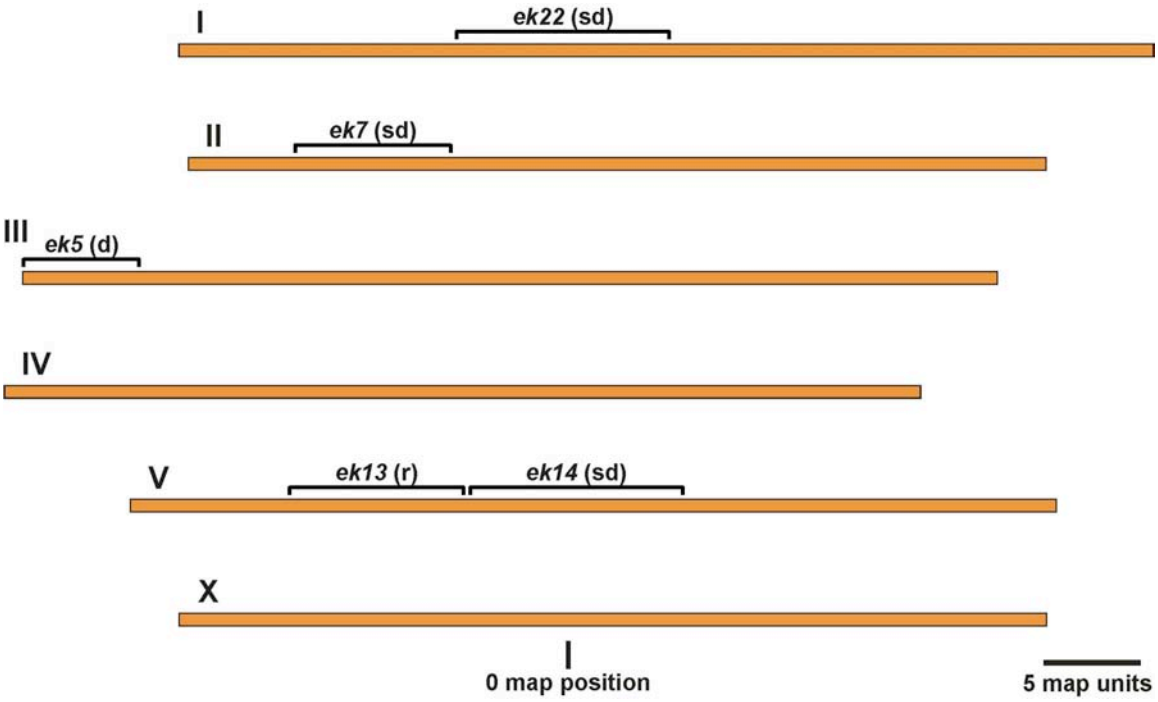
I
ek22 (sd)
II
ek7 (sd)
III
ek5 (d)
IV
V
ek13 (r)
ek14 (sd)
X
0 map position
5 map units

CHAPTER 6

DISCUSSION

Protein degradation by the ubiquitin proteosome system is one of the major pathways by which intracellular proteins are degraded. Central to the ubiquitin proteosome system are the ubiquitin ligases that facilitate the transfer and assembly of a polyubiquitin chain on the substrate. This work involves the study of CUL-2 ubiquitin ligase and its substrate recognition subunit ZYG-11.

CUL-2 and ZYG-11 are required for the initiation of anaphase II and meiotic progression

C. elegans is a self-fertilizing hermaphrodite that first produces sperm in the fourth larval stage and switches to oocyte production at the young adult stage. The process of meiosis involves several stages, such as the decision to switch from sperm to oocyte production, homologous chromosome pairing, synapsis formation, oocyte maturation, fertilization, and the completion of the two meiotic divisions. This study sheds light on the progression of the second meiotic division in *C. elegans.*

In zygotes devoid of *cul-2* and *zyg-11,* anaphase II fails to occur and meiosis II lasts three to four times longer than wild type. The chromosomes remain in the metaphase configuration for an extended period of time. The cohesin REC-8 which is required to hold the sister chromatids together is degraded in *cul-2* zygotes. Thus, the

failure to proceed to anaphase is due to a failure in chromosomes to move apart (Liu et al., 2004; Sonneville and Gonczy, 2004).

During meiotic anaphase II in *C. elegans*, the microtubules near the meiotic spindle poles appear to depolymerize whereas the amount of midzone microtubules between the separating chromosomes increases dramatically. This suggests that during meiotic anaphase the chromosomes are pushed apart by microtubule polymerization. In *cul-2* zygotes, the meiotic spindle maintains its normal size and shape for an extended period of time during metaphase II. However we never observe any anaphase structures based on tubulin immunofluoresence suggesting a defect in the initiation of microtubule depolymerization at the spindle poles and polymerization between sister chromatids. After a prolonged metaphase II arrest, the meiotic spindle eventually shrinks, loses the barrel shape and is observed as a disorganized mass of microtubules near the meiotic DNA. CUL-2 therefore is required to promote microtubule polymerization between the separating pieces of chromosomes during meiotic chromatid segregation (Liu et al., 2004).

In mammalian meiosis, the chromosomes are segregated by a different mechanism. The chromosomes are pulled apart by the microtubules and if the functions of CUL-2 are conserved across species, it would be of interest to investigate the role of CUL-2 in mammalian meiosis (Woods et al., 1999).

The role of CUL-2 and ZYG-11 in cyclin degradation during meiosis

Degradation of Cyclin B1 is a key regulatory step in progression through and exit from mitosis. Using a CYB-1::GFP reporter, we observed that maternally provided cyclin B1

is degraded upon fertilization and completely disappears by the end meiosis. In *cul-2* and *zyg-11* zygotes CYB-1::GFP is stabilized during both meiosis I and II. Depletion of CYB-1 by RNAi in *cul-2* zygotes partially rescued the meiosis II delay of *cul-2 (ek1)* embryos (Liu et al., 2004).

Sonneville and Gonczy have demonstrated that *cul-2* and *zyg-11* zygotes not only have an extended metaphase II but also a lengthened anaphase II. They investigated whether the persistence of CYB-3 may be causing delayed metaphase exit in *cul-2* mutants. They observed an increase in CYB-3::GFP levels during meiosis II in *cul-2* and *zyg-11* zygotes compared to wild type. Upon depletion of cyclin B3 in such embryos, the metaphase to anaphase transition of meiosis II is delayed. However the anaphase II delay is abolished (Sonneville and Gonczy, 2004).

These results suggest that degradation of cyclin B1 and cyclin B3 are required for timely exit from metaphase II and anaphase II respectively. Cyclin B1 levels are also regulated by the APC component *apc-11* in *C. elegans.* Exactly how the levels of cyclins are regulated by APC components, *cul-2* and *zyg-11* will require further investigation. It has been proposed that either cyclins B1 and B3 are substrates of the CUL-2 ligase or the upregulation of cyclins B1 and B3 could be an indirect result of a failure to degrade other CUL-2 targets.

Polarity reversals in *cul-2* and *zyg-11* zygotes

Establishments of the anterior-posterior axis is essential for the normal development of *C. elegans.* In wild type, the first signs of polarized PAR-2 is observed shortly after meiosis II. In *cul-2* and *zyg-11* zygotes, stable PAR-2 is observed on the anterior cortex

near the meiotic spindle during the extended metaphase. In APC mutant zygotes arrested in meiosis I, the meiotic spindle can initiate the localization of PAR-2 at the anterior cortex. It has been proposed that the establishment of AP polarity in the *C. elegans* zygote is a microtubule directed process (Wallenfang and Seydoux, 2000). Interestingly in *cyb-3 (RNAi)* zygotes that are also delayed in meiosis II but at a different stage than *cul-2* and *zyg-11* zygotes, no reversals in PAR-2 localizations was observed. (Sonneville and Gonczy, 2004). These results suggest that the ability of the meiotic spindle to localize the PAR proteins in a wild-type background is questionable and that in *cul-2* and *zyg-11* mutants the meiotic spindle acquires the ability to polarize the zygote.

Upon depletion of the meiotic spindle by RNAi of tubulin, lateral cortical PAR-2 was still observed in *cul-2* zygotes at a reduced but significant levels (Liu et al., 2004). Thus during meiosis, CUL-2 prevents localization of PAR-2 near the meiotic spindle and on regions away from the meiotic spindle. An important direction of research would be in the identification of substrates that must be degraded to prevent polarity establishment during meiosis II. We speculated that PAR-2 could serve as a substrate for the CUL-2 $^{ZYG-11}$ ligase, however we did not detect any interaction between ZYG-11 and PAR-2 through the yeast two-hybrid system (unpublished data).

Apart from reversals in the intiation of polarity. A full reversal of PAR localization at the two cell stage, reversals in P-granule locaization, and migration of the sperm pronucleus centrosomal complex are observed in *cul-2* zygotes (Liu et al., 2004). What triggers the reversals in these downstream events is not known. Perhaps the initial reversal of PAR-2 followed by its stabilization is responsible for the reversals in downstream events (Liu et al., 2004; Vasudevan et al., 2007).

ZYG-11 interacts with CUL-2 *in vivo*

ZYG-11 produces meiotic and polarity reversal defects similar to those observed in *cul-2* mutants, suggesting that the two proteins function in the same pathways. We have identified ZYG-11 in CUL-2 pulldowns suggesting that ZYG-11 is a CUL-2 complex component (Vasudevan et al., 2007).

ZYG-11 has a VHL box motif and serves as the substrate recognition subunit for CUL-2

ZYG-11 is a leucine rich repeat protein and this protein-interaction motif is found in a number of substrate recognition subunits for the CUL-1 based E3 complexes. It is therefore possible that ZYG-11 functions as the substrate recognition subunit for the CUL-2 based E3 complexes to promote meiosis, degrade cyclin B1 and establish anterior-posterior polarity.

To qualify as a substrate recognition subunit for CUL-2, the candidate protein must interact with the adaptor protein Elongin C through a conserved motif called the VHL box (Kamura et al., 2004). We have identified a *C. elegans* specific VHL box that is notably different from that in humans. We have also been able to demonstrate interaction of ZYG-11 with Elongin C, and this interaction was abolished when the VHL box was mutated (Vasudevan et al., 2007). The conserved sequences of the VHL box can be used to search protein databases for additional CUL-2 substrate recognition subunits.

ZYG-11 homologues are CBC complex components

We identified ZER-1, the ZYG-11 paralog as a CUL-2 complex component which is also known to contain the VHL box. The human orthologs of ZYG-11 and ZER-1 also contain the VHL box motif and interact with human CUL2 through Elongin C. It would be important to know the functions of ZYG-11 in higher animals to elucidate these CUL-2 mediated processes.

ZYG-11 substrates and regulators

To identify the substrates and regulators of the CBC^{ZYG-11} complex, we have performed a suppressor screen with a temperature sensitive *zyg-11* mutant and have recovered several suppressors. At present no information is available on why cyclin B1 is failed to be degraded and meiosis II is delayed in *zyg-11* and *cul-2* zygotes. Also the substrates that are linked to inverted polarity are unknown. The information obtained from the study of these suppressors here will be crucial in understanding the regulation of meiosis by CUL-2 and ZYG-11.

REFERENCES

Kamura, T., Maenaka, K., Kotoshiba, S., Matsumoto, M., Kohda, D., Conaway, R.C., Conaway, J.W., and Nakayama, K.I. (2004). VHL-box and SOCS-box domains determine binding specificity for Cul2-Rbx1 and Cul5-Rbx2 modules of ubiquitin ligases. Genes & development *18*, 3055-3065.

Liu, J., Vasudevan, S., and Kipreos, E.T. (2004). CUL-2 and ZYG-11 promote meiotic anaphase II and the proper placement of the anterior-posterior axis in C. elegans. Development (Cambridge, England) *131*, 3513-3525.

Sonneville, R., and Gonczy, P. (2004). Zyg-11 and cul-2 regulate progression through meiosis II and polarity establishment in C. elegans. Development (Cambridge, England) *131*, 3527-3543.

Vasudevan, S., Starostina, N.G., and Kipreos, E.T. (2007). The Caenorhabditis elegans cell-cycle regulator ZYG-11 defines a conserved family of CUL-2 complex components. EMBO reports *8*, 279-286.

Wallenfang, M.R., and Seydoux, G. (2000). Polarization of the anterior-posterior axis of C. elegans is a microtubule-directed process. Nature *408*, 89-92.

Woods, L.M., Hodges, C.A., Baart, E., Baker, S.M., Liskay, M., and Hunt, P.A. (1999). Chromosomal influence on meiotic spindle assembly: abnormal meiosis I in female Mlh1 mutant mice. The Journal of cell biology *145*, 1395-1406.